

A METHOD TO PREDICT DEFORMATIONS FOR
PARTIALLY DRAINED CONDITIONS IN BRACED
EXCAVATIONS

by

Theodore von Rosenvinge IV

B.S. Eng. Northeastern University

(1978)

Submitted in partial fulfillment
of the requirements for the degree of
Master of Science

at the

Massachusetts Institute of Technology

(August 1980)

© Theodore von Rosenvinge IV

Signature of Author _____

Department of Civil Engineering, August 14, 1980

Certified by _____

Thesis Supervisor

Accepted by _____

Chairman, Departmental Committee on Graduate

Students of the Department of Civil Engineering.

ARCHIVES
MASSACHUSETTS INSTITUTE
OF TECHNOLOGY

OCT 9 1980

A METHOD TO PREDICT DEFORMATIONS FOR
PARTIALLY DRAINED CONDITIONS IN
BRACED EXCAVATIONS

by

Theodore von Rosenvinge IV

Submitted to the Department of Civil Engineering
on August 14, 1980 in partial fulfillment of the
requirements for the degree of Master of Science in
Civil Engineering

ABSTRACT

The purpose of this thesis is to develop a method to predict deformations in braced excavations, which includes the effects of excess pore pressure dissipation. The time variables considered are time for construction compared with time required for pore pressure equilization due to altered flow conditions and shear. The method will apply the Stress Path Method to determine appropriate soil parameters to use in the existing finite element program, BRACE III in a way that accounts for time effects.

The method will be applied to an actual case to demonstrate its applicability and illustrate its use.

Thesis Supervisor: Dr. William Allen Marr

Title: Research Associate

To M.E. and Marta

ACKNOWLEDGMENTS

The author is grateful to Dr. William Allen Marr for his interest and guidance during the work on this thesis. The author is also grateful to Professor T.W. Lambe for his support, providing information and soil specimens tested for the case study.

The author also wishes to acknowledge the generous advice and discussion provided by Dr. Walter E. Jaworski of Northeastern University during the early stages of this thesis.

Special thanks is due to my wife, M.E., and young daughter, Marta for their patience during my education. M.E.'s tireless hours on the word processor are gratefully acknowledged. The sustaining humor was supplied by Marta's often welcome distraction while her father was working on his "thēthiss". And a note of thanks to my entire family for their continued support and encouragement during the last several years.

TABLE OF CONTENTS

	<u>Page</u>
TITLE PAGE	1
ABSTRACT	2
DEDICATION	3
ACKNOWLEDGEMENTS	4
TABLE OF CONTENTS	5
LIST OF TABLES	9
LIST OF FIGURES	10
CHAPTER ONE INTRODUCTION	
1.0 <u>INTRODUCTION</u>	14
1.1 <u>THESIS OBJECTIVE</u>	19
1.2 <u>THESIS SCOPE</u>	19
CHAPTER TWO THE ROLE OF TIME	
2.0 <u>INTRODUCTION</u>	21
2.1 <u>STRESS PATHS</u>	21
2.1.1 <u>Undrained Shear</u>	21
2.1.2 <u>Dissipation of Pore Pressure Following</u> <u>Shear</u>	22
2.1.3 <u>Stress Paths - Summary</u>	25
2.2 <u>THE PERFORMANCE OF BRACED EXCAVATIONS VS. TIME</u>	25
2.2.1 <u>Braced Excavations in Cohesionless Sand</u>	25
2.2.2 <u>Piping, Suffosion</u>	26
2.2.3 <u>Effects of Frost Action</u>	26
2.2.4 <u>Braced Excavations In Normally</u> <u>Consolidated Clay</u>	27

	<u>Page</u>
4.4.2 <u>Stress Paths from Initial BRACE III</u>	
<u>Analysis</u>	87
4.4.3 <u>Laboratory Tests and Revised Soil</u>	
<u>Profile</u>	89
A. <u>Soil Classification</u>	89
B. <u>Stress Path Tests</u>	90
C. <u>Coefficient of Consolidation</u>	91
D. <u>Revised Soil Profile</u>	91
E. <u>Contours of Equal Vertical Strain</u>	95
4.4.4 <u>Revised BRACE III Analysis for Partially</u>	
<u>Drained Conditions</u>	95
A. <u>General</u>	95
B. <u>Computation of Partially Drained</u>	
<u>Moduli</u>	96
1. <u>Undrained Shear Strains</u>	96
2. <u>Consolidation Strains Due to</u>	
<u>Dissipation of Excess Pore Pressure</u>	
<u>Within the Excavation</u>	97
3. <u>Consolidation Strains Due to</u>	
<u>Dissipation of Excess Pore Pressure</u>	
<u>Behind the Excavation</u>	98
4. <u>Contours of Moduli</u>	100
5. <u>K_o</u>	102
6. <u>Anisotropy</u>	102
C. <u>Predicted Loads, Deformations and</u>	
<u>Stability</u>	103

	<u>Page</u>
1. <u>General</u>	103
2. <u>Deformations</u>	103
3. <u>Loads</u>	106
4. <u>Stability</u>	107
CHAPTER FIVE SUMMARY AND CONCLUSIONS	
5.0 <u>GENERAL</u>	152
5.1 <u>LIMITATIONS</u>	153
5.2 <u>SUGGESTIONS FOR FURTHER RESEARCH</u>	154
5.3 <u>CONCLUSIONS</u>	156
LIST OF SYMBOLS	161
REFERENCES	163
APPENDIX A GRAINSIZE PLOTS AND SQUARE ROOT OF TIME CONSOLIDATION PLOTS - NAKAGAWA SOIL SPECIMENS	167
APPENDIX B VERTICAL EFFECTIVE STRESS VERSUS DEPTH- NAKAGAWA	182

LIST OF TABLES

<u>Table No.</u>	<u>Title</u>	<u>Page</u>
3.1	GEOTECHNICAL PERFORMANCE	81
3.2	STRESS PATH METHOD	82
4.1	SOIL INDEX PROPERTIES, AND CLASSIFICATION	115
4.2	SUMMARY OF COEFFICIENT OF CONSOLIDATION DATA FROM STRESS PATH TESTS	121
4.3	SUMMARY OF SHEAR STRENGTH DATA	124
4.4	SUMMARY OF DETERMINATION OF PARTIALLY DRAINED STRESS STRAIN MODULI	129
4.5	SUMMARY OF STRENGTHS FOR AVERAGE ELEMENTS IN STABILITY ANALYSIS	151

10
LIST OF FIGURES

<u>Figure No.</u>	<u>Title</u>	<u>Page</u>
1.1	EFFECT OF FORCED DELAY ON A CRITICAL CONSTRUCTION EVENT	20
2.1.1	EXAMPLE BRACED EXCAVATION GEOMETRY	48
2.1.2	STRESS PATHS FOR UNDRAINED UNLOADING OF NORMALLY AND OVER CONSOLIDATED SOIL ELEMENTS	49
2.1.3a	STRESS PATHS FOR UNDRAINED UNLOADING FOLLOWED BY PORE PRESSURE DISSIPATION FOR NORMALLY CONSOLIDATED SOIL-NO DEWATERING	50
2.1.3b	STRESS PATHS FOR UNDRAINED UNLOADING FOLLOWED BY PORE PRESSURE DISSIPATION FOR NORMALLY CONSOLIDATED SOIL-WITH DEWATERING	51
2.1.3c	STRESS PATHS FOR UNDRAINED UNLOADING FOLLOWED BY PORE PRESSURE DISSIPATION FOR OVER CONSOLIDATED SOIL-NO DEWATERING	52
2.1.3d	STRESS PATHS FOR UNDRAINED UNLOADING FOLLOWED BY PORE PRESSURE DISSIPATION FOR OVERCONSOLIDATED SOIL-WITH DEWATERING	53
2.1.4	DETERMINATION OF TOTAL HEAD SUBJECT TO EXCAVATION AND/OR DEWATERING	54
2.1.5	STRESS PATHS FOR ACTIVE AND PASSIVE CONDITIONS FOR NORMALLY AND OVERCONSOLIDATED SOIL	55
2.2.1	STRESS PATHS FOR EXCAVATION IN COHESIONLESS SAND	56
2.2.2	PIPING/SUFFOSION MECHANISMS	57
2.2.3	INCREASE IN STRUT LOAD VS. TIME FOR A BRACED CUT IN STIFF FISSURED CLAY	58
2.2.4	VARIATION IN COEFFICIENT OF CONSOLIDATION	59
2.2.5	SOIL PROFILE, EXCAVATION, AND INSTRUMENTATION DETAILS FOR A BRACED SLURRY WALL IN SOFT CLAY, OSLO	60
2.2.6	SUMMARY OF OBSERVATIONS FOR BRACED CUT IN SOFT CLAY, OSLO	61

		<u>Page</u>
2.2.7	STRESS DATA FOR PIEZOMETER P-1, BELOW THE CAES FOUNDATION EXCAVATION	62
2.2.8	SOUTH COVE SUBWAY EXCAVATION TEST SECTION PIEZOMETER P-4	63
2.2.9	STRUT LOAD AND PORE WATER PRESSURE VS. TIME -SOUTH COVE TEST SECTION	64
2.2.10	MEASURED AND PREDICTED STEADY STATE PORE PRESSURES-SOUTH COVE TEST SECTION	65
2.2.11	TIME DEPENDENT BEHAVIOR OF TEST CUT IN STIFF FISSURED CLAY	66
2.2.12	EFFECT OF VARIATION OF TIME TO FAILURE ON STRENGTH IN UNDRAINED TRIAXIAL TESTS	67
2.2.13	EXCAVATION PENETRATING SILT: MBTA TEST SECTIONS A & B	68
2.2.14	MEASURED AND PREDICTED PORE PRESSURE MBTA TEST SECTIONS A AND B	69
2.3.1a	TERZAGHI & PECK DESIGN ENVELOPES	70
2.3.1b	TERZAGHI & PECK DESIGN ENVELOPES	71
2.3.2	CONSOLIDATION AT THE END OF ONE-DIMENSIONAL EXCAVATION	72
2.3.3a	CONTOURS OF NEGATIVE EXCESS PORE PRESSURE FOR TWO-DIMENSIONAL EXCAVATION	73
2.3.3b	CONTOURS OF NEGATIVE EXCESS PORE PRESSURE FOR TWO-DIMENSIONAL EXCAVATION	74
3.1	CONTOURS OF EQUAL VERTICAL STRAIN	83
4.2.1	PLAN VIEW AND PROFILE OF NAKAGAWA SEWAGE TREATMENT PLANT EXCAVATION - SITE B	110
4.2.2	SITE B CONSTRUCTION SCHEDULE	111
4.4.1	INITIAL PROFILE AND FINITE ELEMENT MESH	112
4.4.2	DETAIL OF FINITE ELEMENT MESH IN ZONE OF EXCAVATION	113
4.4.3	TYPICAL TOTAL STRESS PATHS INITIAL BRACE III ANALYSIS LINEARLY ELASTIC MODULUS	114

		<u>Page</u>
4.4.4	PLASTICITY CHART	116
4.4.5a	STRESS PATH TEST TC-1	117
4.4.5b	STRESS PATH TEST TC-2	118
4.4.5c	STRESS PATH TEST TE-1	119
4.4.5d	STRESS PATH TEST TE-2	120
4.4.6	REVISED SOIL PROFILE	122
4.4.7	UNDRAINED STRENGTH TRIAXIAL TEST RESULTS VERSUS SAMPLE DEPTH	123
4.4.8a	ESTIMATED CONTOURS OF EQUAL STRAIN - COMPRESSION	125
4.4.8b	ESTIMATED CONTOURS OF EQUAL STRAIN - COMPRESSION	126
4.4.8c	ESTIMATED CONTOURS OF EQUAL STRAIN - EXTENSION	127
4.4.9	SIXTH EXCAVATION STAGE SIMPLIFIED PROFILE	128
4.4.10	SUPERPOSITION OF TOTAL STRESS PATHS ON CONTOUR PLOT OF EQUAL STRAIN	131
4.4.11	DEPTH OF EXCAVATION VS. TIME	132
4.4.12a	TIME FACTOR VS. AVERAGE DEGREE OF CONSOLIDATION	133
4.4.12b	NORMALIZED DEPDTH VS. CONSOLIDATION RATIO	133
4.4.13	NORMALIZED DEPTH VS. CONSOLIDATION RATIO FOR TRIANGULAR INITIAL EXCESS PORE PRESSURE	134
4.4.14a	VOLUMETRIC STRAIN VS DISSIPATION OF PORE PRESSURE	135
4.4.14b	VOLUMETRIC STRAIN VS. LOGARITHMIC DISSIPATION OF PORE PRESSURE	136
4.4.15	CONTOURS OF MODULI - BRACE III ANALYSIS - REVISED RUN B	137
4.4.16	CONTOURS OF MODULI - BRACE III ANALYSIS - FINAL RUN C	138
4.4.17	DEFORMED FINITE ELEMENT MESH	139

		<u>Page</u>
4.4.18	SELECTED LINES OF LATERAL DISPLACEMENT	140
4.4.19	SELECTED LINES OF VERTICAL HEAVE	141
4.4.20	CONTOURS OF SHEAR STRESS	142
4.4.21	CONTOURS OF TOTAL SIGMA Z	143
4.4.22	CONTOURS OF TOTAL SIGMA X	144
4.4.23	CONTOURS SHOWING TRENDS OF NEGATIVE EXCESS PORE PRESSURE	145
4.4.24	COMPARISON OF PECK'S CHART WITH SETTLEMENT BEHIND THE NAKAGAWA EXCAVATION	146
4.4.25	ESTIMATED TOTAL STRESS DISTRIBUTION BEHIND THE STEEL PILE WALL	147
4.4.26	TERZAGHI BASAL HEAVE ANALYSIS	148
4.4.27	SIXTH EXCAVATION STAGE - STABILITY ANALYSIS	149
4.4.28	STRESS PATHS FOR STABILITY ANALYSIS	150
5.1	LINEAR VS. NON LINEAR STRESS STRAIN	159
5.2	HYPERBOLIC STRESS STRAIN CURVES	160
A.1-A.6	COMBINED GRAINSIZE ANALYSIS PLOTS	168
A.7-A.14	SQUARE ROOT OF TIME CONSOLIDATION PLOTS	174
B.1	VERTICAL EFFECTIVE STRESS VS. DEPTH, NAKAGAWA	183

CHAPTER ONE

INTRODUCTION1.0 INTRODUCTION

An engineer should carefully consider the role of time and specifically the role of excess pore pressure dissipation, in designing and constructing "deep" or major excavations. Design economy, safety, and the potential for damage to the excavation and adjacent facilities can be highly influenced by the effect of time on the response of the soil mass.

Presently the usual practice of engineers is to idealize the excavation or "unloading" case and assume "undrained" or "drained" conditions. For excavations in clay the most common approach is to use "undrained" strength and deformation parameters for design. This approach assumes the following:

- (1) Construction occurs rapidly.
- (2) No dissipation of excess pore pressure occurs during construction (i.e., no drainage occurs).
- (3) The soil strength is the in-situ undrained shear strength.

The assumptions above are applicable only for an "instantaneous" excavation. Actual excavations in cohesive soils are not "instantaneous" and are partially drained.

Although for some situations (i.e. rapid temporary excavation in soil with a very low permeability) the undrained assumption is nearly valid at least for design purposes, many major braced excavations are open for months or even years. Significant pore pressure dissipation following shear stressing of the soil or altered flow conditions may occur. Undetected layers of pervious soil may facilitate rapid drainage. As a consequence unpredicted and significant increases or decreases in soil strength may occur as well as variation in the stress/strain characteristics of the soil with time.

Although relatively few studies of instrumented excavations have been made to observe the effect of time on the performance of braced cuts, some significant observations have been made. To briefly summarize several cases:

- (1) Bjerrum & DiBiagio (1956) reported on an experimental 4 meter deep trench in stiff-fissured clay instrumented for the purpose of studying the influence of time on earth pressure. They observed the average force per meter as measured in the struts increase from 2.3 tons/meter to 7.17 tons/meter over several months (Sept. to Dec.).
- (2) Measurements from a braced slurry wall in stiff Boston Blue Clay reported by Jaworski (1973) indicate a gradual and significant increase in

earth pressure after excavation to the design depth.

(3) DiBiagio & Roti (1972) reported earth and pore pressure measurements for a braced slurry wall excavation in soft clay. Significant decreases and increases in earth and pore pressures during and after completion of excavation to the final depth were observed.

(4) Lambe (1968) reported piezometer data for an excavation 22 feet deep penetrating an overconsolidated medium Boston Blue Clay. Negative excess pore pressures in the clay at the bottom of the excavation decreased during the 24 day period the cut was open. This indicated an overall decrease in the strength of the soil as well as a decreasing factor of safety with time.

The above observations reflect the fact that time is an important variable to be recognized by the engineer.

Recently Clough & Osaimi (1979) investigated pore pressure dissipation for excavations, including braced excavations using a finite element model to determine how long the undrained case was applicable. From the results the authors concluded that pore pressure dissipation for excavation in clay is likely to occur to a greater degree than previously believed and that the undrained assumption should be used with care.

Determining the degree to which dissipation of pore pressure occurs for a given braced cut can be a complex and difficult task. For sands time may be a factor with respect to other phenomena such as soil transport (piping).

The engineer should attempt to assess the importance of several variables prior to design:

- (1) The rate of excavation and total time for which the design support system is to be in service (i.e. temporary or permanent).
- (2) The character of altered groundwater conditions due to the imposition of new boundary conditions and groundwater control.
- (3) The changes in total stress distribution due to excavation.
- (4) The effect of excess pore pressure dissipation on the soil strength and deformation parameters.
- (5) The effect of forced delay-(i.e. labor strikes etc).

Although construction time may be accurately estimated for reasonable weather and contractor conditions unforeseen events such as labor strikes may unexpectedly extend construction time and hence influence performance.

Critical excavation events such as placing support or bracing after an excavation stage can be most influenced by such delays. Clough & Davidson (1977) report one case where a final phase of construction (just prior to casting and backfilling pile caps and slab) at the bottom of a foundation excavation for a major office building, was

adversely affected by an unexpected delay. The slab was to be used to support raker bracing for the sheet pile wall. A carpenter strike delayed pile cap formwork for six days during which the excavation stayed open and the walls crept inward. After 20 centimeters of movement had occurred some remedial support was applied by temporary filling of the pile cap excavation to retard further movement. Eventually over 30 centimeters of wall movement occurred. A large crack appeared behind the wall. Figure 1.1 shows movement versus time and the pertinent events for this excavation.

Corbet, Davies and Langford (1974) reported on a braced excavation in stiff London Clay where a national building workers strike led to delay of a critical period in the excavation. Although the specific results of this delay are not reported, the authors state that the delay was a cause of concern for the stability of the excavation.

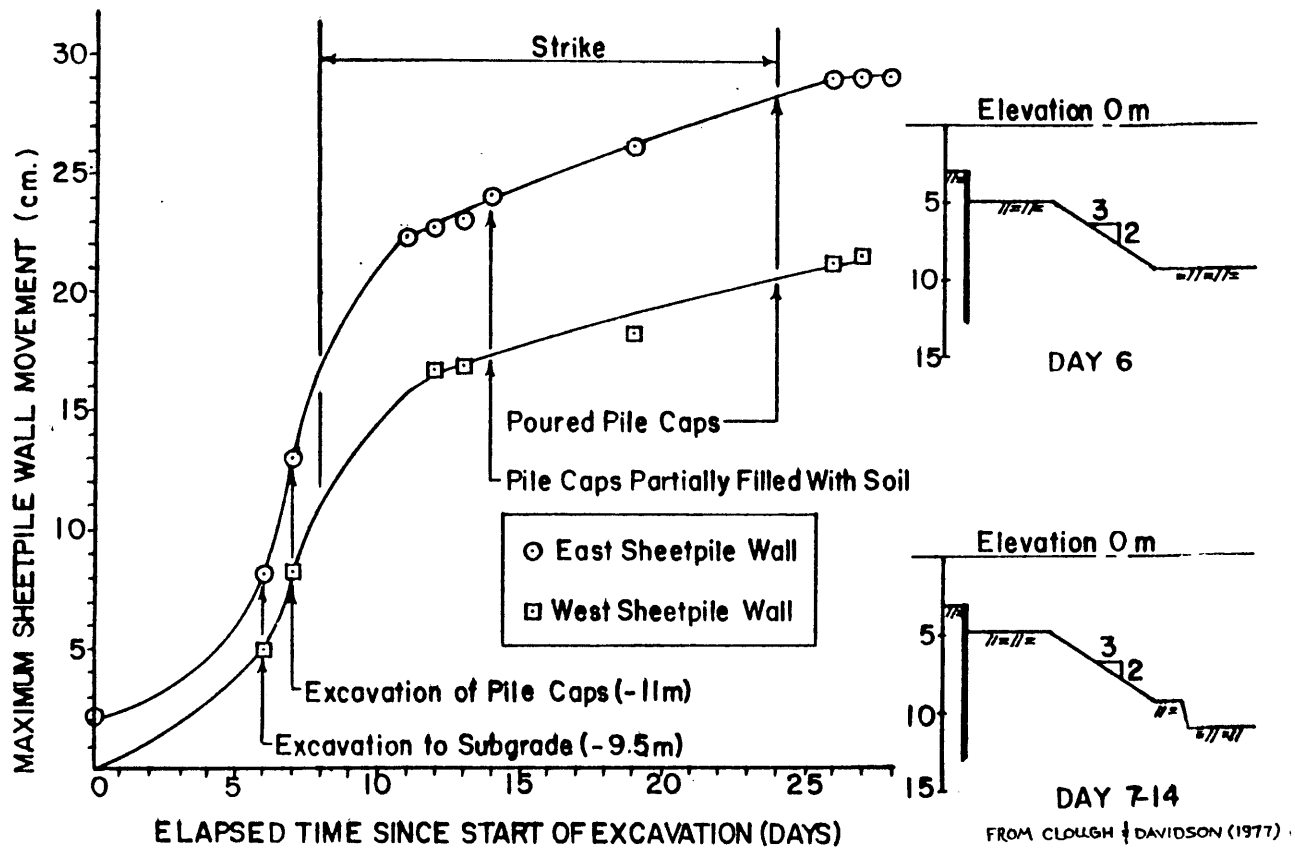
It is apparent to the author that the profession would benefit from additional research and measurements of excavation performance vs. time. The behavior of excavations penetrating intermediate soils between the clay and sand types such as silts, clayey silts and clayey sands etc. are of particular interest. The demand for the engineer to design with economy and safety warrant a better understanding of the role of time and drainage on behavior of soil subject to excavation unloading.

1.1 THESIS OBJECTIVE

The objective of this thesis is to formulate and apply a method which includes the effects of pore pressure change with time to predict deformations of an excavation.

1.2 THESIS SCOPE

Following the discussion of the effect of time for several simple cases, the significance of measurements made over time for several braced excavations will be discussed. Several current design and analysis approaches will be discussed. A Stress Path Method approach will be outlined and applied for a type A prediction of a case study. This method will include a composite of finite element analysis, and stress path testing of soil specimens in the lab to predict the role of time in the study of a deep braced excavation.



EFFECT OF FORCED DELAY ON A CRITICAL CONSTRUCTION EVENT

FIG. 1.1

CHAPTER TWO

THE ROLE OF TIME2.0 INTRODUCTION

In this chapter the effect of time on strength and deformation for several simple examples will be discussed to outline the importance of excess pore pressure dissipation for braced excavations. Related observations and measurements of pressure and time from the literature will be discussed. Various current methods of analysis and design will be reviewed on the basis of how the methods incorporate time effects. Limitations and assumptions made for each method are discussed.

2.1 STRESS PATHS

Use of stress paths and the Stress Path Method (Lambe 1967, Lambe & Marr 1979) provides an organized framework within which the field problem can be studied. Stress paths for field situations can be modeled using standard laboratory tests, such as the three dimensional triaxial test.

2.1.1 Undrained Shear

At this point it is convenient to refer to Figures 2.1.1 and 2.1.2 constructed by the writer. Shown in the figures are an example of braced excavation geometry and total and effective stress paths for normally and overconsolidated clay soil elements adjacent to the excavation.

The total stress paths between points 1A and 1B and between 2A and 2B represent the type of unloading typically experienced by soil elements 1 and 2. The mode of total stress change for element 2 at the center line of the excavation is extension unloading. Soil element 1 behind the wall experiences compression unloading or an "active" stress condition.

Typical effective stress paths for the undrained shear can be traced between points 1A and 1C and points 2A and 2C on each p-q plot. The horizontal width of the shaded area at any given value of q is the value of excess pore pressure generated by shear.

The shaded region also represents the region within which the effective stress paths lie for partially drained conditions. There are an infinite number of possible effective stress paths in this region. Rapid excavation in a material such as silt for example, may exhibit partially drained behavior.

2.1.2 Dissipation Of Pore Pressure Following Shear

Strength and stress-strain modulus of the soil are dependent on the effective stress path. Since changes in pore pressure directly affect the effective stress path, these changes are important in the field and when estimating soil parameters for design.

Figure 2.1.3a-d shows stress paths for the example geometry of Figure 2.1.1 for typical overconsolidated and

normally consolidated clays. The plots in the figure exhibit a range of situations bracketing the type of pore pressure behavior likely to occur during and after excavation to the design depth. A simplifying assumption is made in order to draw these plots; undrained shear due to excavation occurs first and then is followed by dissipation of excess pore pressure.

Excess pore pressure results from the total stress release due to excavation and/or from decrease in pore pressure due to altered flow conditions (i.e. construction dewatering). With respect to dissipation of excess pore pressures the following qualitative conclusions can be made after construction of the Figure 2.1.3 plots:

Normally Consolidated Clay

- (1) 2.1.3a--This soil will undergo a minor decrease in strength (i.e. move towards the failure envelope) following dissipation of excess pore pressure to the original pore water pressure. This occurs at both the bottom of the excavation and behind the excavation wall. Consolidation heave will occur.
- (2) 2.1.3b-- Consolidation due to dissipation of positive excess pore pressure caused by dewatering will result in settlement. The soil will experience an increase in strength with consolidation. Net vertical strain will be higher with dewatering for element 1 due to additional compressive strains at

constant shear stress. However the net vertical strain for element 2 will be less than the strain associated with no dewatering. If two dimensional steady state flow conditions are attained the steady-state pore pressure can be determined from a flow net. Although it may be unlikely that full steady state flow conditions will be reached, this condition represents an outside bound.

- (3) 2.1.3c--For an increasing over consolidation ratio the effective stress path will shift to the right due to the generation of large negative excess pore pressures. Subsequent consolidation will result in a substantial decrease in strength and a consolidation heave.
- (4) 2.1.3d--If the absolute value of change in pore pressure due to altered flow conditions is equal to or greater than the absolute value of the excess pore pressure due to shear, the strength will increase. Otherwise the strength will decrease with time.

For a given excavation with excess pore pressures generated by shear and dewatering the net excess pore pressure can be estimated by super-imposing or adding the two. Lambe (1968) discusses this. Figure 2.1.4 schematically illustrates the procedure for simplifying the field situation.

2.1.3 Stress Paths---Summary

The use of stress paths to illustrate the various possibilities assists the engineer in his judgement. Qualitatively the pore pressure-strength-strain relation is clarified in one's mind. Similarly Henkel (1970) uses stress paths to illustrate active and passive earth pressures for excavation in normally and highly overconsolidated clays. For comparison, several of Henkel's plots are reproduced in Figure 2.1.5 showing a slightly different graphical portrayal of stress paths. Henkel recognizes the utility in applying this type of approach as an aid to the engineer in his understanding of how a given excavation may behave.

2.2 THE PERFORMANCE OF BRACED EXCAVATIONS VS. TIME

Cohesive soils are assigned low permeabilities compared to cohesionless soils which have high permeabilities. In general for the time associated with most construction projects involving loading or unloading of the soil or changes in flow conditions, some degree of drainage occurs in cohesive soils. For sands the condition of full drainage is achieved rapidly.

2.2.1 Braced Excavations In Cohesionless Sand

For excavations in sand deposits steady-state seepage conditions are achieved rapidly. Figure 2.2.1 shows stress paths illustrating this behavior. Since sand has a relatively high permeability pore pressure dissipation is virtually instantaneous. The total stress path equals the

effective stress path and the steady state pore pressure can be obtained from a flow net. Therefore time does not play a significant role. Although the following two sections are not specifically bound to the thesis objective, they serve to illustrate the different type of role time plays in the excavation in cohesionless soil (vs. cohesive soil).

2.2.2 Piping, Suffosion

Where silts and sands or gravels, are present, time plays a role with respect to migration or erosion of soil particles via high seepage gradients into the excavation. This migration is referred to as piping or suffosion. Figure 2.2.2 graphically illustrates the mechanisms responsible for suffosion and/or piping. Peck (1969) points out that inadequate groundwater control may lead to damaging settlements resulting from migration of sand into the cut. Over a period of time migration of silt size particles can clog construction dewatering wells and render them ineffective. Particles can also be piped through cracks or holes in a sheet pile wall. Serious conditions can be anticipated by field monitoring of flow into and out (pump effluent) of the excavation for the presence of suspended soil particles. Also at the bottom of the excavation piping failure by heave may occur. The mechanics of this phenomena were elucidated by Terzaghi (1942) and discussed by Terzaghi & Peck (1967) and D'Appolonia (1971).

2.2.3 Effects of Frost Action

Field observations have shown the effect of frost action

to be substantial. Several cases show the loads in the struts may increase several fold. Pappas & Sevsmith¹ monitored performance of a deep braced cofferdam in sensitive Leda clay. Abnormally large increases in strut load were detected during December excavation. Since heating of the adjacent soil resulted in rapid load reduction, the problem was concluded to be one of frost action.

DiBiagio & Bjerrum (1956) observed after ground freezing within and at the surface of an excavation trench, decreases in load in the uppermost struts, and severe increases in the lower bracing levels buckling some of the walers and struts. Although reliable deformation measurements were not available, visual observations led to the conclusion that an upward expansion of the soil during freezing caused the unusual changes in distribution of pressure. Figure 2.2.3 shows the dramatic time vs. strut load behavior.

Terzaghi & Peck (1967) report that braced cuts in Oslo & Chicago were subjected to below freezing weather. They observed earth pressures climb to magnitudes several times greater than those prior to freezing.

Ground freezing as these cases illustrate can result in unpredictable and radical behavior. Since the formation of frost lenses is time dependent, the potential for damage can be anticipated by monitoring the wall movements and strut loads.

¹ Refer to Clough and Davidson (1977)

2.2.4 Braced Excavations In Normally Consolidated Clay

For clays one expects a soft normally consolidated clay to have a lower coefficient of consolidation than an overconsolidated clay since this value is generally found to be higher in recompression than in primary consolidation as shown in Figure 2.2.4 for a varved clay. We would therefore expect soft clay to dissipate excess pore pressures at a slower rate.

At least one braced excavation case illustrates that for normally consolidated clay the ideal undrained condition is not sustained over the course of time for a temporary excavation. DiBiagio and Roti (1972) measured the magnitude of total earth pressure, pore pressure and deformations of a braced slurry-trench wall in a soft clay in Oslo. Below the clay the wall was keyed into a pervious bedrock. Measurements were made before, during and after excavation. Figure 2.2.5 shows the soil profile and geometry of the excavation as well as the instrumentation layout. Instrumentation included fifteen earth pressure cells and two piezometers.

The measurements during the excavation stages shown in Figure 2.2.6 indicate only minor decreases in pore pressure occurred until the excavation approached bedrock and groundwater control was facilitated through this layer. Consequently, the pore pressure at the bottom of the clay was significantly reduced, accompanied by a marked reduction in total earth pressure on the wall. The excavation remained open to this depth for approximately 200 days. A

downward gradient in the clay contributed to consolidation settlements during this period before the "sealing" of the excavation bottom with the construction of a base slab. The pore pressure built up steadily from this point on decreasing the rate of settlement and increasing the total earth pressure back towards its initial value.

Over the course of the construction of this excavation the total earth pressure varied dramatically due primarily to changes in pore pressures. For the center of the clay layer, piezometer PZ-9 shows a small decrease in pore pressure over the time of construction. Coupled with the fact that the location of the resultant earth force moved upward towards the center of the layer with time, this writer concludes that this central point of the soft clay behaved partially drained. As a practical matter, in this specific zone the undrained assumption may be reasonable. However, looking at the clay mass as a whole the assumption is not correct as piezometer PZ-8 clearly shows. After careful study, the writer concludes that because the decrease in pore pressure in PZ-9 occurred before dewatering and remained relatively constant, dewatering did not significantly affect the center of the clay and the negative increment of pore pressure was due solely to changes in total stress. Conversely the lower portion of the clay layer shows the effect of both changes in total stress and changes in flow conditions.

Although admittedly this is only one case, it illustrates that pore pressure dissipation can be a factor even for impervious walls in soft clay. Dissipation of positive excess pore pressures resulting from dewatering can lead to large pressure decreases against the wall during construction. More rapid dissipation of excess pore pressures can be expected for sheet pile and other non-slurry-trench walls which are characteristically more permeable.

2.2.5 Braced Excavation In Overconsolidated Clay

Some interesting conclusions from field data suggest the undrained assumption to be seriously in error for the overconsolidated clay.

Referring now to Figure 2.2.7, Lambe (1968) observed piezometer readings from the medium clay layer at the bottom of a temporary braced excavation for the CAES building foundation at MIT. The excavation was open for 24 days. Very little dewatering was attempted in this excavation. The stress paths for a point at piezometer P-1 are reproduced in the figure. Note that u_0 , is the pore pressure immediately after excavation. Thereafter the pore pressure increased to a value greater than u_0 but still less than u_s (the pre-excavation static porewater pressure). The dissipation of negative excess pore pressure moves the effective stress path towards failure and results in a consolidation heave. It follows as Lambe concludes that there is a progressive decrease in strength leading to a decreasing factor of

safety with time. Therefore the end of the unloading period is the most critical time for this excavation. The end of the unloading period is defined as just before the load is replaced in the excavation. Hence, the most critical condition occurs some time after completion of the excavation.

Observations and measurements were made for braced slurry-trench and sheet pile walls in stiff clay for a subway excavation in Boston (see Figure 2.2.8). Pore pressures, deformations and strut loads were measured. Figure 2.2.9 shows a redrawn compilation of strut load and pore pressure versus time for a test cross section at the slurry wall. Observations of piezometers indicate excavation was accompanied by steady decreases in water pressure behind the wall from an initial total head of 106 feet decreasing to 82 feet measured in piezometer P-4 behind the wall after the final cut had been made. Following mud slab placement, axial strut loads increased steadily as did pore water pressure measured in the piezometer P-4 as shown in the figure. Since measurements showed very little outward wall movement (less than 1 inch) the change in pore water pressure can be associated with altered flow conditions resulting from construction. Seepage through wall panel joints was observed. Figure 2.2.10 shows measured pore pressure vs. depth. Steady state seepage predictions compared well with end of construction pore pressure measurements. Hence, it can be argued that the

drained parameters, \bar{c} and $\bar{\phi}$ are more applicable for this "end of construction" case.

In contrast to the slurry wall case in the soft clay in Oslo, pore pressures throughout the stiff clay drop significantly. Imposition of new boundary water pressure conditions are met with a relatively quick drainage. Also the strut loads at the end of excavation do not accurately reflect the strut loads which the bracing will experience over the life of the structure. The trend in the figure shows an increase in strut load by a factor of approximately 1.5. Similar trends are seen in adjacent struts.

2.2.6 Braced Excavation In Stiff Fissured Clay

One interesting case for excavation in this type of soil is the experimental trench in stiff marine clay Bjerrum & DiBiagio (1956) studied. Figure 2.2.11 shows a section of the excavation, corresponding soil profile and test data. Strut loads during the Autumn (Sept. to mid Nov.) show a gradual and marked increase followed by enormous winter load increases attributed to frost action and previously discussed in section 2.2.3 (see also Figure 2.2.3). Autumn rainfall data compared to the total earth pressure show sharp load increases following periods of rainfall. The most intense period of rainfall is followed by the maximum value of pore pressure observed for Autumn in mid November. Pore pressures plotted in Figure 2.2.11 show the measured pore pressure versus time over this period. The fissures in the clay facilitate access of water to the clay mass. Total

stress release from excavation in fissured and weathered clays can lead to further opening of the fissures and increases in permeability. Prolonged construction under such conditions leads to progressive weakening or softening, as well as increases in the susceptibility of the soil to rapid changes in pore pressure.

The effect of fissuring on stability is dramatically illustrated by the short term slip failure of an unsupported excavation in London Clay reported by Skempton and LaRochelle (1965). The results of this study lend understanding to braced excavation in stiff fissured clay as well. The slip occurred shortly after excavation had been completed. The estimated mobilized shear strength in the clay mass was approximately 55% of the average undrained strengths measured from triaxial tests. The authors attributed the difference between the measured strengths in the triaxial tests and the actual failure to (1) pore pressure migration within the intact clay, and (2) fissuring. It was shown that by increasing the time to failure for the triaxial tests, strength decreased. Conventional tests run at a time to failure of 15 minutes correspond to strain rates much higher than and unrepresentative of the strain rate due to excavation. This influence of strain rate on strength is attributed to pore pressure migration. Figure 2.2.12 shows the results of strength versus time to failure for a series of undrained triaxial tests performed to study this behavior. Secondly,

the authors conclude that at least five factors related to the fissuring can weaken the clay during excavation. Several of the important factors are, absorption of water along fissures leading to increases in water content (softening), reduction of strength to zero as fissures open, and progressive failure.

Quantifying the effect of fissures and the rate of softening on stability and deformation to predict performance is difficult.

Corbet et al (1974), and Cole and Burland both reported observations made for a raker braced diaphragm wall in a 20 meter deep excavation for a basement in stiff fissured London Clay. In view of the uncertainties cited in the previous paragraph, detailed construction performance monitoring was undertaken. Wall movement and verticality were monitored. Earth pressure however, was not monitored. Several of the conclusions drawn by the authors after observing the construction performance are reiterated below.

- (1) Wall movements showed a clear time dependence.
- (2) Early internal support placement is essential to minimize movements.
- (3) Performance monitoring is important for construction control and is of research value for future excavations.
- (4) Inward wall movement is associated with a progressive softening and reduction in stiffness of the clay. The greatest reduction in stiff-

ness was found to be near the ground surface behind the wall. This is attributed to the opening of fissures due to lateral stress release.

In summary, one can clearly see that time is a very significant factor for load and deformation behavior of excavation in stiff fissured clay. Although additional observations and measurements of field situations are needed to advance our understanding of this case we can make several conclusions of practical value at this time. The undrained assumption is not applicable to excavations in stiff fissured clay which remain open for several months, construction performance monitoring is important and is recommended, and minimizing construction time is desirable.

2.2.7 Braced Excavation in Silt

Very little well documented information on excavation performance in silt has been reported in the literature. Lambe (1969), et al, and MIT (1972) reported on a study of two instrumented Boston subway cuts in fill overlying organic silt, underlain by glacial till as seen in Figure 2.2.13. The test sections, Section A and Section B were monitored for stresses and deformation and compared against predicted behavior. No significant strut load variation with time was measured. However, one conclusion reached in the studies was that for braced excavation in sands and silts the pore pressure behind the excavation can be expected to be less than static due to construction. Some agreement between the final measured pore pressures and

steady state pore pressures predicted by finite element analysis (FEDAR, Taylor and Brown 1967) indicates the pore pressure in the silt was probably in a transient state near steady state. See Figure 2.2.14.

Although these two test sections penetrate silt, soil conditions are not truly representative of an excavation in silt due to the upper fill and stiff lower strata. Therefore general conclusions by the writer regarding excavation in silt cannot be made. However the cases are representative of the fact that many excavations do penetrate several soil types and cannot be easily categorized.

These studies are valuable case histories. They illustrate the type of construction monitoring data which predictions of construction performance can be evaluated from. As a result, our understanding of braced excavations can be extended. The reader is referred to the references for additional details. Use of finite element computer programs like BRACE and FEDAR to model braced excavation and flow respectively showed encouraging predictive capabilities.

2.3 METHODS OF ANALYSIS AND DESIGN

The following currently used methods of analysis and design will be discussed as they relate to the incorporation of time effects.

- (1) Semi-empirical Methods
- (2) Numerical Analysis Methods
- (3) The Stress Path Method

2.3.1 Semi-empirical Methods

Several well known semi-empirical design methods are the:

- (1) Terzaghi and Peck Method (1948, 1967)
- (2) Tschebotarioff Method (1973)
- (3) DM-7 (Navdocks) Method (1971)

These methods are similar and are commonly used in practice. They are intended to estimate maximum lateral strut loads. Only the Terzaghi and Peck Method (1967) will be discussed to illustrate this design approach.

Terzaghi and Peck presented the original apparent pressure envelopes in 1948 for braced excavations in sand or in clay. Peck, Hansen & Thornburn (1974) is the most recent published version. The design envelopes were derived from classical earth pressure theory and actual measurements of strut loads in excavations. Hence the method is referred to as semiempirical. Difficulty in reliably measuring stresses against the sheeting required the apparent stress distribution to be inferred or backfigured from the strut loads. The envelopes are intended to give maximum values of strut load to be experienced and are not truly representative of the actual stress distribution. Over the years modifications and adjustments have been made to accomodate newer observations and experience. Figures 2.3.1a and 2.3.1b show the design envelopes of the Terzaghi and Peck Method for sand and clay.

The pressure envelope for sand is based in part on strut load measurements for braced excavations in New York,

Munich, and Berlin. An equivalent uniform earth pressure was fit through the apparent pressures in the excavation. Several qualifications attend the application of this method for sand.

- (1) The authors emphasize that the diagram has been developed from a limited number of excavations varying in depth from 28' to 40'.
- (2) The diagram is a pressure distribution for estimating the maximum values of strut loads to be expected for similar cuts.
- (3) The groundwater level is assumed to be below the bottom of the cut. Consequently, (in the writer's opinion), seepage or static water pressures should be added to the pressure distribution. Ries (1973) points out that for impervious diaphragm type walls which typically retard drainage of the soil behind the wall, this assumption (water level below cut) is likely to be seriously in error.

For sands detrimental time related effects have been associated with piping and piping heave at the bottom of the excavation. This problem cannot simply be incorporated into any pressure envelope. Application of the Terzaghi and Peck method for sands must accompany an awareness of such conditions. Also, in the writer's opinion the groundwater pressures which may be experienced over the life of the structure should be added especially since these pressures can be substantial.

Several relevant facts one should be aware of when using the clay envelopes of the Terzaghi and Peck method are summarized below.

- (1) Cuts are assumed to be temporary. The " $\bar{\sigma} = 0$ " condition or undrained condition is assumed to prevail. Average undrained strength of the clay along the side the cut is used.
- (2) Although the data from the test cuts (Oslo and Chicago) from which the envelopes evolved included measurements showing large increases in strut load due to freezing during cold weather, these measurements were not used for formulation of the envelopes. Therefore the effects of freezing should be considered separately.
- (3) The authors (1967) admit that due to little available data on cuts in stiff intact clays, sandy clays, and clayey sands etc., design envelopes have yet to be worked out. However more recently, Peck (1969) reports that the trapezoidal clay envelope fit the measured values of five cuts in stiff clay conservatively and therefore could be used as a guideline. Peck suggests that limited data for at least one deep cut in dense clayey sand and stiff sandy clay shows drained behavior and the appropriate drained strength parameters can be input into an equation for K_a . Presumably, the equation for earth pressure for excavation in sand

is then modified to include this expression.

- (4) Use of the trapezoidal envelope for stiff fissured clay is discussed by the authors (Terzaghi and Peck 1967, Peck 1969) in light of the measurements made by DiBiagio and Bjerrum (1957) which showed time dependent behavior. This case has been discussed by the writer in earlier sections of this paper. The authors suggested that the lower value for maximum design pressure, $.2\sigma'_H$ be used if movements of the sheeting are minimal and construction time is short. If these conditions do not apply, use of the higher pressure value of $.4\sigma'_H$ is recommended. Hence Terzaghi and Peck, in an indirect way have assigned some importance to time effects for stiff fissured clay.

In summary, it is the writer's opinion that these methods provide a useful guideline for estimating maximum strut loads. The method has been tempered with experience although to extend the scope of the Terzaghi and Peck method more experience for a large variety of cuts is required. The limitations of the method should be realized and may be understood by studying the evolution of its formulation. Major braced cuts open for extended periods should not be designed on the basis of this method alone. The engineer's understanding of the excavation problem may benefit by using other more fundamental techniques.

2.3.2 Finite Element Analysis

Over recent years the advent of the high speed digital computer has enabled numerical analysis to become a popular and viable technique for solving complex engineering problems. The use of the electronic computer to solve large sets of equations by matrix algebra allows the engineer to mathematically model problems in detail. Previously such sets of equations could be set up but the solution was too complicated to achieve practically by hand.

Application and theory of the Finite Element Method is now well documented in the literature (Desai and Abel 1972, Zienkiewicz 1967, Bathe and Wilson 1976) for engineering analysis. Subsequently, over the last decade several finite element computer programs to model construction of braced excavations have been developed and used by several investigators including Wong (1971), Jaworski (1973) and Clough and Duncan (1971).

Advantages of using this technique include:

- (1) Complex soil and structure geometries and properties can be modeled.
- (2) Construction sequence and details can be simulated.
- (3) Detailed information on stress changes and deformations can be obtained.
- (4) Parameter studies can reveal the relative importance of input data (strengths, moduli, sheeting stiffness and penetration etc.) for a given excavation.
- (5) Critical stages of excavation can be predicted.

Some limitations have yet to be overcome. One such limitation lies in the difficulty in modeling the soil structure interaction (i.e., soil sheeting interface). Nevertheless, even in the relatively young stage of development for finite element modeling of excavation, encouraging results and insights have been gained. Indeed, in practice, MIT (1972), Cole and Burland (1972), Palmer and Kenney (1972), Clough and Tsui (1974), Duncan and Chang (1970), and others have demonstrated the powerful applicability of the method.

The finite element program developed at MIT for analysis of excavation is called BRACE. The reader is referred to the theses by Wong (1971) and Jaworski (1973) for details. The program in its present form will model the stress strain behavior of the soil via a linear or bi-linearly elastic modulus. The program does not model the effects of time on strength, modulus, loads or deformations. If necessary, these effects must be indirectly considered by inputting soil parameters which include the effect of time (e.g., pore pressure dissipation). Conventional soil parameter input for such a program is the undrained soil strength and undrained modulus to model the undrained case (total stress analysis) or drained parameters, \bar{c} and $\bar{\phi}$ for the drained case (effective stress analysis).

Pore Pressure Dissipation

Recently, new insight into the evaluation of the validity of the undrained assumption and total stress

analysis for excavation has been presented by Clough and Osaimi (1979). The authors used the finite element technique to model excavation sequence for given rates of excavation (meters per day). The purpose of the study was to show how pore pressure dissipation occurs during and after excavation. The name of this computer program is TIME-CONSTRUCT and at this writing is not available for distribution (Clough 1980) since its documentation is not complete. In any event, the published results by the authors are of interest to the engineer and will be discussed in the following paragraphs.

Using TIME-CONSTRUCT Clough and Osaimi analyzed several cases. Results of the analysis of a one dimensional excavation are shown in Figure 2.3.2. For wide excavation the one dimensional unloading and drainage represent the central portion of the bottom of the cut. The figure shows that decreasing the excavation rate corresponds to an increase in the percentage of consolidation at the end of construction for the wide range of permeabilities analysed.

Figures 2.3.3a and b summarize the analysis results for two dimensional excavation for cases of both linear and nonlinear soil behavior. Contours of negative excess pore pressure shown indicate that the pore pressure response at the bottom of the excavation is essentially one dimensional. Dissipation of the excess pore pressures will occur vertically. Of general interest, in Figure 2.3.3a contours of negative excess pore pressure for no wall in

place are shown for comparison with the supported excavation in the linearly behaving soil. As would be expected the presence of an impervious wall markedly inhibits consolidation. Therefore we can conclude that for the realistic case of a more pervious wall (sheetpile), the magnitudes of negative excess pore pressure would be at values somewhere between the two cases. In any event more consolidation would occur for the sheet pile wall than for the impermeable type.

Note that this analysis by Clough and Osaimi does not consider the role of drainage due to dewatering which accompanies excavation construction. As a result, the dissipation of excess pore pressures due to shear alone will produce an upward movement of the soil mass behind the wall. Since measurements and observations for many case studies consistently show settlement occurs behind the wall with time, we can conclude for such excavations one or more of the following:

- (1) The dissipation of negative excess pore pressure due to shear behind the wall is negated by equal or larger positive excess pore pressures resulting from dewatering.
- (2) The heave movements are non-existent behind the wall due to greater settlement resulting from inward wall movement and/or loss of ground towards the bottom of the excavation with time.

- (3) Other factors including surcharging by traffic or equipment as Clough & Osaimi suggest.

One important conclusion was drawn by Clough and Osaimi as a result of their study. The undrained, "end of construction" case is unlikely to occur even in thick deposits of low permeability clay. They further note that consolidation in the field is likely to occur more rapidly. This latter conclusion is probably based on the commonly accepted fact that consolidation in the field generally occurs several times more rapidly than predicted by available methods. Extrapolating test results using small specimens in the lab in analyses of the field situation where undetected drainage layers may exist may explain some of the discrepancy.

2.3.3 The Stress Path Method

Lambe's Stress Path Method is a useful method for both understanding and analyzing a given geotechnical engineering problem. Lambe (1967) and Lambe and Marr (1979) describe the fundamentals and applications of this method. By selecting and analyzing representative or "average" soil elements, one can attempt to estimate the stresses and strains that will occur in the field for each phase of construction.

For a supported excavation one can subject representative soil specimens to the in-situ initial stresses, apply the total stress changes associated with excavation and measure the strains, pore pressures (and

hence, effective stresses), and coefficients of consolidation and lateral earth pressure, K_0 .

Of course the method has some limitations one should be aware of. Sample disturbance affects measured values of coefficient of consolidation, strength, and modulus. K_0 determined from reloading to the initial stresses is not truly representative of the initial K_0 in the field. Stress path tests can be both expensive and difficult to run. Many of these limitations however, are present to varying degrees in the other methods available to the geotechnical engineer. The advantages of the method outweigh the limitations, particularly if the engineer is aware of the limitations. The value and the applicability of this method lie in the evaluation of the predicted versus measured performance of actual geotechnical projects.

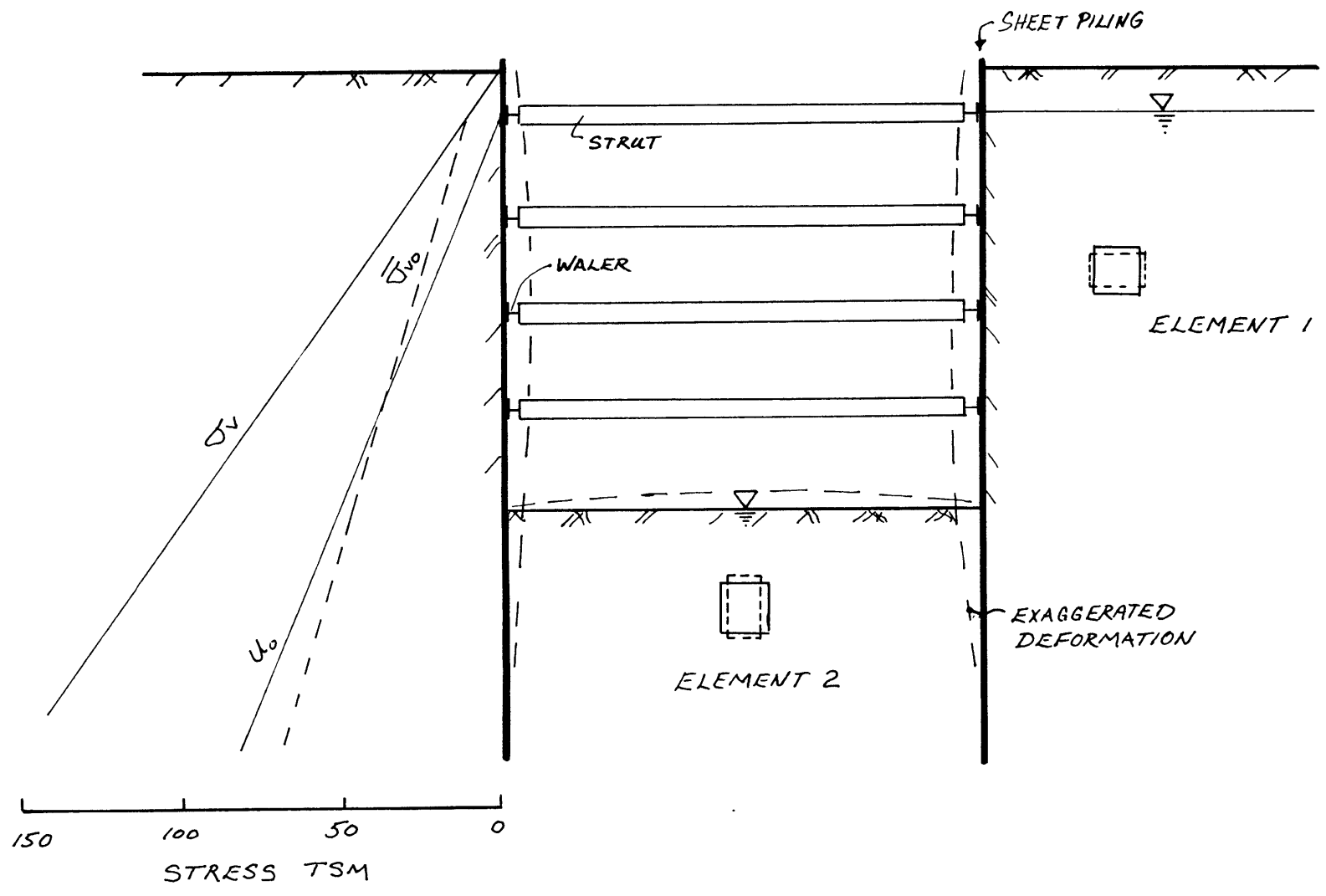
2.4 CONCLUSIONS

The measurements from the case histories cited from the literature show that time effects (pore pressure dissipation) are of significant importance in braced excavation. For cohesive soils partially drained conditions exist during construction and the undrained assumption is only a design simplification which is in error and may be seriously in error in some excavations.

Recent numerical techniques allow analysis which may include the effects of time, but most use linear stress-strain parameters. Other numerical techniques which have non-linear parameter models, are expensive and

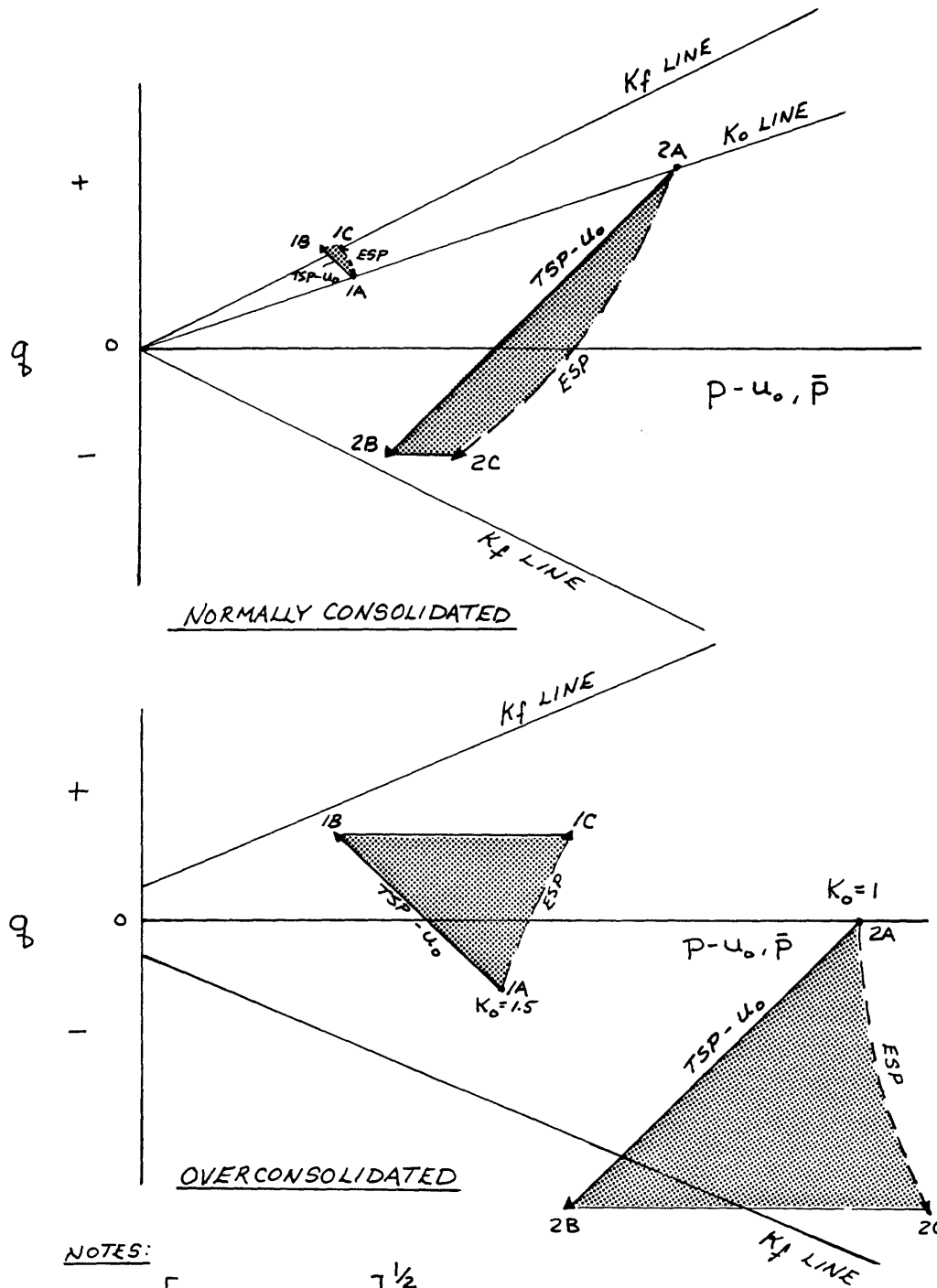
difficult to use and don't consider time effects. Although Clough and Osaimi have developed a computer program (TIME-CONSTRUCT), which considers non-linear and time dependent stress strain behavior, their studies to date have only treated a simple, hypothetical excavation. Nevertheless their work is a significant advance in this area of study. The writer looks forward to an evaluation of predicted versus actual performance of an actual excavation using TIME-CONSTRUCT.

The Stress Path Method provides a rational way to select soil parameters which include time effects. One may combine the Finite Element Method with the Stress Path Method. The powerful numerical technique can be used to model sequential excavation and obtain the complex stress distribution in conjunction with the Stress Path Method used to determine the appropriate soil parameter input. The deformations of an excavation could then be predicted using this fundamental approach.



EXAMPLE BRACED EXCAVATION GEOMETRY

FIG. 2.1.1



NOTES:

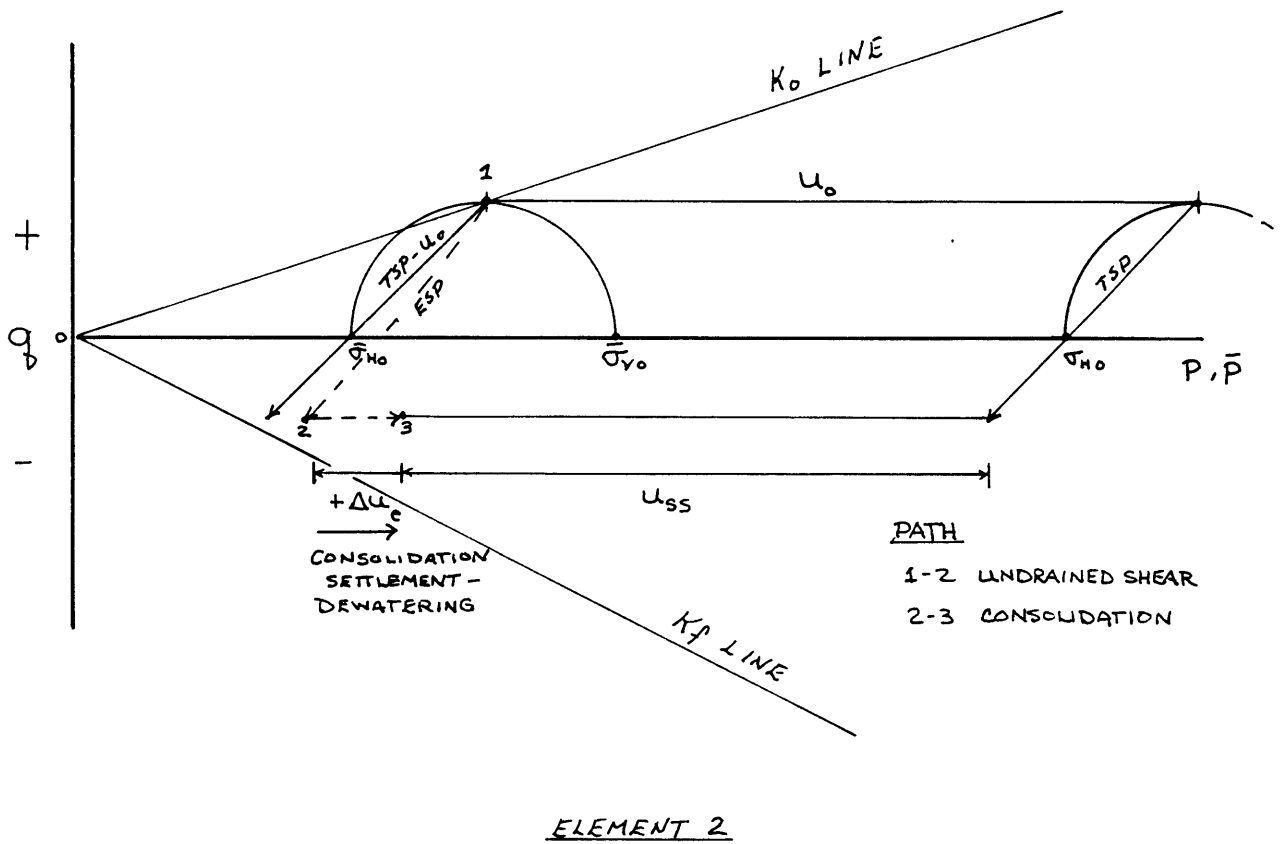
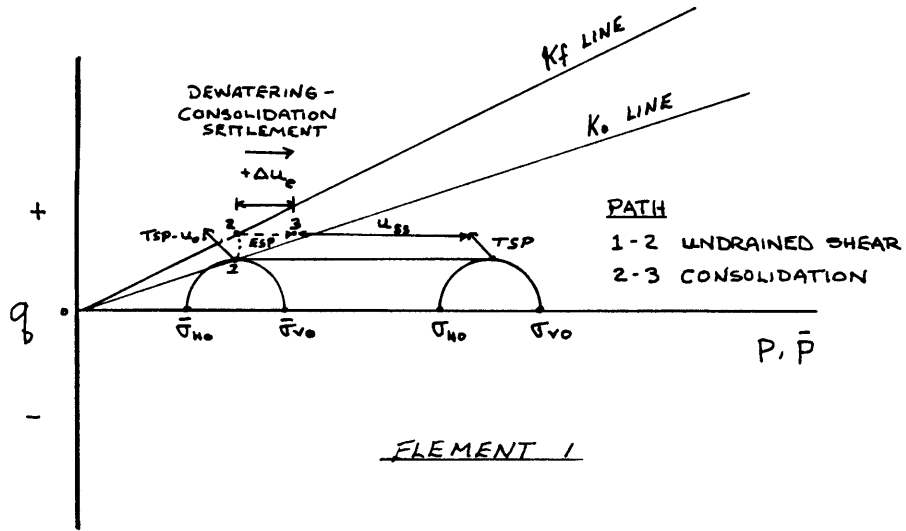
$$q = \left[\left(\frac{\sigma_v - \sigma_H}{2} \right)^2 + \tau_{vH}^2 \right]^{1/2}$$

$$p = \frac{\sigma_v + \sigma_H}{2}$$

$$\bar{p} = \frac{\bar{\sigma}_v + \bar{\sigma}_H}{2}$$

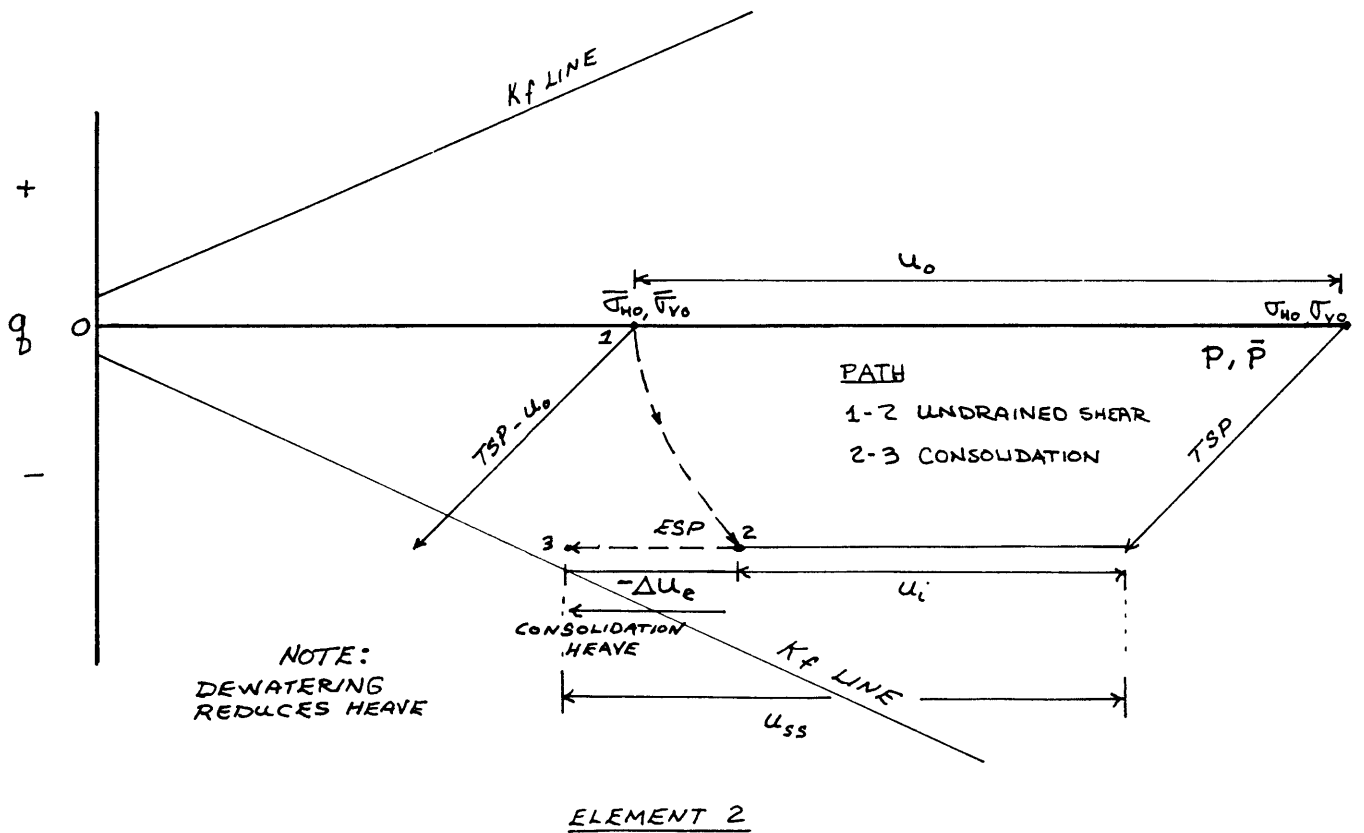
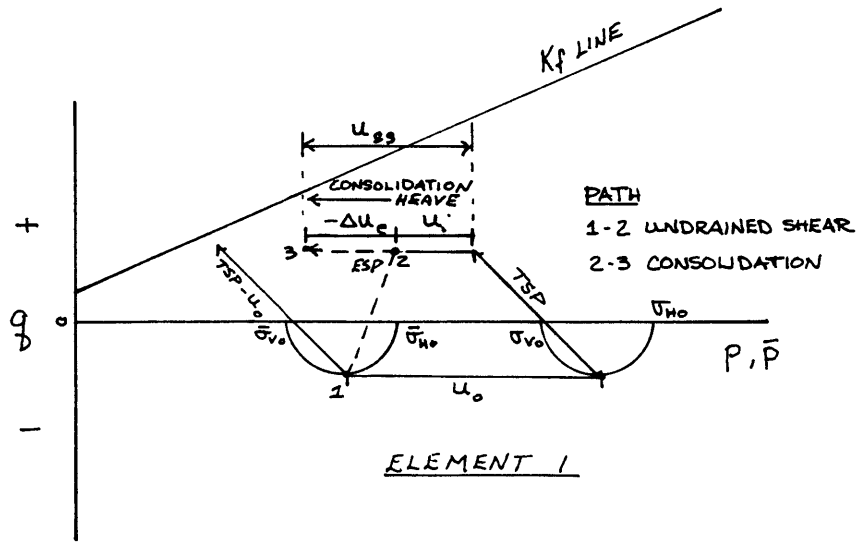
STRESS PATHS FOR UNDRAINED UNLOADING OF NORMALLY AND OVER CONSOLIDATED SOIL ELEMENTS

FIG. 2.1.2



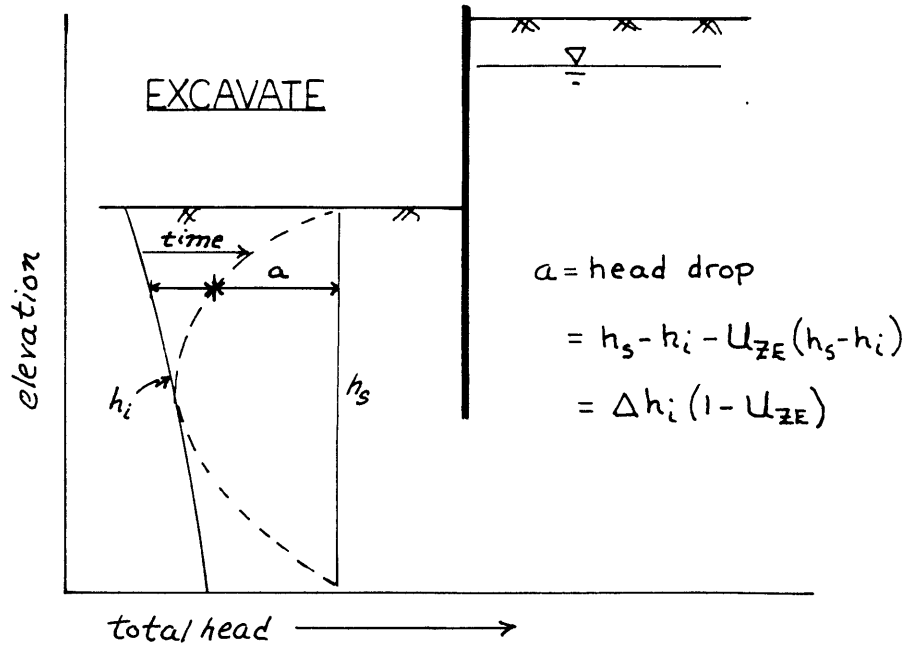
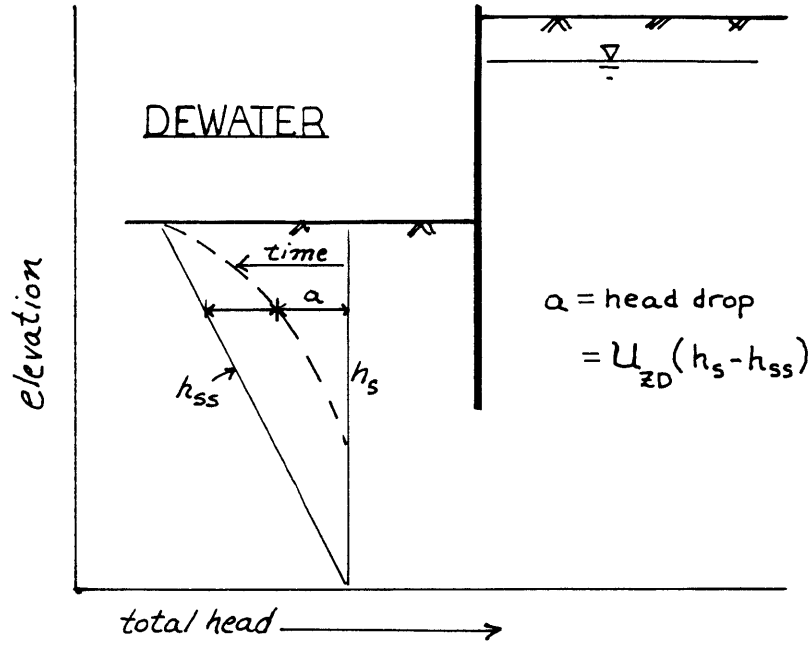
STRESS PATHS FOR UNDRAINED UNLOADING FOLLOWED BY PORE PRESSURE DISSIPATION FOR NORMALLY CONSOLIDATED SOIL-WITH DEWATERING

FIG. 2.13b



STRESS PATHS FOR UNDRAINED UNLOADING FOLLOWED BY PORE PRESSURE DISSIPATION FOR OVERCONSOLIDATED SOIL-WITH DEWATERING

FIG. 2.13d



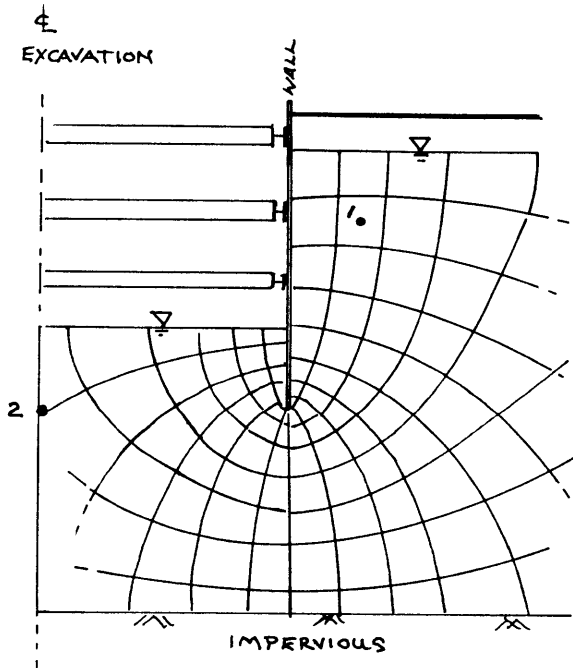
DEWATER + EXCAVATE total head = $h_s - a_{\text{dewater}} - a_{\text{excavate}}$

after Lambe (1968)

DETERMINATION OF TOTAL HEAD SUBJECT

TO EXCAVATION AND/OR DEWATERING

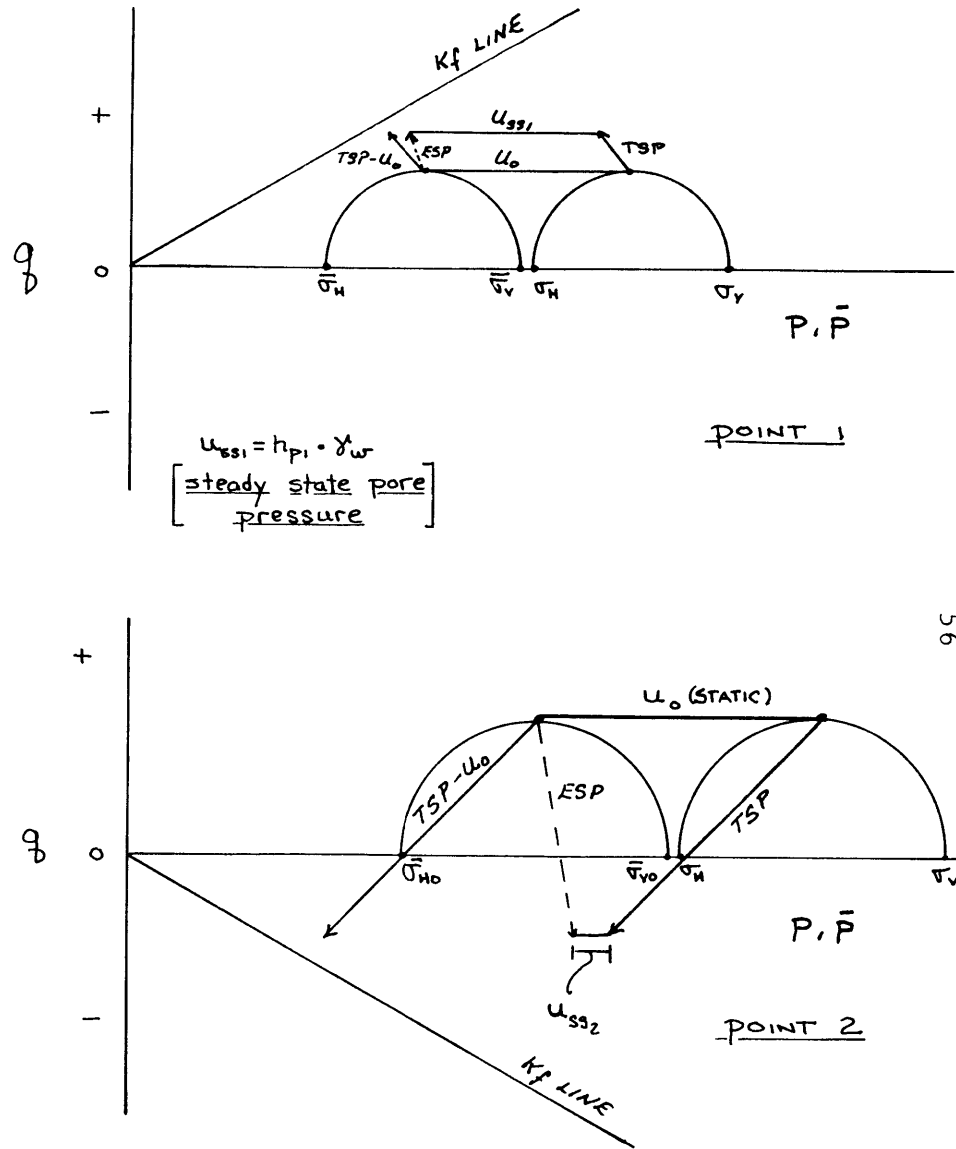
FIG. 2.14



FLOW NET

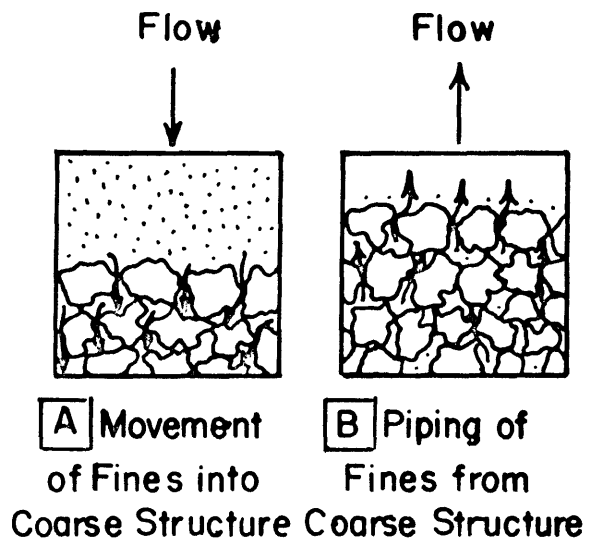
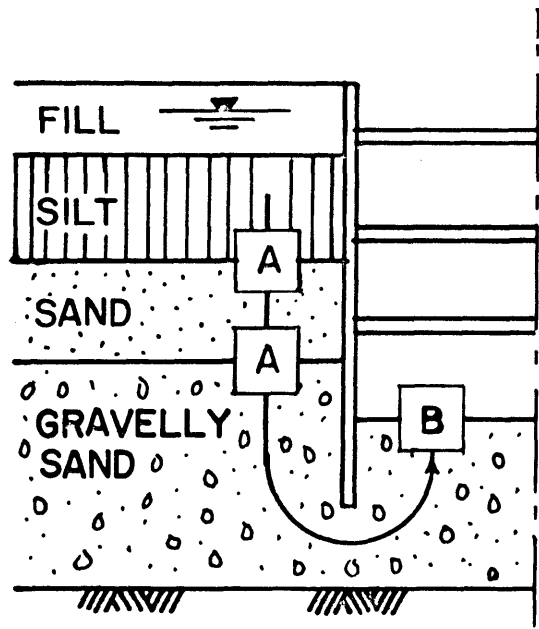
$$h_{p1} = h_t - h_{e1}$$

$$\frac{\text{pressure}}{\text{head}} = \frac{\text{total}}{\text{head}} - \frac{\text{elevation}}{\text{head}}$$



STRESS PATHS FOR EXCAVATION IN COHESIONLESS SAND

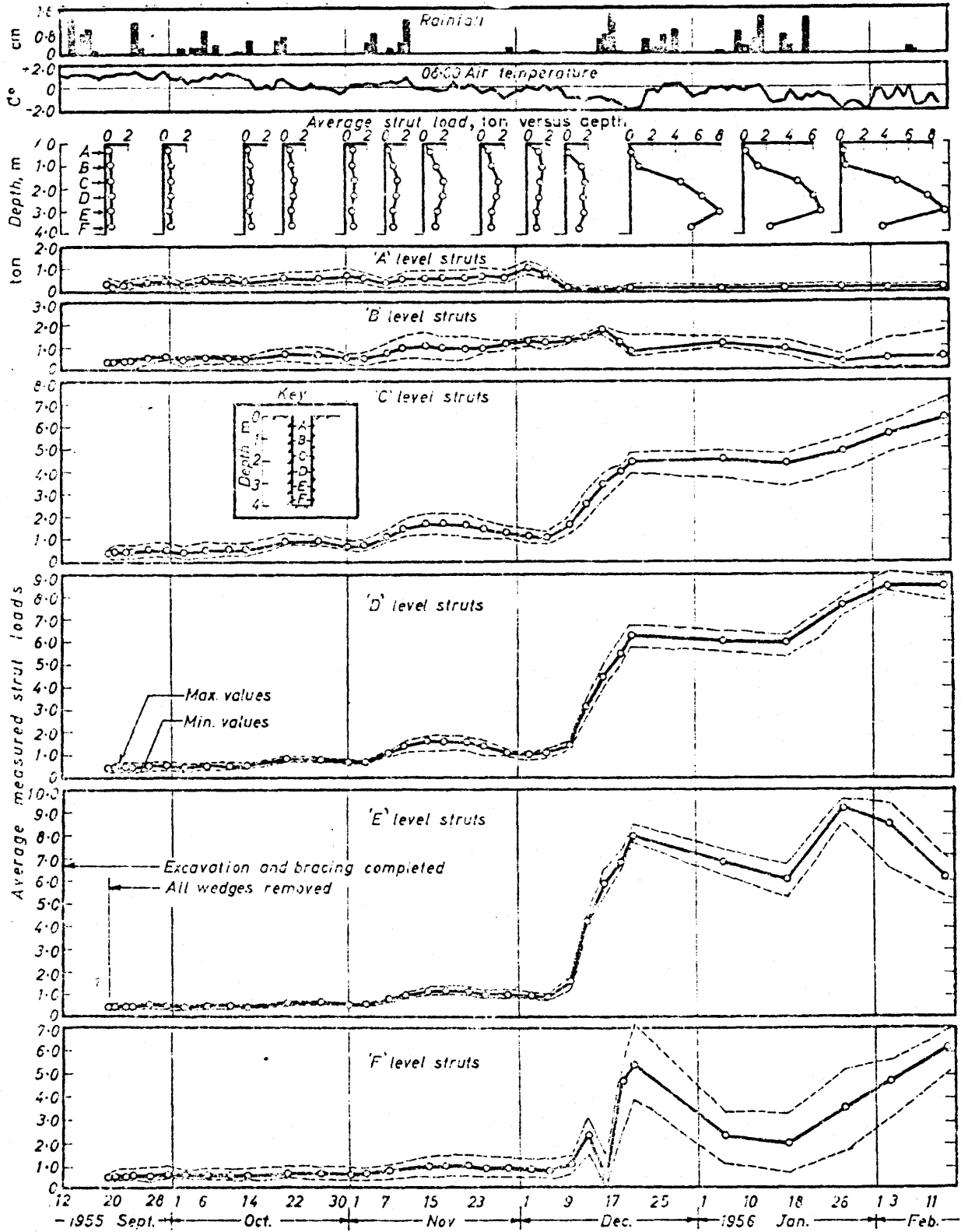
FIG. 2.2.1



FROM CLOUGH & DAVIDSON (1977)

PIPING/SUFFOSION MECHANISMS

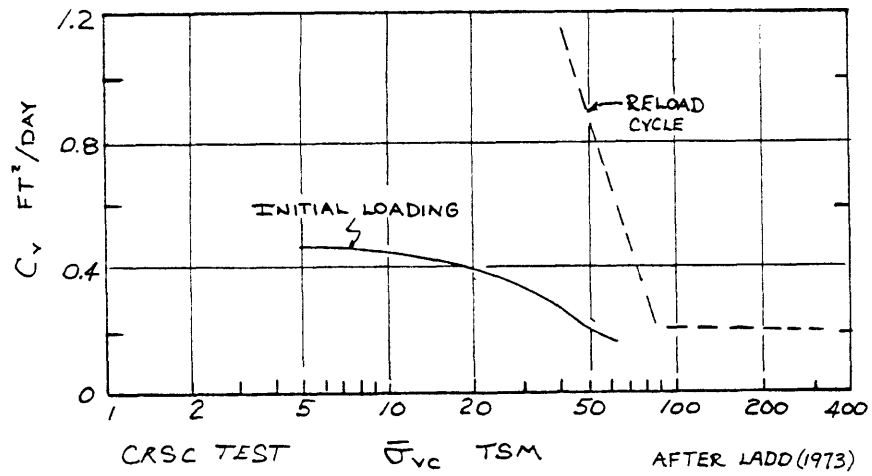
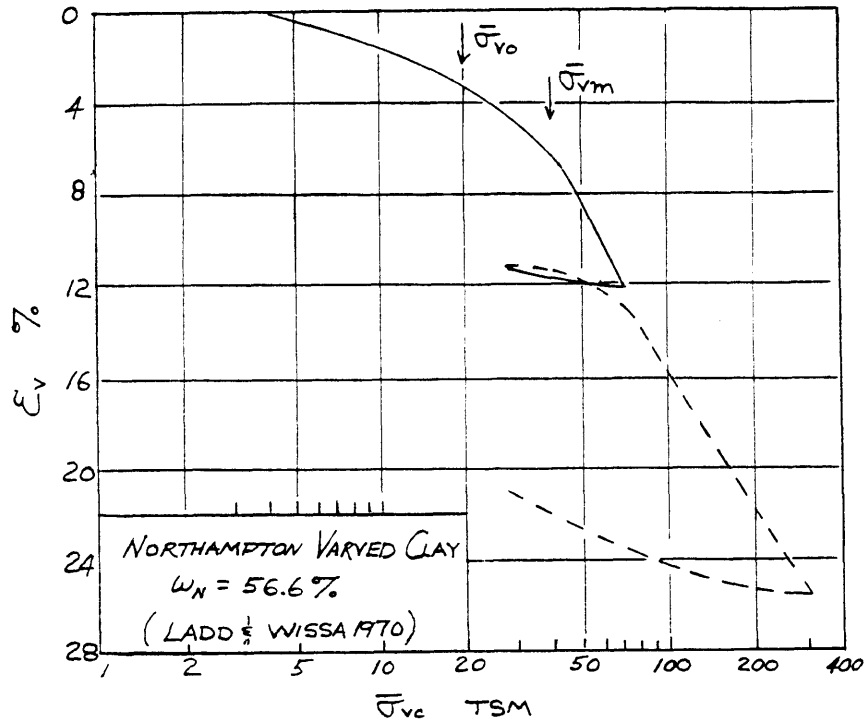
FIG. 2.2.2



DIBIAGIO & BJERRUM (1957)

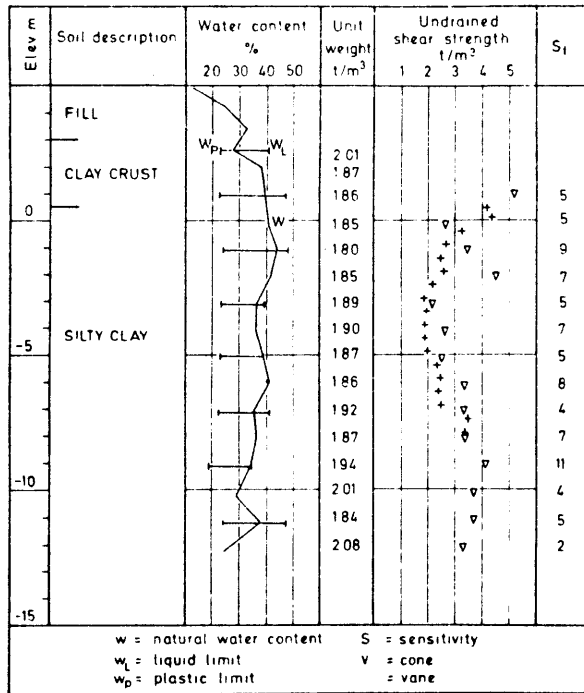
INCREASE IN STRUT LOAD VS. TIME FOR A BRACED CUT IN STIFF FISSURED CLAY

FIG. 22.3

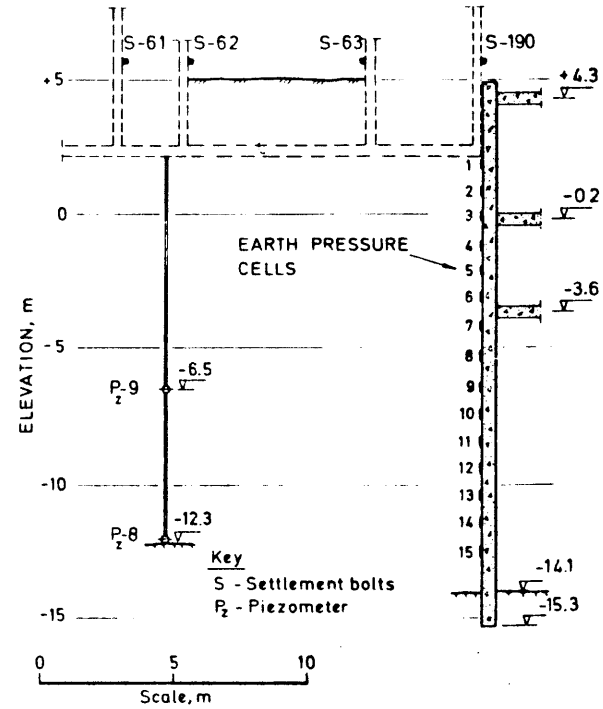


VARIATION IN COEFFICIENT OF CONSOLIDATION

FIG. 2.24



Typical soil data

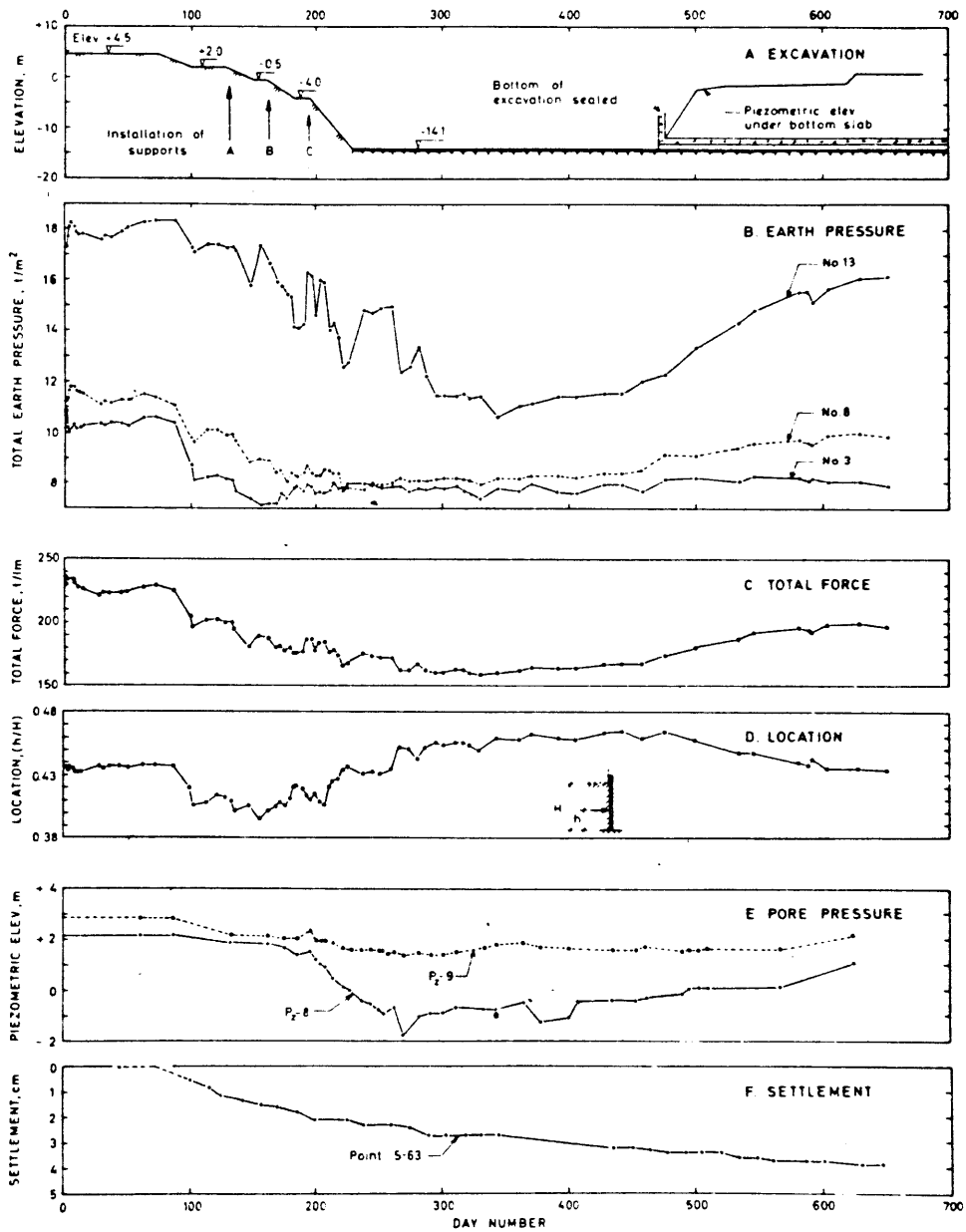


Instrumentation details - Telefonhuset.

FROM DiBiagio & Roti (1972)

SOIL PROFILE, EXCAVATION, AND INSTRUMENTATION DETAILS FOR A BRACED SLURRY WALL IN SOFT CLAY, OSLO

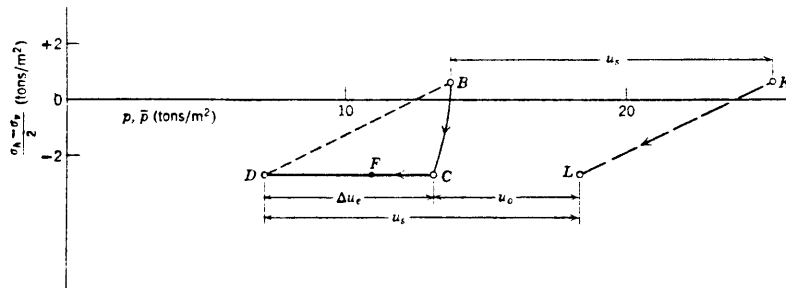
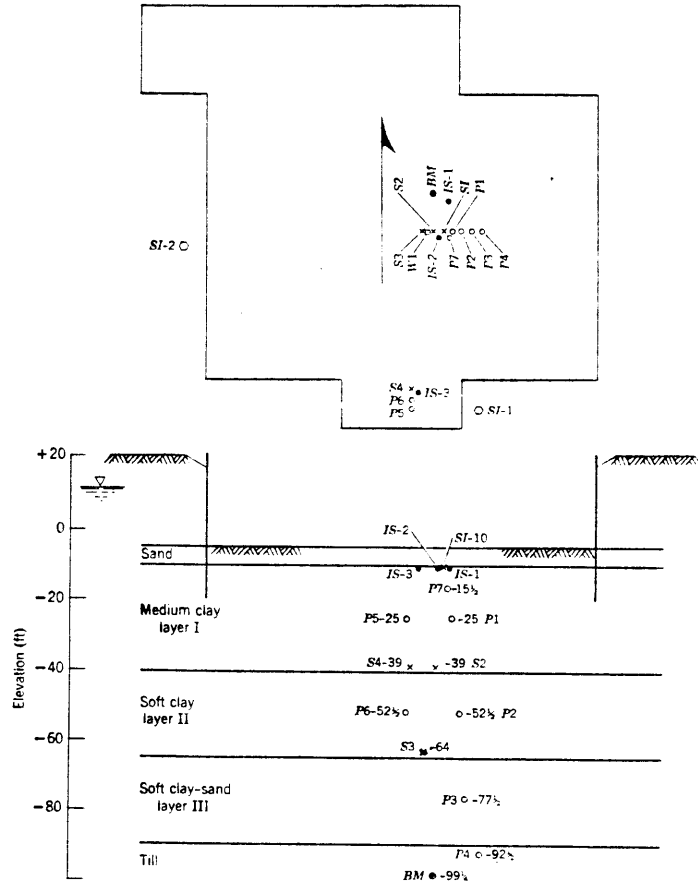
FIG. 2.25



Summary of observations from Dec. 1969 to Sept 1971
 FROM DiBiagio & Roti (1972)

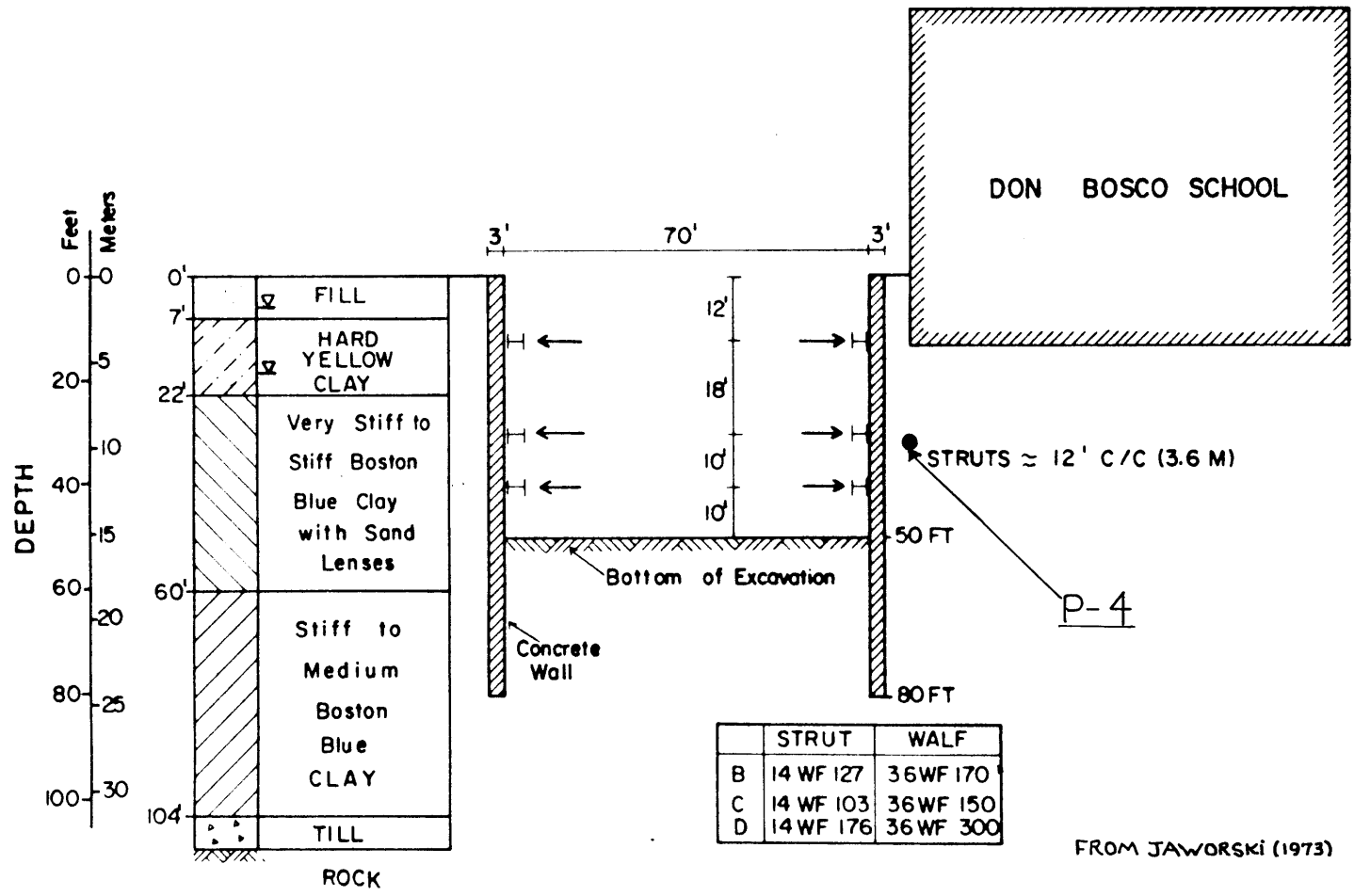
SUMMARY OF OBSERVATIONS FOR BRACED CUT IN SOFT CLAY, OSLO

FIG. 2.2.6



STRESS PATH FOR PIEZOMETER P-1
BELOW THE CAES FOUNDATION EXCAVATION

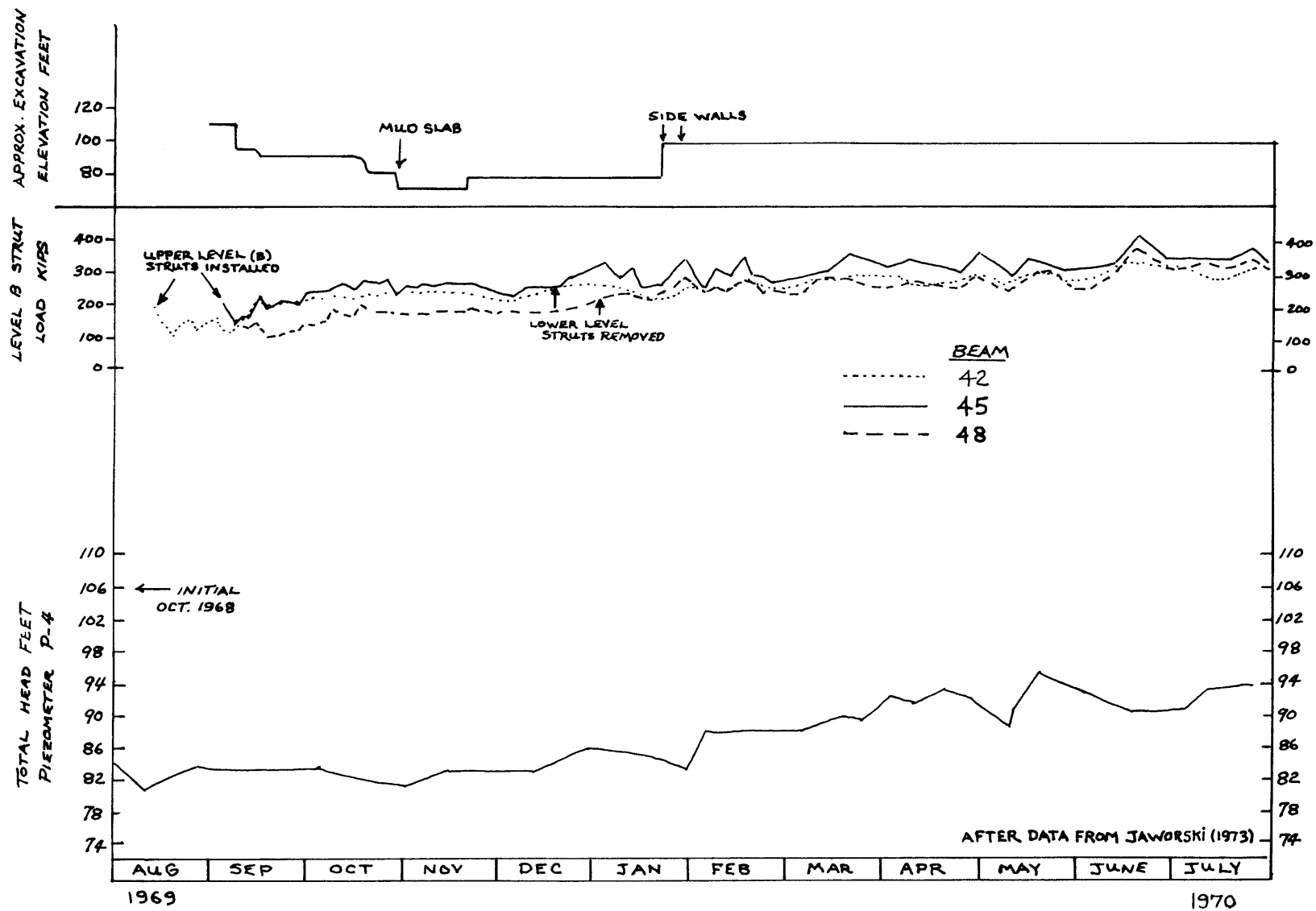
FIG.22.7



63

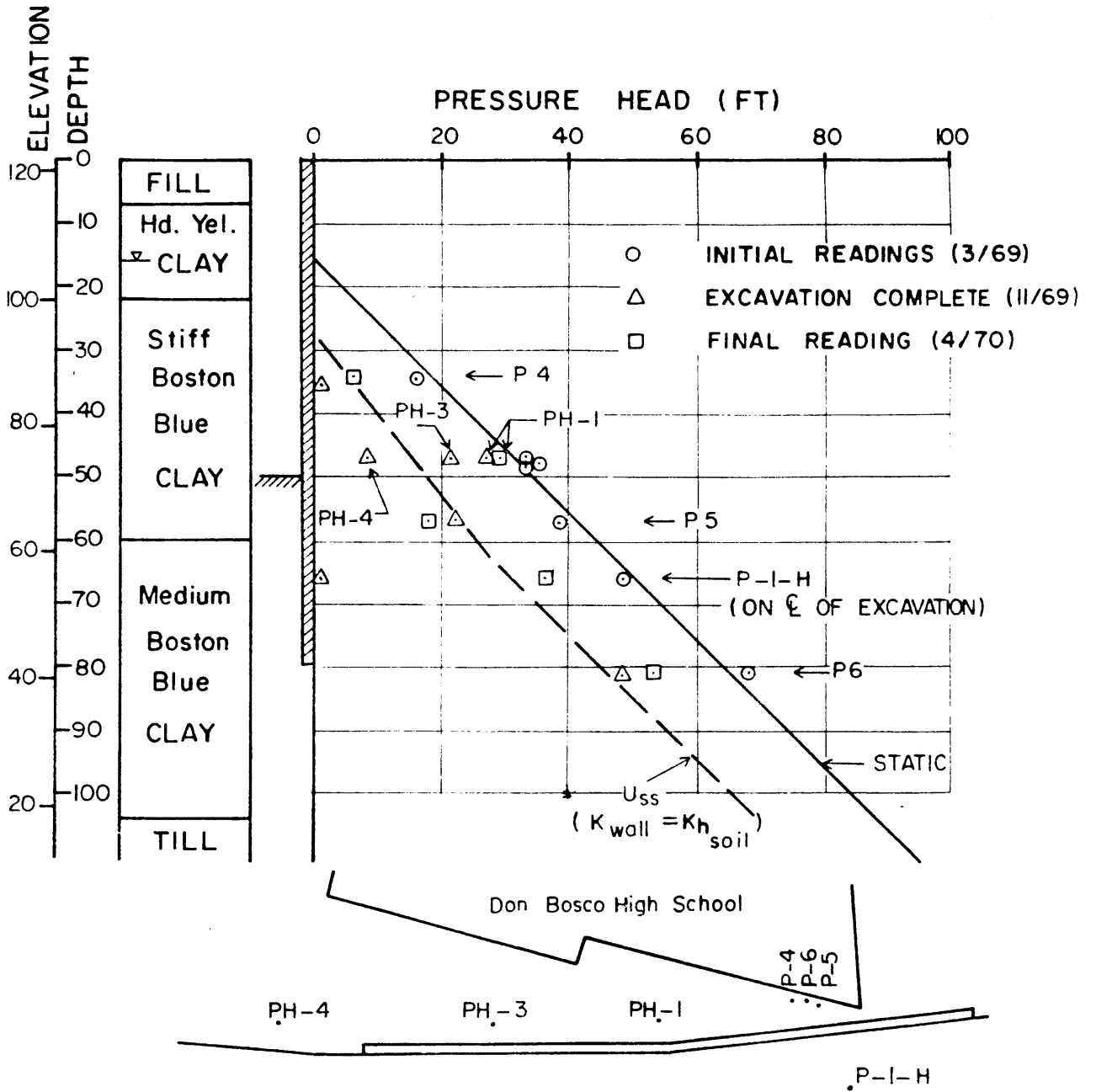
SOUTH COVE SUBWAY EXCAVATION TEST SECTION PIEZOMETER P-4

FIG. 2.2.8



STRUT LOAD AND PORE WATER PRESSURE VS. TIME-SOUTH COVE SECTION

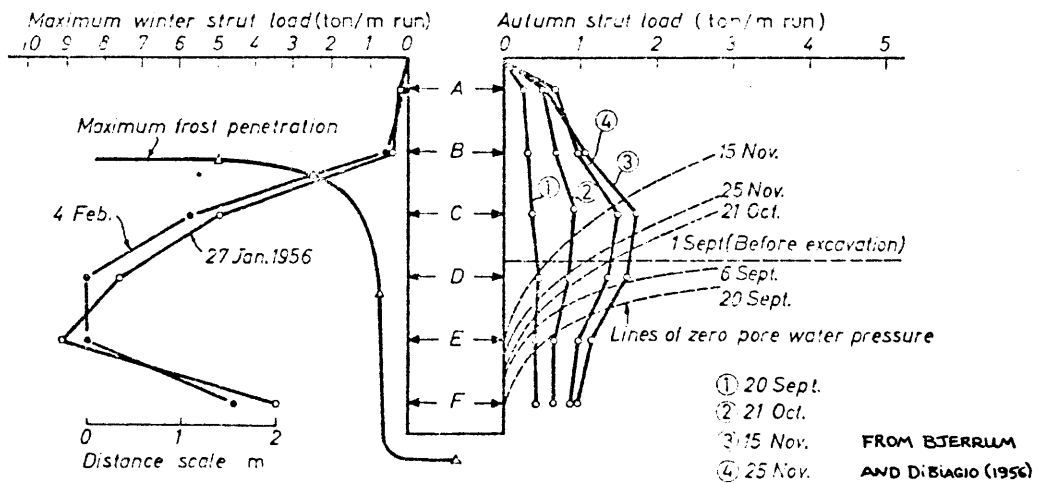
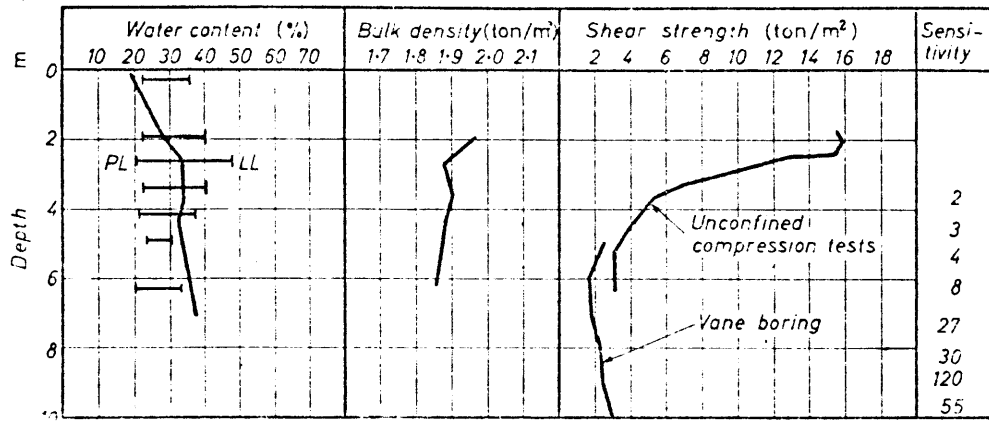
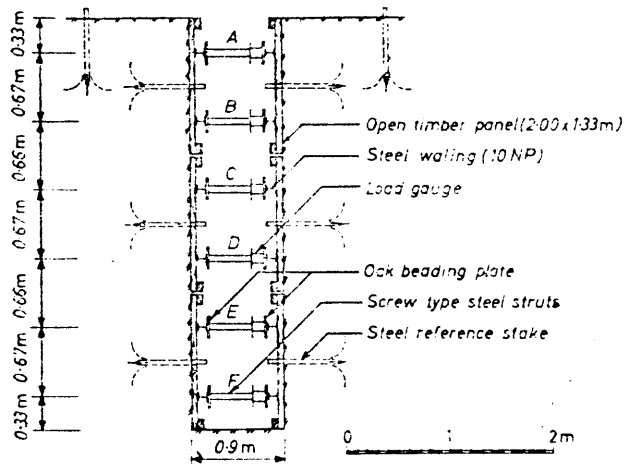
FIG. 2.29



FROM JAWORSKI (1973)

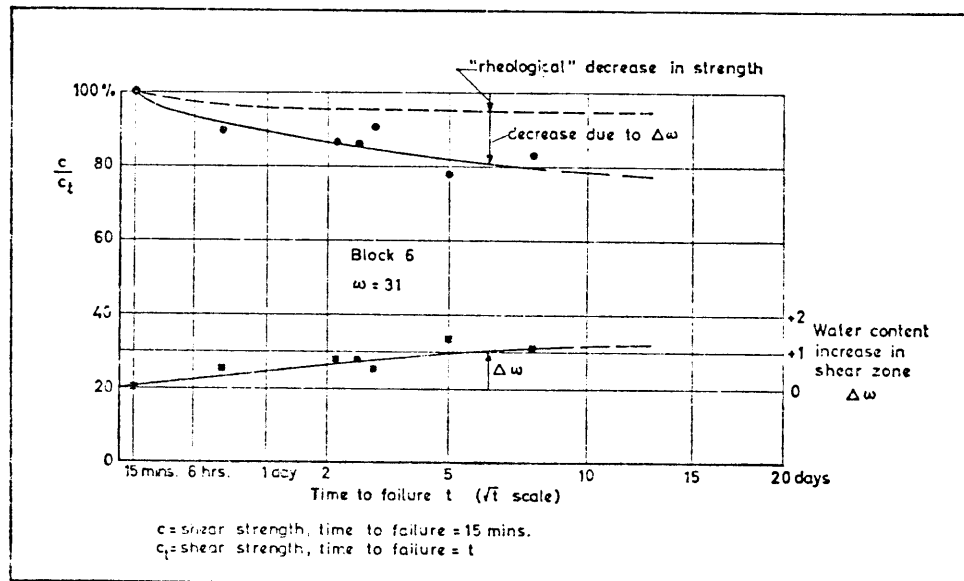
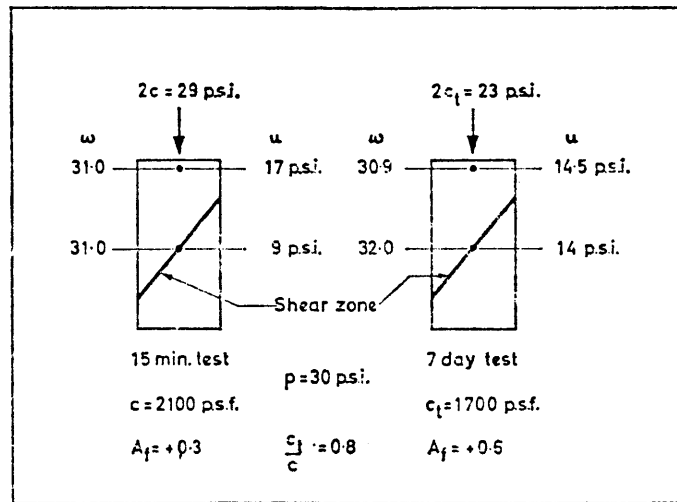
MEASURED AND PREDICTED STEADY STATE PORE PRESSURES-SOUTH COVE TEST SECTION

FIG. 2.2.10



TIME DEPENDENT BEHAVIOR OF TEST CUT IN STIFF FISSURED CLAY

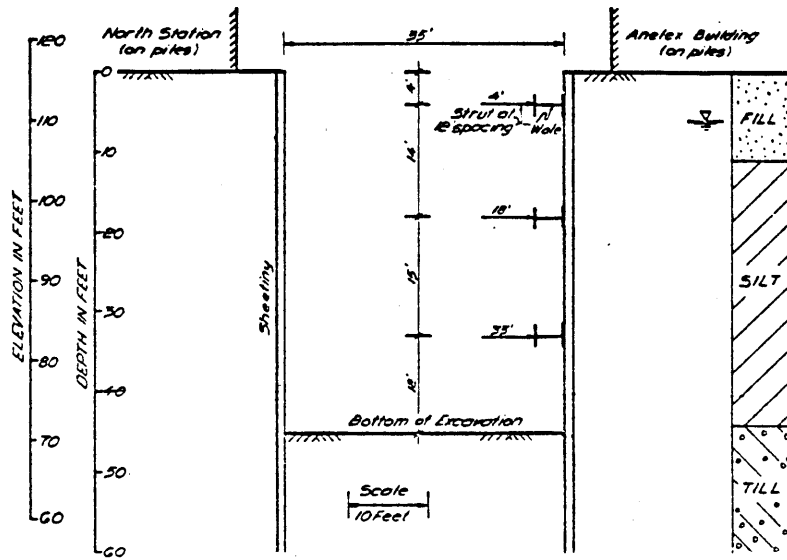
FIG. 22.11



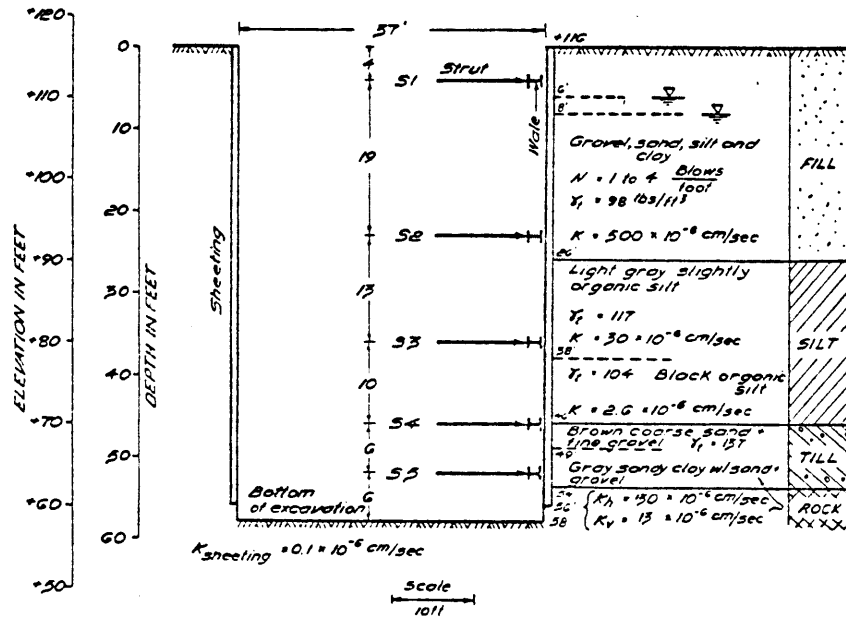
FROM SKEMPTON AND LAROCHELLE (1965)

EFFECT OF VARIATION OF TIME TO FAILURE
ON STRENGTH IN UNDRAINED TRIAXIAL TESTS

FIG. 2.2.12



TEST SECTION A

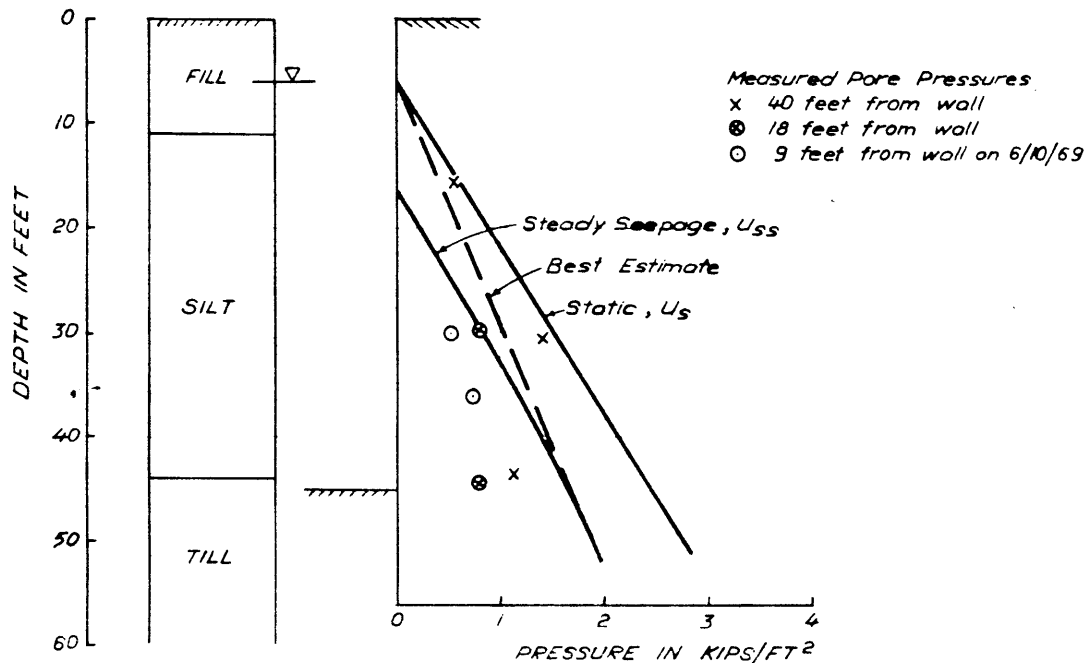


TEST SECTION B

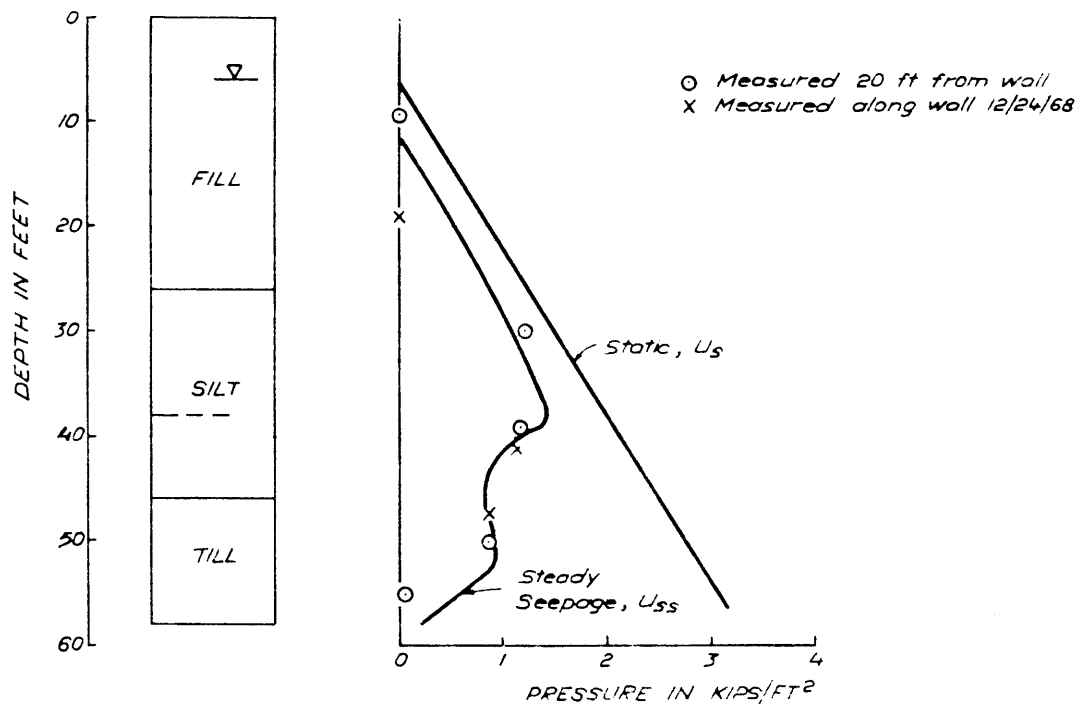
FROM LAMBE (1970)

EXCAVATION PENETRATING SILT: MBTA TEST SECTIONS A & B

FIG. 2.2.13



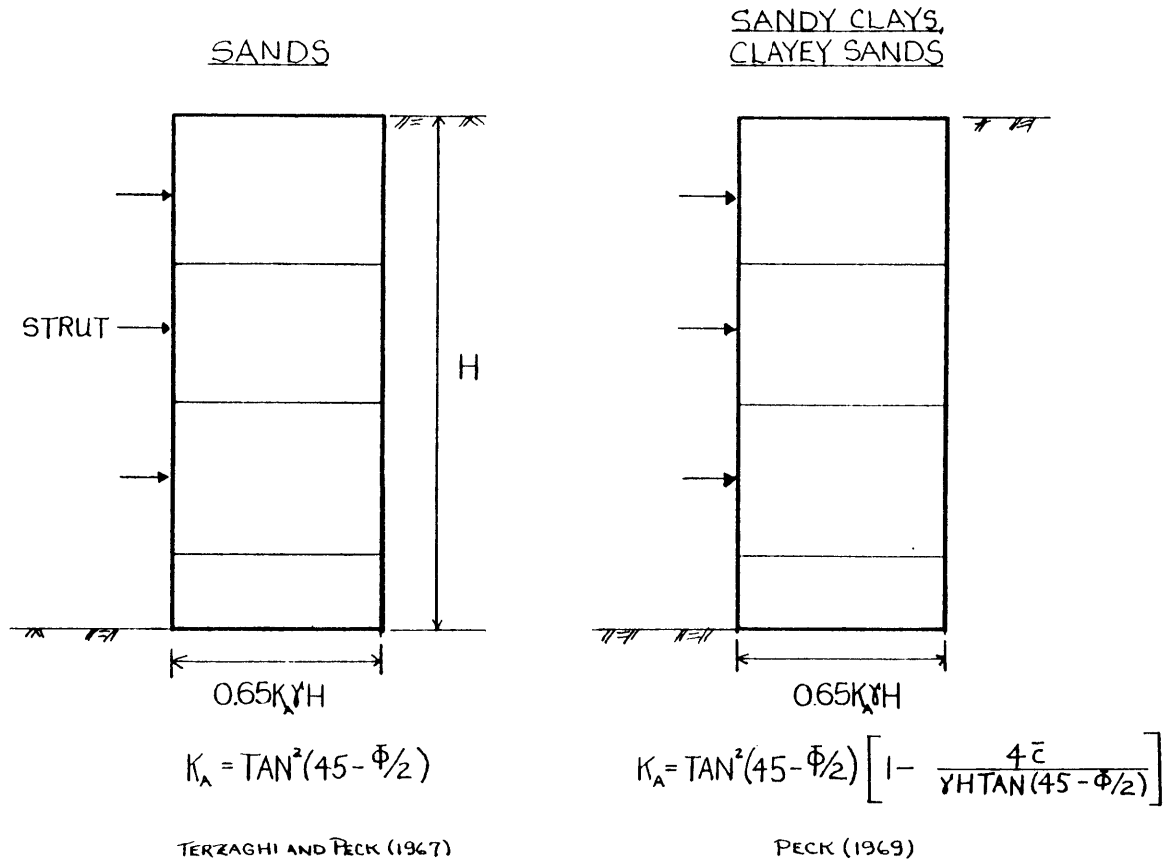
PORE PRESSURE SECTION A



PORE PRESSURE SECTION B

MEASURED AND PREDICTED PORE PRESSURE
MBTA TEST SECTIONS A AND B

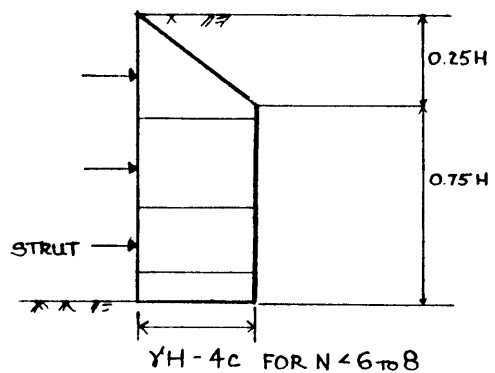
FIG. 2.2.14



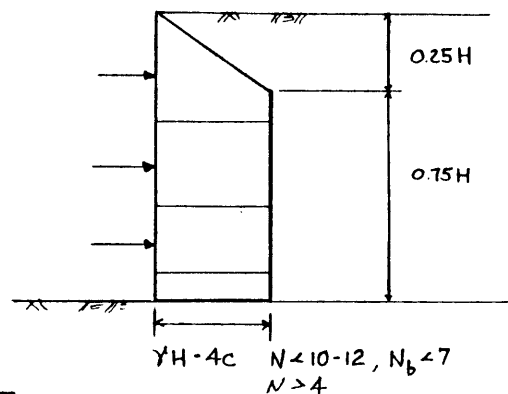
TERZAGHI & PECK DESIGN ENVELOPES

FIG. 2.3.1a

PECK (1969)



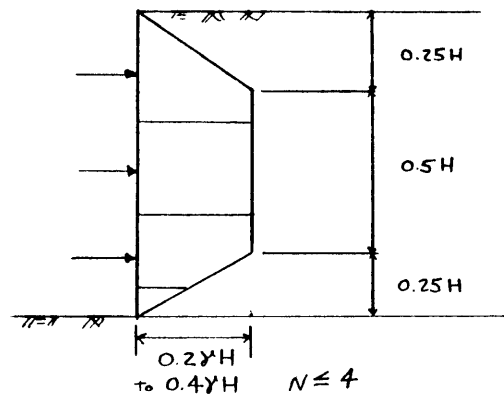
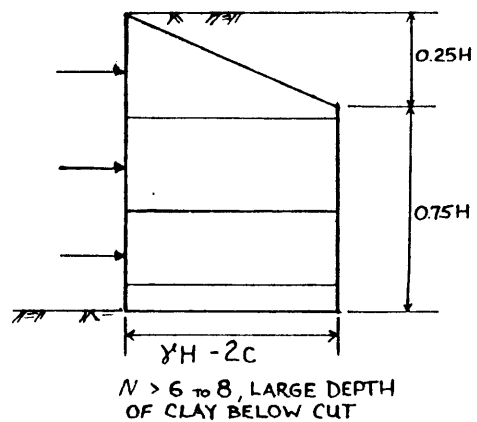
PECK, HANSON AND THORNBURN (1974)



CLAYS

$$N = \frac{\gamma H}{c}$$

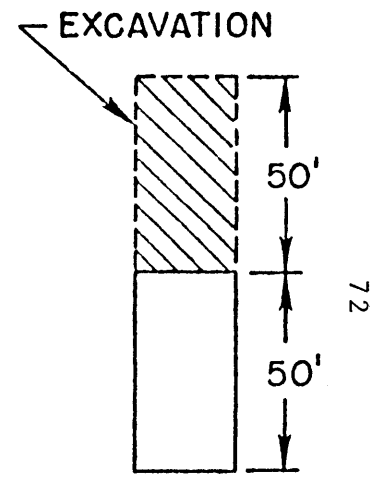
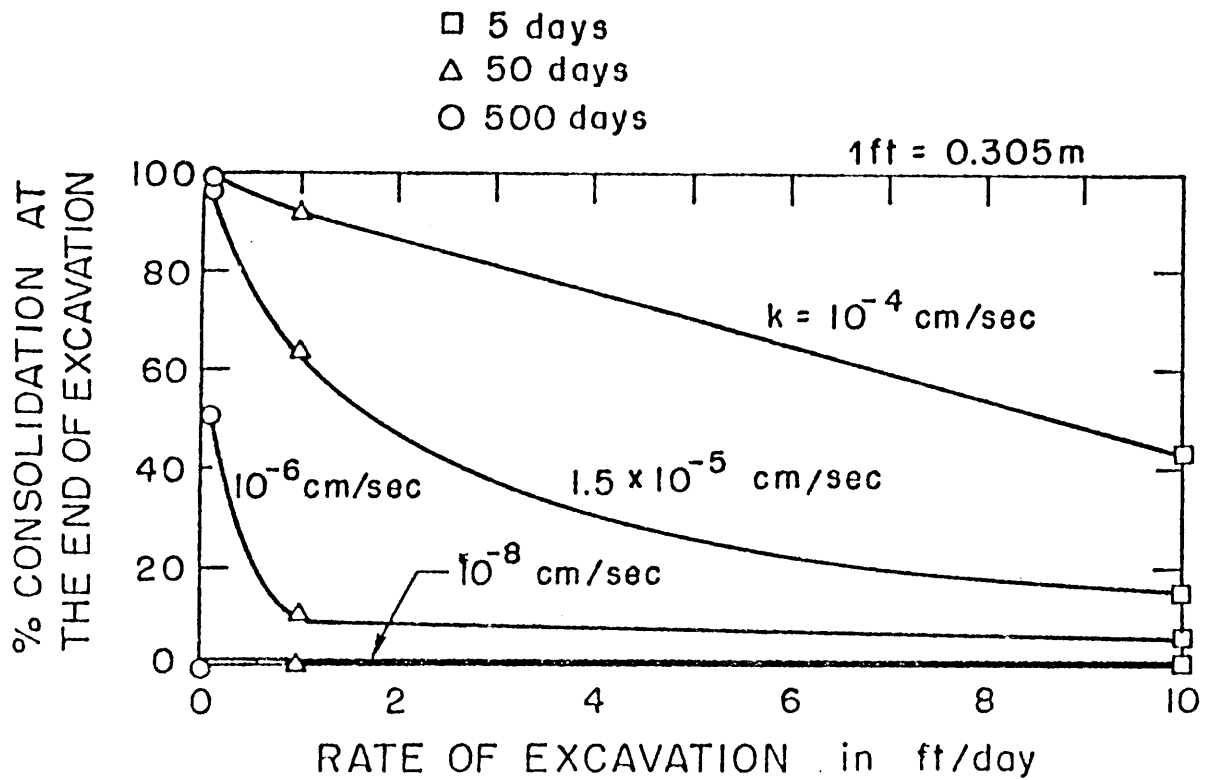
$$N_b = \frac{\gamma H}{c_b}$$



TERZAGHI & PECK DESIGN ENVELOPES

FIG. 23.1b

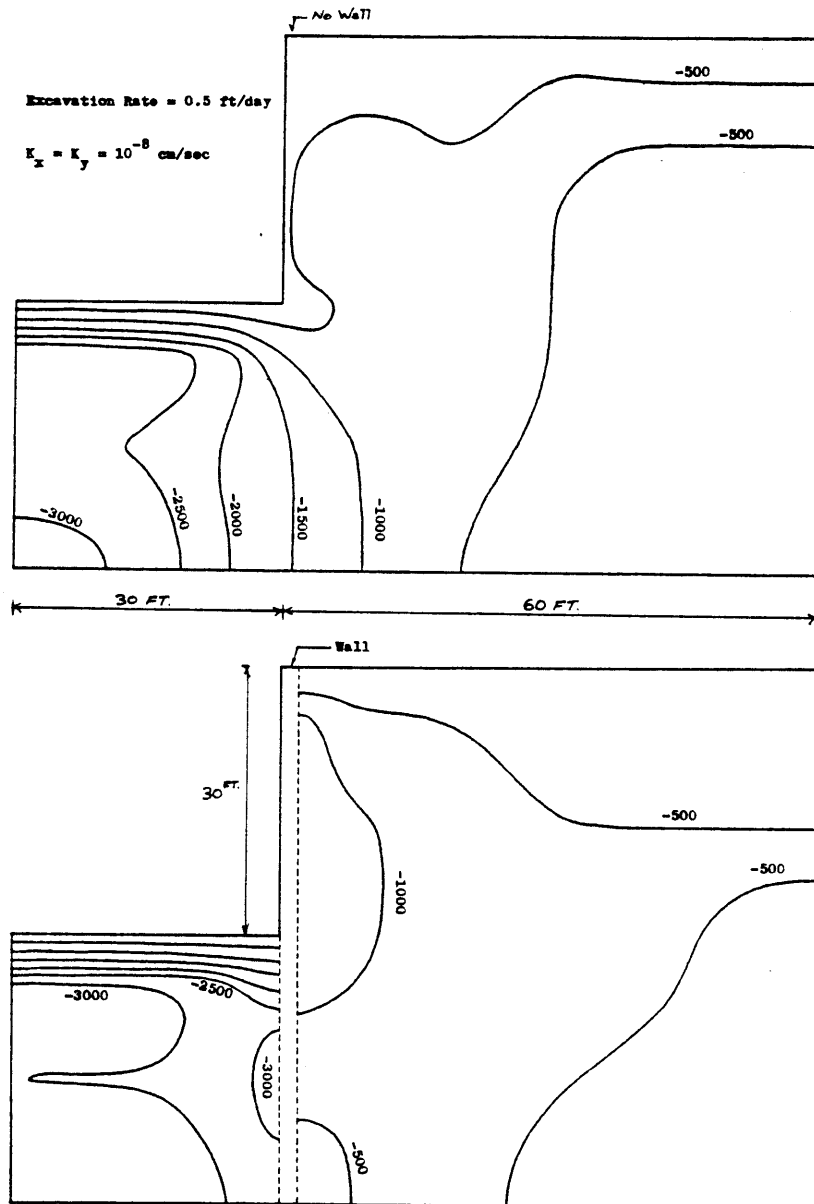
TIME TO COMPLETE EXCAVATION



FROM CLOUGH AND OSAIMI (1979)

CONSOLIDATION AT THE END OF ONE-DIMENSIONAL EXCAVATION

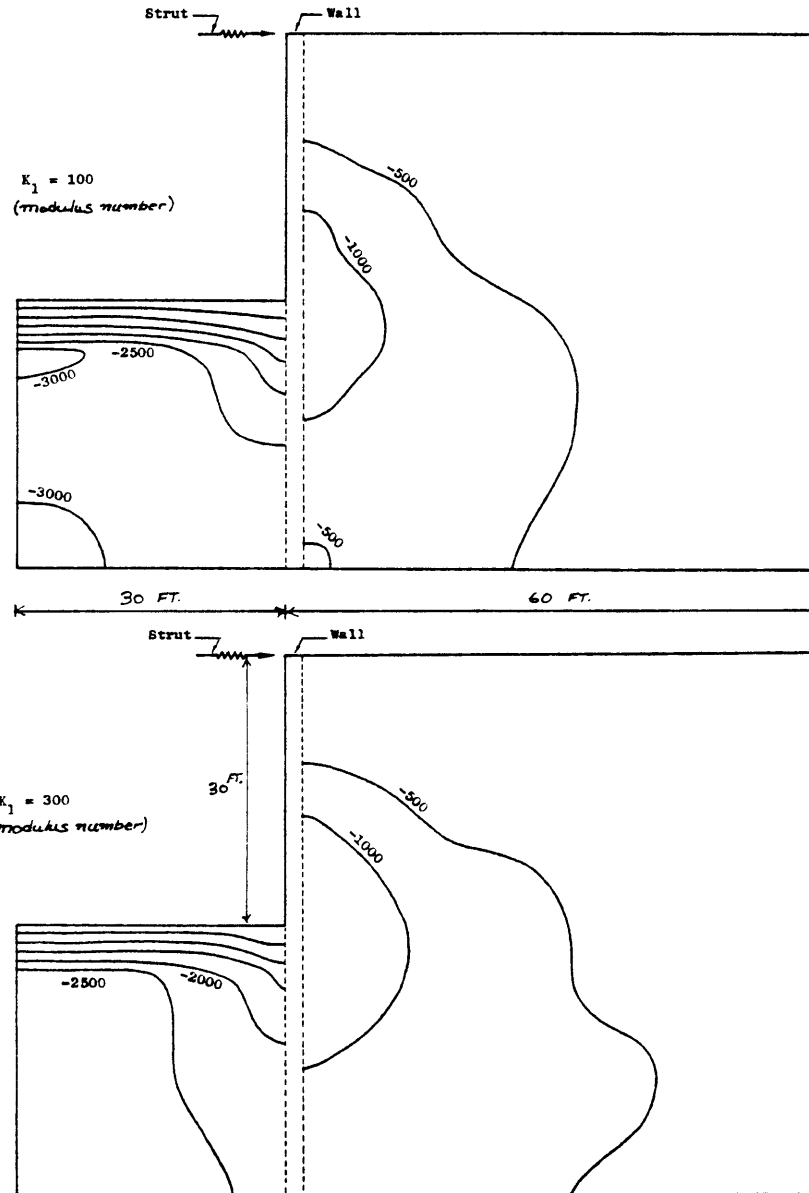
FIG. 2.3.2



FROM OSAIMI (1977) CONTOURS OF EXCESS PORE PRESSURE (psf) AT THE END OF EXCAVATION.

CONTOURS OF NEGATIVE EXCESS PORE PRESSURE
FOR TWO-DIMENSIONAL EXCAVATION

FIG. 23.3a



FROM OSAMI (1977) CONTOURS OF EXCESS PORE PRESSURE (psf) AT THE END OF EXCAVATION.

CONTOURS OF NEGATIVE EXCESS PORE PRESSURE
FOR TWO-DIMENSIONAL EXCAVATION

FIG. 23.3b

CHAPTER THREE

PROPOSED PROCEDURE FOR INCORPORATING
TIME IN THE PREDICTION OF THE PERFORMANCE OF A
BRACED EXCAVATION

3.0 INTRODUCTION

In this chapter the writer outlines a proposed procedure to incorporate a major time effect (pore pressure dissipation) in the prediction of construction performance. Acknowledging advantages of certain aspects of available Finite Element techniques and the Stress Path Method, lead the writer to use both in a composite procedure. Hence this procedure integrates the use of a sophisticated computer model as a tool for a Stress Path Method approach.

The fundamental basis for this method is the Stress Path Method. The most recent edition is presented by Lambe and Marr (1979). The basic principle behind the Stress Path Method is the effective stress principle, which states that the effective stress equals the total stress minus the pore pressure.

$$\bar{\sigma} = \sigma - u$$

Soil behavior is dependent on the effective stress history and future changes in effective stress.

Table 3.1 illustrates the types of geotechnical problems; force, deformation, stability, and flow, which the geotechnical engineer must face in practice. Generally, he

must predict the performance of constructed facility. Table 3.2 summarizes the steps used in the Stress Path Method to predict performance for the classes of problems presented in Table 3.1. The method developed in this chapter by the writer follows the steps in Table 3.2 for force and deformation.

3.1 OUTLINE OF THE PROPOSED METHOD

This procedure is an iteration whose solution can be improved with each pass through the steps outlined. Actual field performance measurements during construction can be input to update or adjust the solution. The proposed procedure is as follows:

- | <u>Step</u> | <u>Description</u> |
|-------------|--|
| (1) | Using a finite element computer program which models braced excavation (i.e. BRACE), <u>input an initial geometry and initial soil and structure properties</u> (i.e. strength, moduli, pore pressure parameters). |
| (2) | From Step (1) <u>obtain total stresses</u> (approximate). |

$$\Delta \sigma$$

- | | |
|-----|---|
| (3) | From Step (2) <u>obtain u_E (the excess pore pressure generated by the change in total stress due to excavation)</u> . |
| (4) | <u>Estimate u_D (the excess pore pressure resulting from the altered flow conditions associated with</u> |

the excavation). A hand drawn flow net or other method (FEDAR) may be necessary if steady state conditions are anticipated.

- (5) Run dissipation analysis for actual drainage condition (i.e. one, two, or three way drainage) with estimated coefficient of consolidation.¹ Estimate the percentage of dissipation, D.
- (6) Select a representative element(s) or prediction point and an undisturbed soil sample(s).
- (7) Consolidate the soil specimen(s) to the estimated in-situ stresses. Measure the coefficient of consolidation.
- (8) Shear the sample by applying a total stress path obtained for the representative element. In other words apply $\Delta\sigma$. Measure the actual u_e and the shear strains ϵ_s . The first set of tests might be sheared under conditions of no drainage. If a second set are executed after the first pass through the procedure, partially drained tests may be required.
- (9) Using the results of (5) and of (7) and the estimated time t for the excavation construction, determine the percentage of dissipation, D.
- (10) Then,

$$\Delta u_T = D(u_o + u_e)$$

1. One might use superposition as shown previously in Figure 2.1.4 to obtain the initial net excess pore press.

- (11) Apply Δu_T to the soil specimen. Measure the consolidation strain, ϵ_c .
- (12) Find;

$$\epsilon_T = \epsilon_s + \epsilon_c$$

This is a convenient simplification of the actual, partially drained behavior. Here it is assumed that the summation of the strains for undrained shear followed by consolidation are equal to the strain for a partially drained stress path terminating at the same final effective stress. Later, one might use stress path tests with partial drainage to refine the solution.

- (13) Compute a soil modulus, E and Poisson's ratio, ν ;

$$E = \frac{\Delta \sigma_v}{\epsilon_v} + \frac{\epsilon_{vol} - \epsilon_v}{\epsilon_v^2} \cdot \Delta \sigma_H \quad \nu = -\frac{\epsilon_H}{\epsilon_v} = -\frac{\epsilon_{vol} - \epsilon_v}{2\epsilon_v}$$

Here we assume that the actual stress strain curve can be replaced with a single modulus passing passing through the actual stress level.

- (14) Re-input parameters established from the test data into the computer program (BRACE). For a series of tests, contours of equal strain can be plotted as seen in Figure 3.1. From such plots moduli can be determined for any element by plotting the total

stress path on this plot, estimating the "undrained" strains and adding them to the estimated consolidation strains.

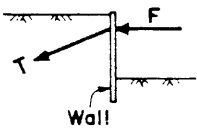
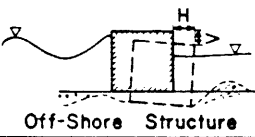


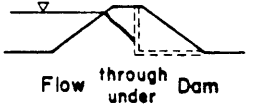
- (15) Check against original total stress paths and reiterate procedure if necessary to refine solution.

Below are summarized the main simplifications and assumptions made in the presentation of the method;

- (1) Deformations for an undrained unloading followed by consolidation to a final effective stress point equal deformations for a partially drained stress path terminating at the same final effective stress.
- (2) The actual stress strain curve can be replaced with single modulus passing through the actual stress level.
- (3) The dissipation analysis is not too affected by details of initial pore pressure distribution.
- (4) Contour plots of equal vertical strain can be constructed similar to the plot for the normally consolidated soil in Figure 3.1.

Obviously this method relies on a laboratory testing technique to obtain a soil modulus. Sample disturbance and other factors influence this value. Another limitation lies in the difficulty in correctly assessing the pore pressure dissipation. However the writer believes the application of this Stress Path Method type technique is a rational approach for obtaining input for the computer program. As Finite Element parameter studies have shown for supported

excavation, notably the Palmer and Kenney (1971) study, the soil deformation or stress strain modulus is found to have the greatest influence on the solution. One of the proposed method's main objectives is to obtain and use this modulus in a way which considers the effect of pore pressure dissipation.

TYPE	EXAMPLE	Predicted	Para- meters Needed
Force	 Wall	F T	s, E u, σ_h
Deformation	 Off-Shore Structure	H v	s, E c_v Δu with cycling
Stability	 Dam	FS	s u
	 Natural Slope	FS	σ_h
Flow	 Flow through Dam under	q, h_f Stability of soil particles	k

from Lambe and Marr (1979)

GEOTECHNICAL PERFORMANCE

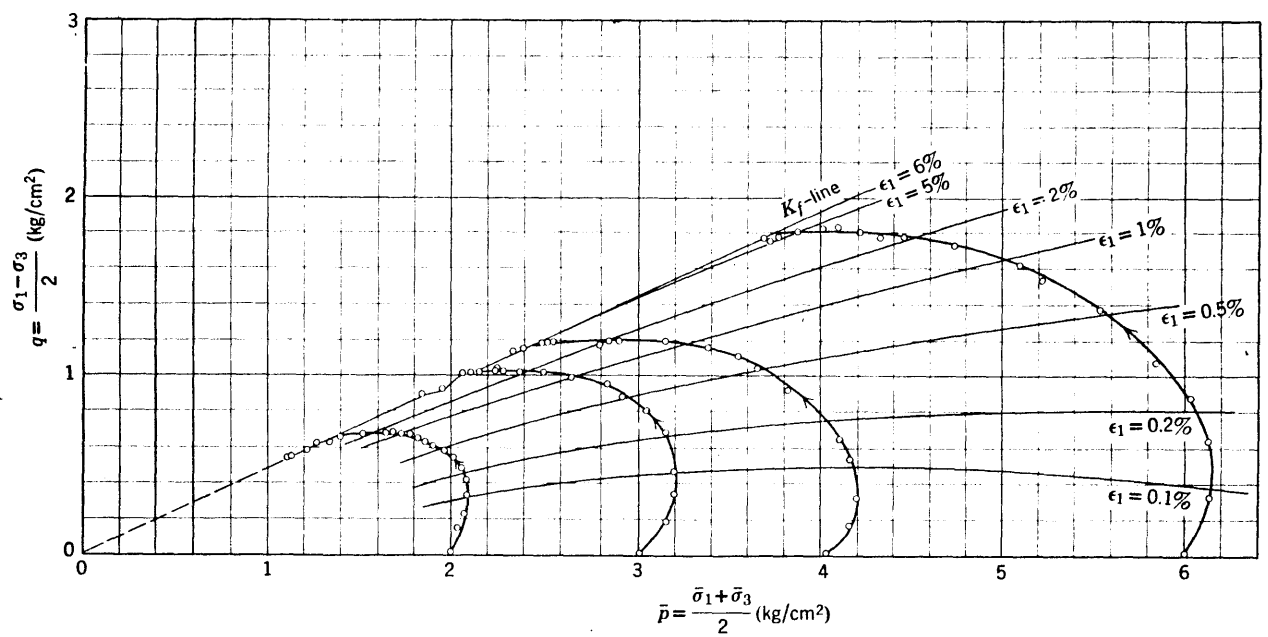
TABLE 3.1

Step (1)	Force and deformation (2)	Stability (3)	Flow (4)
1	Estimate stress-strain pattern	Estimate location of surface of minimum stability	Estimate flow pattern
2	Select average element or select several elements		
3	For selected element(s), determine stress paths for: (a) Geological history, i.e., past; and (b) design life of structure, i.e., future		
4	On soil existing at or near selected elements in field situation Run tests along stress paths determined in step 3 (Orient samples for tests same as in field) (Use field permeant in flow tests)		
5	Obtain stress strain or modulus	Obtain strength or strength parameters	Obtain permeability; Measure any movement of soil fines
6	Force = $f(\text{stress})$ or $f(\text{modulus})$ Deformation = $f(\text{strain or})$ $f(\text{modulus})$	Factor of safety = average strength / average shear stress Average shear stress from: Force polygon; or elastic analysis; or finite element analysis; or stress paths	Determine flow net Evaluate stability of soil to flow

from Lambe and Marr (1979)

STRESS PATH METHOD

TABLE 3.2



LANGUNILLAS CLAY FROM LAMBE & WHITMAN (1969)

CONTOURS OF EQUAL VERTICAL STRAIN

FIG. 3.1

CHAPTER FOUR

ILLUSTRATION AND APPLICATIONOF THE PROPOSED PROCEDURETO A CASE STUDY4.0 INTRODUCTION

To serve as a vehicle to develop and illustrate the application of the method to handle partially drained conditions outlined in chapter 3, the writer will make a prediction of the performance of a braced cut in Tokyo, Japan. The excavation is currently underway and is scheduled to take over two years to reach a design depth of 29.5 meters. Specifically, the writer will attempt to predict the loads and deformations for a critical excavation stage. The excavation depth at this stage is approximately 20 meters.

It is emphasized that the available soil test data is insufficient. Particularly lacking is adequate information on the stress history of the deposit, as well as a lack of good information pertaining to the character of the soil below 45 meters. Initial groundwater conditions (i.e. static or non-static) have not been measured. Summarizing the missing information:

- (1) stress history (oedometer tests)
- (2) u_o
- (3) limited soil samples and tests

Nevertheless, the main purpose of this chapter is to illustrate the proposed method and demonstrate its applicability. In the process a prediction is made using the available test and boring data.

4.1 TYPE OF PREDICTION

In Lambe's (1973) Rankine lecture "Predictions in Soil Engineering", Lambe classified predictions as follows:

<u>PREDICTION</u>	<u>WHEN PREDICTION</u>	<u>RESULTS AT TIME</u>
<u>TYPE</u>	<u>MADE</u>	<u>OF PREDICTION</u>
A	Before event	-----
B	During event	Not known
B1	During event	Known
C	After event	Not known
C1	After event	Known

The writer's prediction will be a classification A prediction. A prediction of early stages of the excavation currently underway would fall into the class B category. The writer did not have measurements of performance of these stages prior to prediction.

4.2 PROJECT DESCRIPTION

4.2.1 General

The excavation is for construction of a pumping station facility for the Nakagawa Sewage Treatment Plant in Tokyo

and is designated site B. The excavation support system is designed as a cross-lot braced, concrete filled pipe pile wall. Plan dimensions of the excavation are approximately 79 meters long and 52.5 meters wide from wall to wall, internal dimension. Cross lot bracing will have intermediate vertical support derived from columns supported by deep concrete piers. Within the excavation, lime stabilization of the upper 25 meters of soil has been executed. Figure 4.2.1 shows a plan view and cross section showing these construction details. Also shown are recent boring locations.

4.2.2 Construction Schedule

Figure 4.2.2 depicts the schedule for construction and pertinent events during this period.

4.3 SUBSURFACE CONDITIONS

4.3.1 Soil Conditions

Limited preliminary soil data indicated that the soil profile consists of intensely stratified deposits of relatively soft sandy silt, fine sands, clayey silt and silty clay extending to a depth of approximately 45 meters. Below these lies a relatively dense stratum of sand and sandy clay layers.

The cohesive soil deposits are of moderate to high plasticity. Blow counts (blows/30cm) in the top 30 meters of soil are typically less than 10, gradually increasing below this depth to approximately 50 at a depth of 50 meters.

4.3.2 Groundwater

Groundwater level is encountered in borings at approximately 1 to 1.5 meters below ground surface. Elevation on the boring logs coincides with depth (i.e. depth = 5 meters, elevation = -5 meters). Unfortunately it is not known to which datum (i.e., sea level) these elevations are referenced to.

Unfortunately initial pore pressure data are not available to verify static or nonstatic groundwater conditions at this site. Static groundwater conditions are assumed in this study. It should be noted however, that previous work in the Tokyo area by Lambe (1968) at a Kawasaki City Site revealed that pore pressures were non-static due to long term pumping from the lower aquifer 55 meters below the ground surface. The total head in this layer was ultimately reduced to -5 meters. Therefore the static initial condition assumption may be in error.

4.4 NAKAGAWA PREDICTION

4.4.1 Initial Model of Field Situation

Following the steps of the outlined procedure in Chapter 3 the writer selected an initial soil profile based on the limited preliminary soil data. A finite element mesh was developed to model this excavation using the BRACE III computer program. The mesh geometry was organized to closely model excavation and bracing levels as well as simplified soil stratification. Areas of anticipated high

stress concentrations (i.e. elements adjacent to wall) are modeled with smaller elements. The initial profile, and finite element mesh are shown in Figure 4.4.1. Figure 4.4.2 is a detail of the excavation and wall zone showing the excavation and bracing levels to model the field situation.

Linearly elastic stress strain moduli were employed for the initial BRACE III analysis. This run will be referred to henceforth as Run A. Values were obtained using an $E_u/\bar{\sigma}_{v_0}$ equal to 75 which corresponds roughly to a value of $E_u/S_u = 250$. These values were used to model the entire deposit. Input values of Poisson's Ratio of 0.45 and 0.40 were selected for cohesive and cohesionless soils, respectively.

4.4.2 Stress Paths from Initial BRACE III Analysis

To check the results of the initial BRACE III analysis, (Run A) total stress paths were plotted on p-q diagrams for selected "average" elements both behind and within the excavation. Several of these total stress paths are shown in Figure 4.4.3 for this linearly elastic analysis. The stress paths illustrate the compression and extension type unloading one might expect behind the wall and at the bottom of the excavation. Within the excavation for soil elements near the wall, (e.g., element No. 345), the total stress paths become less easily categorized, although a straight path extended between the initial and final points indicates the simpler extension mode of unloading.

4.4.3 Laboratory Tests And Revised Soil Profile

General

Five "undisturbed" 1 meter long, 8 cm diameter brass Shelby tubes and 7 jar samples from recent borings adjacent to the excavation were made available to the writer for stress path testing at MIT. In all, 4 anisotropically consolidated undrained triaxial stress path tests, 10 Atterberg limit index tests, and 6 combined sieve analyses (mechanical and hydrometer) were executed by the writer to supplement the available information on soil conditions. Visual classification and torvane tests were also made. Results of one unconsolidated undrained triaxial test performed at MIT were supplied by Mr. Matthew Southworth. In addition to the above, results of six isotropically consolidated compression tests performed in a Japanese lab were also obtained.

Soil Classification

Table 4.1 summarizes the index properties and visual classification of the tube and jar samples. Figures A.1 through A.6 in the appendix give complete grain size plots for the combined sieve analyses. Figure 4.4.4 gives the plasticity chart . Atterberg Limits plot near the A - line.

Stress Path Tests

Figures 4.4.4a through 4.4.4d illustrate results of the stress path tests executed by the writer for four "undisturbed" samples of sandy and clayey silts.

In order to simulate the stress changes that the writer predicted would occur in the field the procedure in Chapter 3 was employed. Based on the length of construction time for this project, it was assumed that consolidation due to altered flow conditions would occur, particularly within the excavation where construction dewatering is inevitable. Consequently the testing procedure consisted of the following 3 steps.

- (1) Consolidating the samples to the estimated in situ stress state.
- (2) Shearing undrained via compression or extension unloading to the failure envelope (define failure envelope while maintaining integrity of the sample). This procedure reflects the trends of Stress Paths from BRACE III Run A which indicated substantial zones of local yielding.

The tests were stress controlled. Pore pressures were allowed to stabilize for each decrement of applied stress.

- (3) Applying a change in pore pressure (back pressure) to simulate post shear consolidation and measure the coefficient of consolidation.

Unfortunately no tests were performed where negative

excess pore pressures were allowed to dissipate although this situation is likely to occur in the field as well. This is mainly because the writer originally assumed deep dewatering was to be implemented, later to learn that this was not the plan. Not having a sufficient knowledge of the initial pore pressure distribution in the field, initial pre-shear effective stresses for the triaxial tests were computed assuming static pore pressure conditions. Admittedly, this assumption may be in error for the actual case.

Coefficient of Consolidation

Table 4.2 summarizes values of coefficient of consolidation computed from both pre-shear and post-shear consolidation. Both square root of time and log time methods were used. The small load increment ratios often yielded type III curves (Ladd, 1973) for log time and the time for 100% consolidation was difficult to obtain from this type of plot. Thus, this writer has more confidence in the reliability of square root of time C_v data. Figures A.7 through A.14 show typical square root of time vs. volume change plots for the triaxial tests.

Revised Soil Profile

Based on the recent soil borings (October 1979) and the results of the tests run at MIT on the samples taken from these borings a revised soil profile was constructed for the prediction. The profile is shown in Figure 4.4.6. Strata

below 45 meters was inferred from older borings in the same general area.

The strength profile shown in the figure was selected for extension and compression unloading. The selection of this simple profile was influenced by:

- (1) available undrained strength data -- although high $S_u/\bar{\sigma}_{v_0}$ values determined from triaxial tests (to be discussed later) indicated some over-consolidation, useful stress history data is missing and would help put such data in perspective. Other factors such as high strain rate used in CIU compression tests and the unquantified effects of the lime stabilization of soil may have increased the test strengths. Because of the lack of better information on this deep deposit, the writer used strength data from the tests run at MIT, selecting the lower values of $S_u/\bar{\sigma}_{v_0}$ to represent the deposit.
- (2) Limitations of the BRACE III computer program -- BRACE III is limited in the number of soil materials that may be input. The writer elected to use the maximum number (20) of materials to model different moduli at the "cost" of assuming a simple strength profile described by two values of the ratio $S_u/\bar{\sigma}_{v_0}$.

The CIU compression tests shown in Figure 4.4.7 are plotted with the triaxial tests performed at MIT. The wide

scatter of strength from the Japanese CIU tests can be attributed to the wide range of confining pressures a series of samples from a given depth were consolidated to and sheared at. The high strain rate at which the shear stress was applied is also a source of error. By increasing the time to failure as Skempton and Larochelle showed (Figure 2.2.12), the measured strength will decrease. Similarly the CIU tests, tested at a strain rate of 0.5% per minute most likely give unrepresentative and higher undrained strengths because pore pressures are not allowed to equalize. This is substantiated by the controlled stress, stress path tests performed by the writer which indicated that it took a significantly longer time (15 ± 5 minutes per increment, increments as shown on Figure 4.4.5) for pore pressures to equalize during undrained shear.

Consequently the writer applied a correction based on the Skempton chart. First, strengths for the sample depths extrapolated from each series of tests were obtained by estimating the strength associated with the insitu octahedral effective stress.

$$\bar{\sigma}_{\text{oct}} = \frac{\bar{\sigma}_{\text{vo}} + 2\bar{\sigma}_{\text{ho}}}{3}$$

In other words for example, if two undrained tests of samples retrieved from a depth of 10 meters were sheared at

consolidated pressures of 5 TSM and 10 TSM, and $\bar{\sigma}_{oct}$ in the field was 6.3 TSM the approximated strength was extrapolated in the following fashion:

$$S_{u_{6.3}} = S_{u_5} + \frac{6.3-5}{10-5} \cdot [S_{u_{10}} - S_{u_5}]$$

This strength was then reduced by 20% to correct for the excessively high strain rate. Table 4.3 summarizes the corrected CIU strengths as well as the other triaxial test data from the MIT tests. The agreement between the two is good for the compression tests. The extension tests have strengths equalling approximately 50% of the strength measured in the compression tests.

In comparison, undrained triaxial test data on normally consolidated Kawasaki Clay (P.I. = 40 ± 10%) with a slightly higher P.I. from Ladd et al (1965) show values of $S_u/\bar{\sigma}_{vo}$ equalling .445 and .225 for compression and extension respectively.

Although the strength data showing large $S_u/\bar{\sigma}_{vo}$ ratios indicates that there is probably some overconsolidation from 18 to 28 meters, stress history data is not available to define the degree of preconsolidation. As previously stated because of the lack of sufficient data, for the purpose of this study the strength for the undrained deposit will be assumed to increase constantly with depth equal to $0.43\bar{\sigma}_{vo}$ for compression and $0.22\bar{\sigma}_{vo}$ for extension. These values agree well with Ladd et al (1965) although they may be

slightly conservative values in the light of test data available from 18 to 28 meters.

Contours of Equal Vertical Strain

Based on the available CIU and CAU tests, plots of equal vertical strain were constructed. Figures 4.4.8a and 4.4.8b show contours of vertical strain on a p-q plot drawn through the effective stress paths for the CIU tests. The two stress path compression tests TC-1 and TC-2 are also plotted and show reasonably good agreement. For extension unloading the two stress path tests TE-1 and TE-2 are plotted on Figure 4.4.8c and estimated contours of equal vertical strain are averaged through these effective stress paths. These plots will be used to extrapolate strains for various loadings at any depth to obtain soil moduli.

4.4.4 Revised BRACE III Analysis for Partially Drained Conditions

A. General

As previously stated, this prediction will address the excavation when it has attained a 20 meter depth. One reason for selecting this depth is illustrated with the help of Figure 4.4.9. This figure shows a simplified soil profile and the Nakagawa excavation geometry for the sixth excavation stage (depth = 19.5 meters). At this depth, bottom stability due to uplift becomes critical. A simple computation for the geometry in the figure determines the critical depth, Z_{CR} for equilibrium of the soil mass against uplift;

$$\begin{aligned}
 z_{CR} &= \frac{z \gamma_T - (z - z_w) \gamma_w}{\gamma_T} \\
 &= \frac{45 \times 1.8 - (45 - 1.5) \times 10}{1.8} \\
 z_{CR} &\cong 21 \text{ METERS}
 \end{aligned}$$

At this excavation depth, the effective stress is zero at 45 meters and the upward force equals the downward force (i.e., the factor of safety is one).

Consequently this prediction will treat the loads and deformations to be anticipated for a depth just prior to the depth where bottom instability is imminent. Two new BRACE III runs B and C are made for this prediction. For the final Run C updated stresses from the previous run are used to obtain moduli.

B. Computation of Partially Drained Moduli

The partially drained moduli incorporate both undrained and consolidation strains in the relation:

$$E = \frac{\Delta \sigma_v}{\epsilon_v} + \frac{E_{VOL} - E_v}{E_v^2} \cdot \Delta \sigma_H$$

where:

$$\epsilon_v = \text{TOTAL VERTICAL STRAIN} \quad E_{VOL} = \text{TOTAL VOLUMETRIC STRAIN}$$

1) Undrained Shear Strains

Using the linearly elastic BRACE III RUN A, the writer selected approximately 50 elements inside and outside of the excavation and tabulated the values of total stress change in terms of $p - u_0$ and q for the initial and sixth excavation

stage. (Table 4.4 shows such tabulated values of stress for the final BRACE III RUN C). Total stress paths are then constructed from these values. Using the appropriate plot of strain contours, (see Figure 4.4.10) the total stress path (minus the static pore pressure) can be superimposed and the undrained strains can be scaled off between contours along the estimated effective stress path.

2) Consolidation Strains Due to Dissipation of Excess Pore Pressure within the Excavation

Given the final effective stress point established by the undrained shear, the excess pore pressure u_E due to shear (typically negative in this case) can be obtained by subtracting the value of $(p_6 - u_0)$ for the sixth excavation stage from the value of \bar{p} . Refer to Figure 4.4.10.

The average degree of consolidation for this geometry is estimated using one dimensional consolidation theory. Within the excavation the impermeable wall is likely to inhibit lateral drainage. The Terzaghi equation for the dimensionless time factor T_v is;

$$T_v = \frac{c_v t'}{H_d^2}$$

For a depth of excavation equal to 20 meters the time factor within the excavation is computed using:

(a) $c_v = 3 \times 10^{-3} \text{ cm}^2/\text{second}$

selected as an average value from the stress path test data

(b) $t' = .5t \approx 8 \text{ months}$ computed from

Figure 4.4.11 to represent an average time for unloading similar to the procedure used to compute settlement time for embankment loading (see Lambe & Whitman p. 414 1969)

$$(c) \quad H_d = (45 - 19.5) \div 2 = 12.75 \text{ meters}$$

The drainage path length for the consolidating cohesive layer. This assumes double drainage.

The time factor then equals 0.05 for this stage of construction for the soil at the bottom of the excavation. For a linear distribution of excess pore pressure this will yield an average degree of consolidation of approximately 25 % obtained from Figure 4.4.12a. Having observed the distribution of negative excess pore pressure within the excavation to be reasonably linear and also considering the study by Osaimi (1977) which indicates a one dimensional vertical dissipation of negative excess pore pressure the writer uses Figures 4.4.12b to approximate the degree of dissipation for negative excess pore pressure for any depth or discrete element below the bottom of the excavation. (Ideally a plot of Z vs. U_z would be derived and constructed to represent the actual initial distribution of excess pore pressure.) By multiplying the specific degree of dissipation U_z times the initial excess pore pressure one estimates the actual negative excess pressure dissipated. This value is then tabulated (Table 4.4), later to be added to the positive excess pore pressure dissipated, due to surficial or shallow dewatering within the excavation.

The excess pore pressure due to shallow dewatering can be analyzed using Figure 4.4.13 for a change in piezometric level at one drainage boundary only. This case also experiences double drainage and therefore the time factor will be the same as previously computed. The dissipated excess pore pressures are obtained using this figure and are computed for various depths and elements (Δu_D).

The summation of $\Delta u_D + \Delta u_E = \Delta u_T$ gives a net value of dissipated pore pressure in TSM. Using Figure 4.4.14a and/or 4.4.14b based on the post-shear consolidation from the series of stress path tests, volumetric and vertical strain can be extrapolated for a given depth. Since stress path tests with dissipation of negative excess pore pressure were not run the plot in Figure 4.4.14a shows inferred lines for this case. Since this is an unloading problem, the strains due to dissipation of negative excess pore pressure are not likely to be in the zone of primary consolidation and therefore are likely to have a similar relationship to changes in pore pressure (but opposite in sign) as the early recompression stage of the stress path tests.

(3) Consolidation Due to Pore Pressure Dissipation Behind the Excavation

The steel pile wall is assumed to be impermeable. The steel interlocks between the piles have been grouted to prevent leakage.

Below the lower silt layer the total head is assumed to remain constant and this stratum is assumed to have free access to a distant source of groundwater.

Given these assumptions, dewatering due to shallow pumping within the excavation will not affect pore pressures behind the wall.

The stress path test TC-1 indicates that the upper organic silt has a coefficient of consolidation of approximately 7×10^{-5} cm²/sec. Computing a time factor for this doubly drained stratum for the time associated with the 20 meter deep excavation we get:

$$T_v \cong .016$$

and from Figure 4.4.12

$$U_{\text{AVG}} \cong 12\%$$

similarly for the lower clayey silt we compute

$$T_v \cong .03$$

$$U_{\text{AVG}} \cong 20\%$$

Continuing with the use of one dimensional theory as was used for within the cut, strains are estimated for consolidation and added to the undrained strains obtained from the contours of equal strain plots. See Table 4.4.

(4) Contours of Moduli

Contours of moduli can then be constructed across the finite element grid using the tabulated values for the

discrete elements analyzed. Figure 4.4.15 shows the contours of moduli in tons per square meter. Stress strain moduli for the granular layers above and below the cohesive soils were estimated using empirical formulas based on blow count (Mitchell and Gardner, 1975) and compared with ranges of modulus for granular soils in the literature. The modulus in the layered lower sand and sandy clay stratum was reduced from 1650 outside of the excavation to 1000 within the excavation to recognize the fact that the shear stress level in this interior zone is higher and therefore the secant modulus will be lower.

The values of modulus from this plot were substituted into the BRACE III computer program by initially assuming 14 soil materials (moduli) and assigning the appropriate values of moduli to the finite elements. Total stresses from this computer Run B were used to improve the solution by determining new or updated moduli as shown in Figure 4.4.16. The final Run C was made using Fig. 4.4.16 and 20 materials. The current version of BRACE III will handle a maximum of 20 soil materials. Ideally zones of soil with similar modulus and Poisson's ratio would be contoured, since these values can also be estimated as shown in Table 4.4 for the final run. Unfortunately, the current version of BRACE III is as previously stated, limited to how many materials may be input.

Ultimately the writer observed that in general Poisson's ratio will follow the trends outlined below:

- a) Zones Inside the Excavation
 - 1) where dewatering prevails and the net excess pore pressure is positive, dissipation will tend to increase Poisson's ratio
 - 2) where the net excess pore pressure is negative, dissipation will tend to decrease Poisson's ratio
- b) Zones Outside of the Excavation
 - 1) where the net excess pore pressure is positive dissipation will tend to reduce Poisson's ratio
 - 2) where the net excess pore pressure is negative, dissipation will tend to increase Poisson's ratio

Ultimately an average value of 0.49 was selected for the cohesive soils, this value at the upper range of typical values (0.2 - 0.5) usually used in finite element analysis modeling of soil. In general the undrained strains in this case tended to dominate the deformations.

(5) K_o

K_o = 0.5 for all soils was selected based on review of stress path K_o consolidation data on these soils, the 1-sin ϕ equation and empirical correlations of K_o versus P.I.

(6) Anisotropy

To account for anisotropic shear strength, The Davis and Christian (1971) yield criterion was used in BRACE III. Also, any yielded Elements are assigned a modulus equalling

1 to 10% of the unyielded modulus, depending on the initial modulus value.

C. Predicted ,Loads Deformations and Stability

(1) General

From the final BRACE III run, contours of deformation and stress are shown in Figures 4.4.17 through 4.4.23. Figure 4.4.23 is a contour plot of undissipated excess pore pressure and is intended to show the approximate trends prior to consolidation.

Related aspects of techniques used in the BRACE III computer program to model the soil structure interaction are discussed in this section.

(2) Deformations

Figure 4.4.17 illustrates the deformed geometry after the sixth excavation stage. Inward movement of the steel pile wall towards the excavation range from 12 centimeters at the top of the wall to a maximum of nearly 44 centimeters at a 27 meter depth. Bottom heave varies from 40 centimeters near the wall to 76 centimeters at the center line. Figures 4.4.18 and 4.4.19 show selected lines of lateral displacement and bottom heave, respectively.

Maximum ground surface settlement behind the excavation is 20 centimeters occurring 25 meters behind the excavation. Figure 4.4.24 compares

ground surface settlement with Peck's chart. Note the uncharacteristic heaving of the excavation face. Ground surface settlement begins to occur at a distance of 3 meters behind the excavation. In the 3 meter wide zone between the wall and this point a very small net upward movement occurs. In the writer's opinion, since this is contrary to the downward movements we would normally associate with past experience, this lifting of the excavation face is due in part to the way which the BRACE III computer program models the soil-structure interaction. When excavation release is simulated the upward forces applied to the nodes on the newly exposed surfaces of the excavation include an upward force applied to the nodes shared by sheeting elements. Consequently, as the bottom of the excavation heaves, the sheeting may also heave slightly.

This behavior is enforced by the technique intended to allow the soil to slip behind the wall. This technique involves setting the axial stiffness of the sheeting equal to either the soil stiffness, or zero above a selected level (usually above the depth of excavation). BRACE III runs in this study set the axial stiffness of the sheeting equal to the soil stiffness.

Simulation of strut installation is made by fixing the node at which the strut is applied in the horizontal direction. A BRACE III computer study by the writer comparing this method with fixing the node in both vertical and horizontal directions indicated that more settlement occurs directly behind the excavation face with the latter method. Although this technique was not implemented in the current BRACE III analyses, fixing the node in both directions may be a more realistic approach. Therein is evidence of the difficulty in modeling the soil structure interaction.

BRACE III Input options used for strut installation in the final Run C included:

- a) no prestressing of struts
- b) zero crushing of shims (or timber wedges) as a percentage of movement already occurred at strut level

Although no prestressing of the struts was employed for the initial linearly elastic Run A and Run B, shim crushing was set to 50%. The first revised Run B (the first of the two runs using the partially drained modulus) showed large inward sheeting movements (up to 1 meter at a 20 meter depth) magnified by the crushing of the shims. Acknowledging this error, the final BRACE III Run C assumed no crushing of shims. Unfortu-

nately, the writer does not have knowledge of the actual prestressing and shimming techniques and details for this excavation.

Movements above the excavation level are also as Jaworski (1973) states, a function of bracing details. The selection of the related input parameters are usually drawn from the engineer's experience or knowledge of actual performance in the field.

(3) Loads

Figure 4.4.25 shows the strut loads and total lateral stresses behind the wall. The negative values in several struts can be attributed at least in part to the lack of prestressing in the struts. Furthermore, since for early stages of excavation the sheeting typically behaves as a cantilever followed by a more convex distribution of displacement, the tendency for the top of the sheeting is to bend back away from the excavation during later excavation stages. This would give negative load to a non-prestressed upper strut, as indeed the upper two strut loads illustrate. Consequently the load is shifted to the lower struts. The unusual negative load in one of the lower level struts is probably a result of several factors. While lack of prestressing may contribute to this result, Jaworski notes that four to five

sheeting elements between strut levels may be required to accurately model the sheeting behavior. Otherwise, uncharacteristic sheeting forces may be transferred to the strut. Only two to three sheeting elements were used between strut levels in this study.

4. Stability

Stability for an excavation of these dimensions is typically analyzed using Terzaghi's bottom heave analysis for shallow excavation ($H/B < 1$) as shown in Figure 4.4.26. Bjerrum and Eide would be used for cases where $H/B > 1$. For comparison recall the basal stability analysis made in section 4.4.4A indicating instability at an excavation level of 21 meters. Also note that for both analyses any beneficial, stabilizing effects of the concrete support piers have been neglected. The plan area of these columns is approximately 13% of the plan view area of the bottom of the excavation.

For the Nakagawa excavation, the average strength along the assumed failure surface can be estimated by:

- (1) selecting several average elements along the assumed failure surface

- (2) constructing stress paths including the effects of pore pressure dissipation
- (3) selecting a strength for each element based on an assumed failure loading path starting from the final effective stress point determined in (2)
- (4) average the strengths and input the Terzaghi equation for Factor of Safety shown in Figure 4.4.26

The extended time for which this excavation remains open has resulted in a dissipation of net negative excess pore pressure for elements outside of the excavation and for the majority of the elements within the cut. Consequently, the soil strength decreases with time as the soil swells and the water content increases. Hence in the stability analysis the actual or "partially drained" value of c is input into the equation below. This method is used instead of the commonly used " $\phi = 0$ " concept where S_u , the undrained strength is substituted for c ;

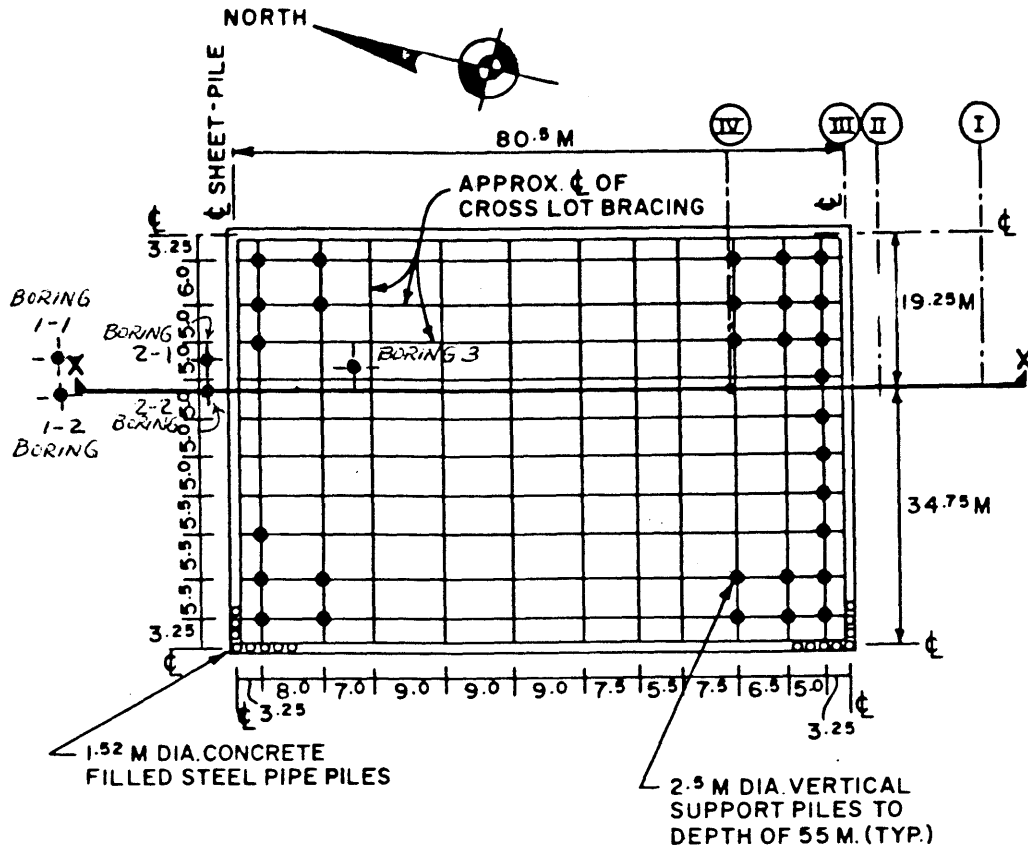
$$\text{Factor of Safety} = \frac{1}{H} \cdot \frac{c N_c}{\gamma - c/\lambda B}$$

Although the " $\phi = 0$ " approach is a convenient simplification, if it is used for this case the

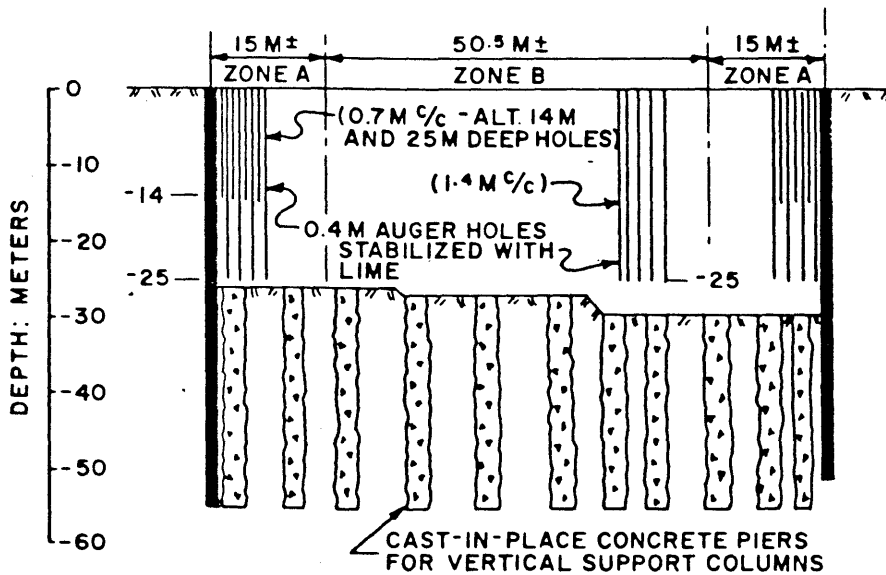
Factor of Safety may be unconservative.

Figure 4.4.27 shows the excavation geometry at the 20 meter stage and several "average" elements. Several of the stress paths for these elements have been plotted in Figure 4.4.28 and an average strength selected from strengths estimated from the stress paths is 8 TSM (refer to Table 4.5).

The resulting factor of safety using this method is 1.6. Using the same strength for the final excavation depth of 29.5 meters, the computed factor of safety is 1.1. Although some error is involved in making this extrapolation because the stress paths for the "average" elements will be different as well as the strengths. In other words, strength does not equal a constant (as the Terzaghi solution assumes) and the factor of safety for the full 29.5 meter depth is probably overestimated.



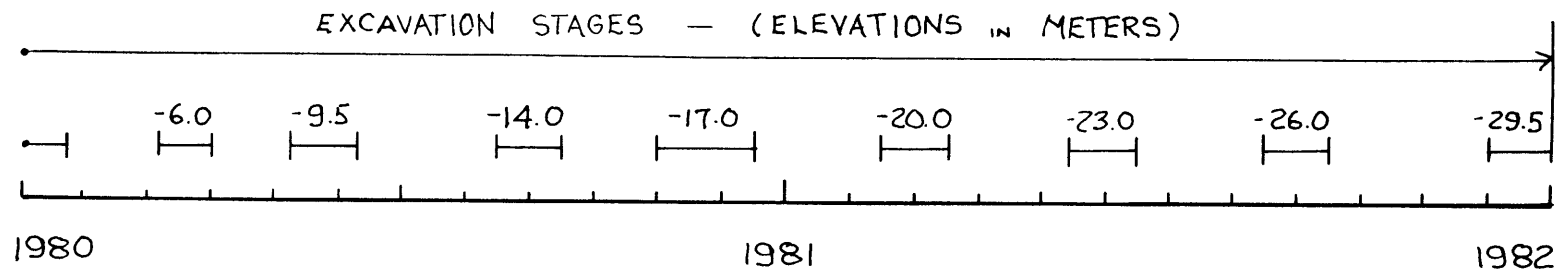
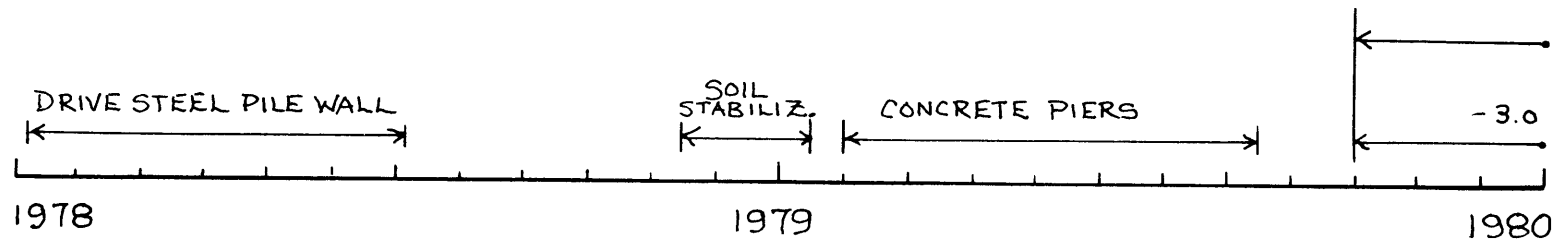
PLAN VIEW



CROSS - SECTION X-X

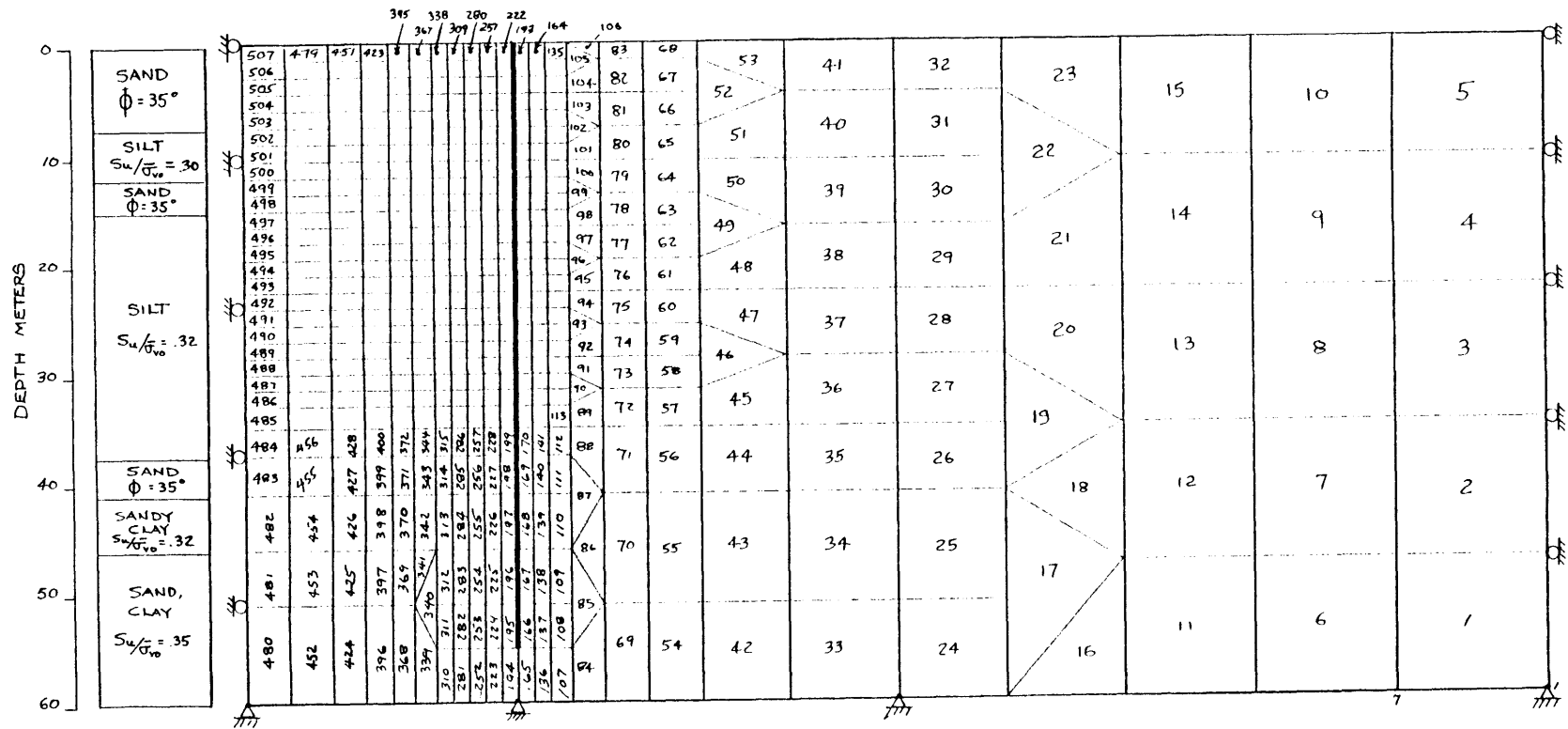
PLAN VIEW AND PROFILE OF NAKAGAWA SEWAGE TREATMENT PLANT EXCAVATION - SITE B

FIG. 4.2.1



SITE B CONSTRUCTION SCHEDULE

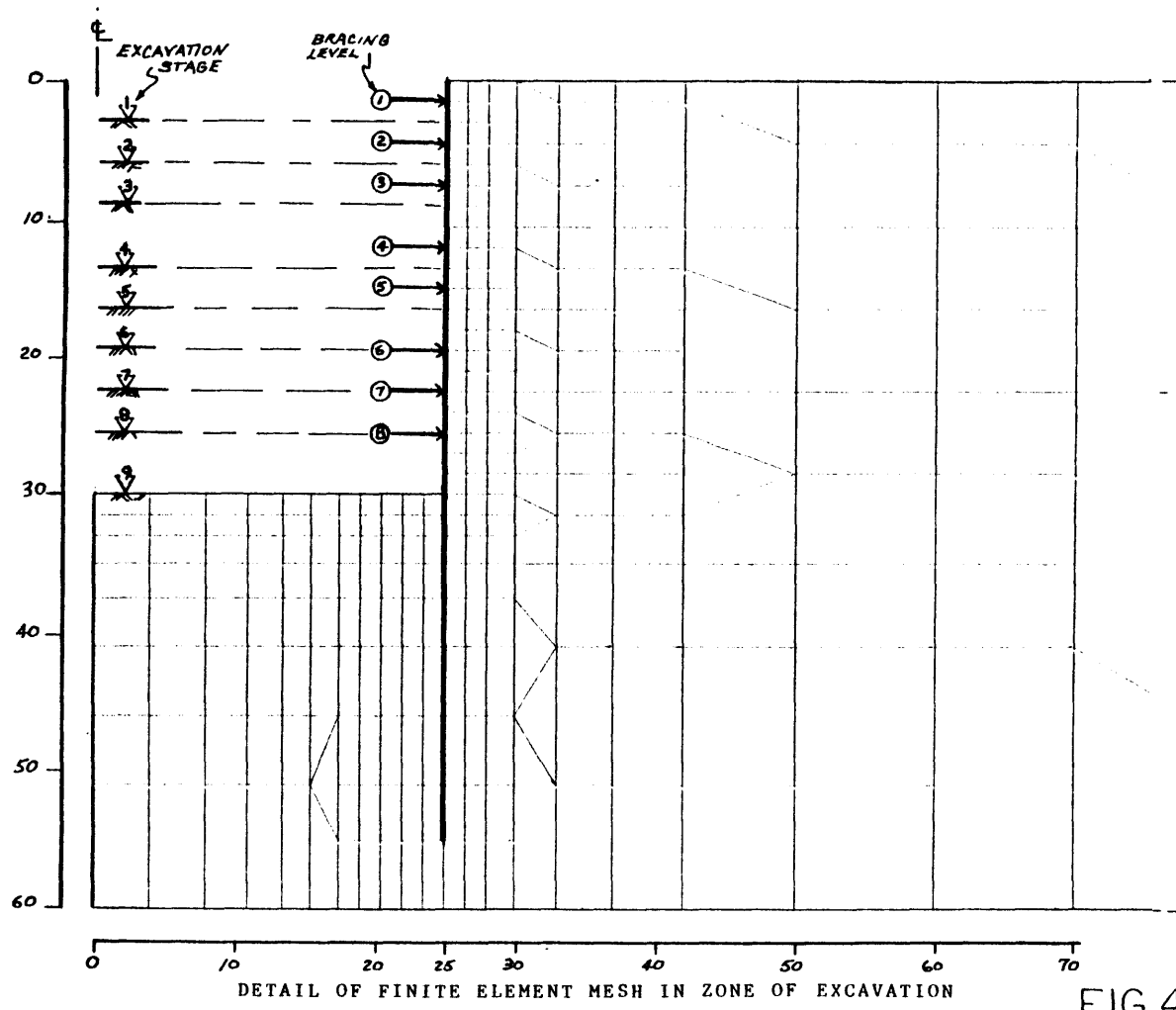
FIG. 4.2.2



ALL SOILS: $\gamma_+ \approx 1.75 \text{ TCM}$, $E/\bar{\sigma}_{vo} = 75$, $K_0 = 0.5$

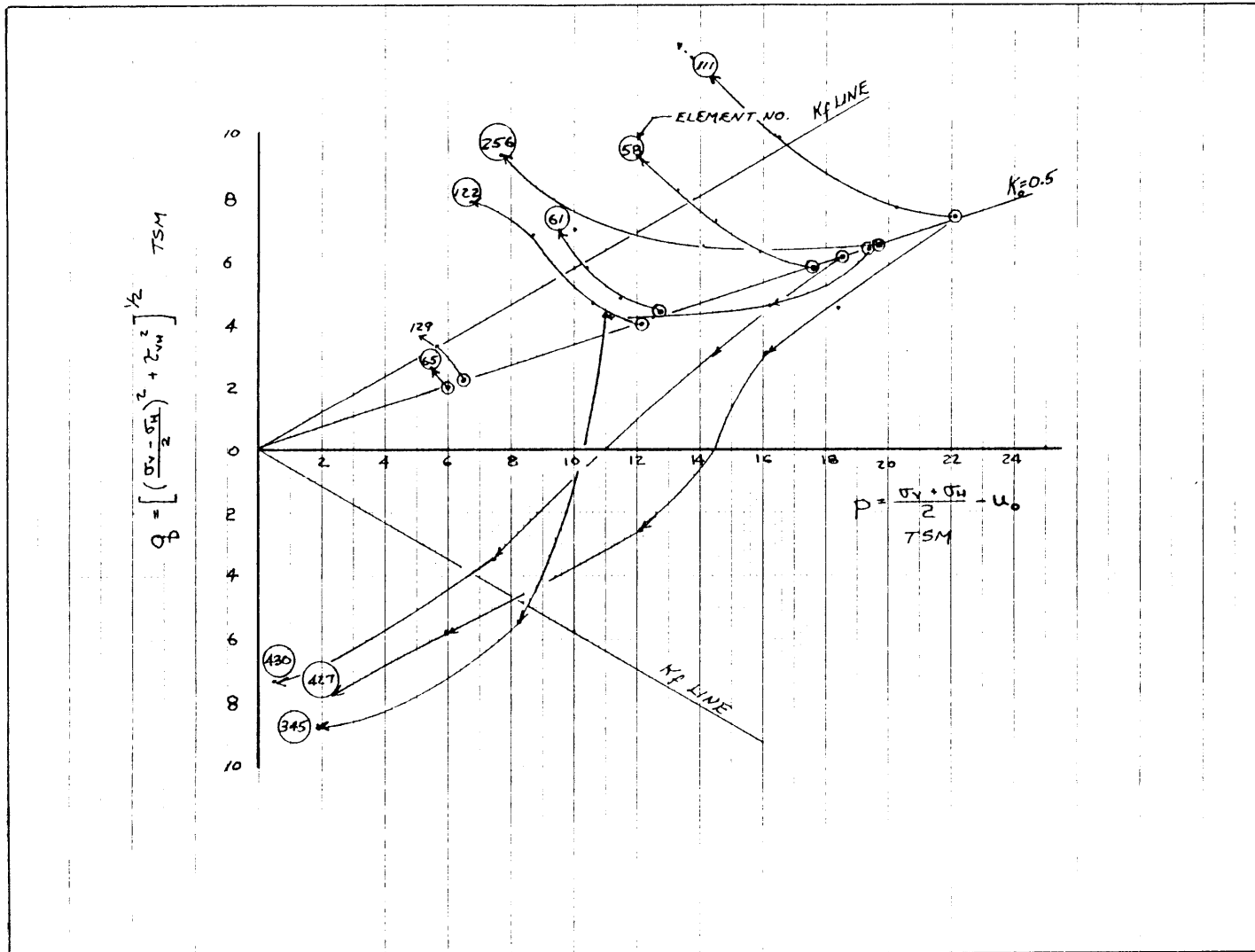
INITIAL PROFILE AND FINITE ELEMENT MESH

FIG.4.4.1



DETAIL OF FINITE ELEMENT MESH IN ZONE OF EXCAVATION

FIG.44.2



TYPICAL TOTAL STRESS PATHS INITIAL BRACE III
ANALYSIS LINEARLY ELASTIC MODULUS

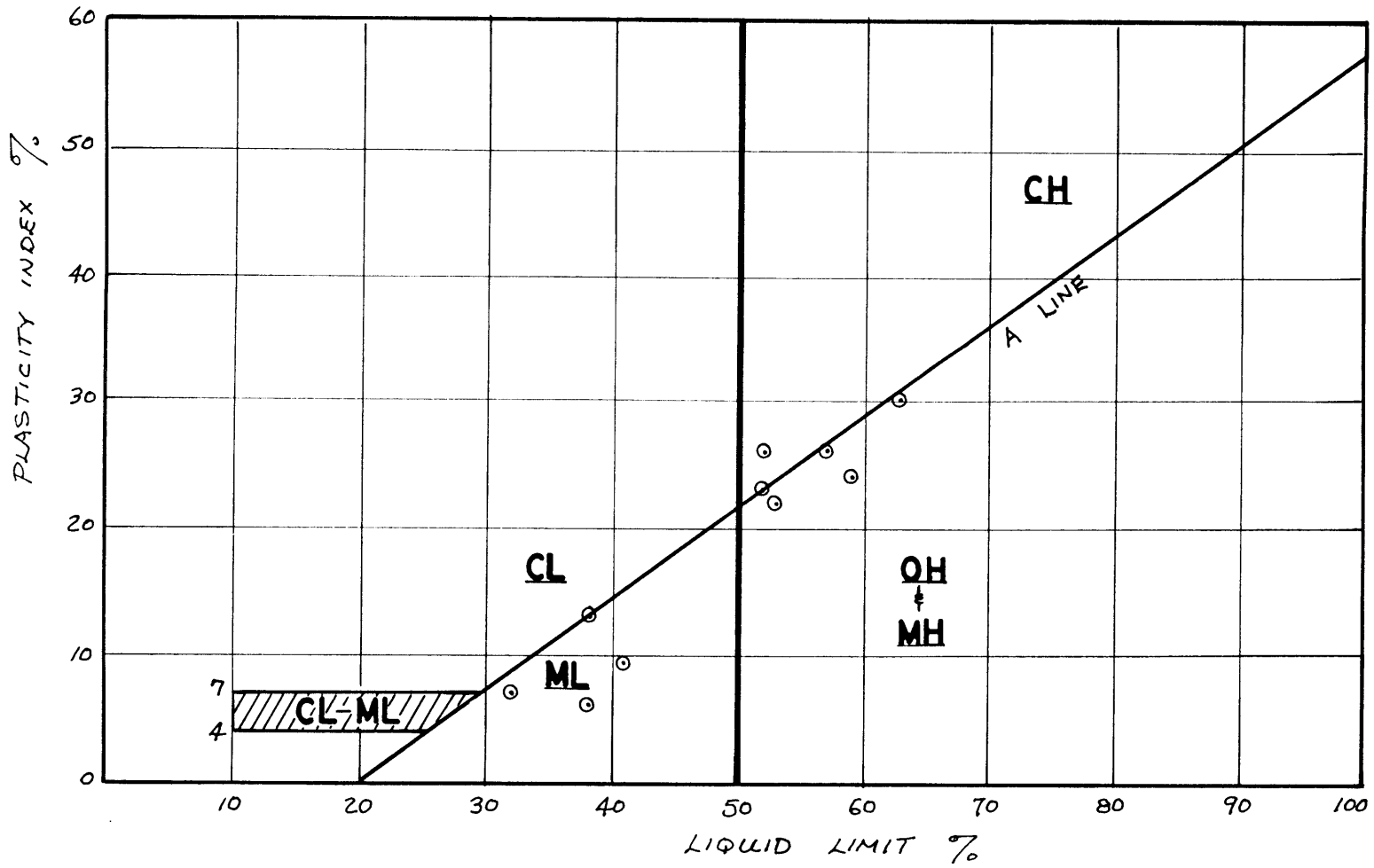
FIG. 4.4.3

SAMPLE DEPTH METERS	BORING	SAMPLE TYPE	w _n %	w _p %	w _p %	P.I.	S _u TORVANE TSM	% WT. < .002 mm	UNIFIED CLASSIF.
10.5	2-2	ST	65.4	63	33	30	2.7	—	OH-MH (TC-1)
10.8	2-2	ST	68.2	58	35	23	2.8	35	OH-MH
19.0	3	ST	44.2	53	31	22	3.5	22	MH (TC-2)
21.4	2-2	ST	55.4	57	31	26	3.2	—	MH
28.0	2-1	ST	50.5	51	29	22	4.1	33	CH-MH (TE-2)
28.8			35.9	31	26	5	—	—	ML
31.3	2-2	JAR	—	38	25	13	—	—	ML-CL
34.0	2-1	ST	40.5	41	32	20	SEE NOTE	28	ML (TE-1)
39.15	2-2	JAR	—	37	32	5	—	12	ML
42.15	2-2	JAR	—	52	26.5	25.5	—	36	CH

ST = SHELBY TUBE NOTE: SANDY SAMPLE - NO TORVANE

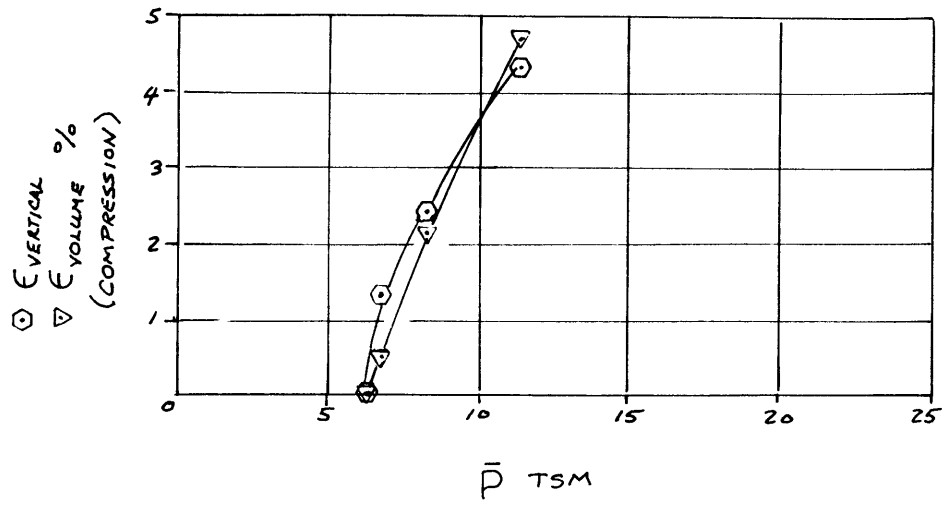
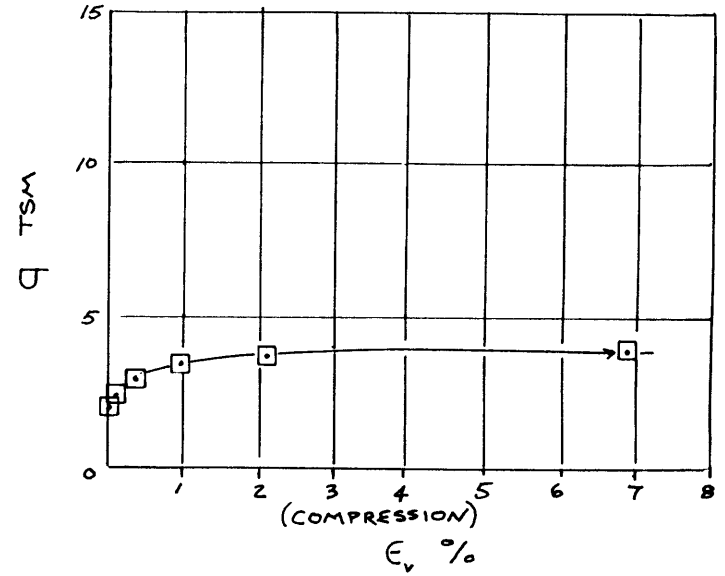
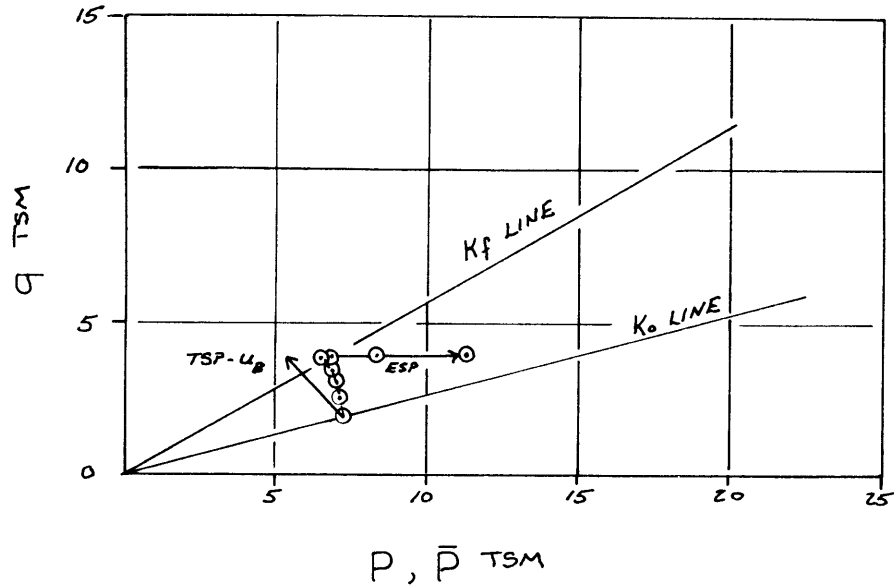
SOIL INDEX PROPERTIES, AND CLASSIFICATION

TABLE 4.1



PLASTICITY CHART

FIG.4.4.4

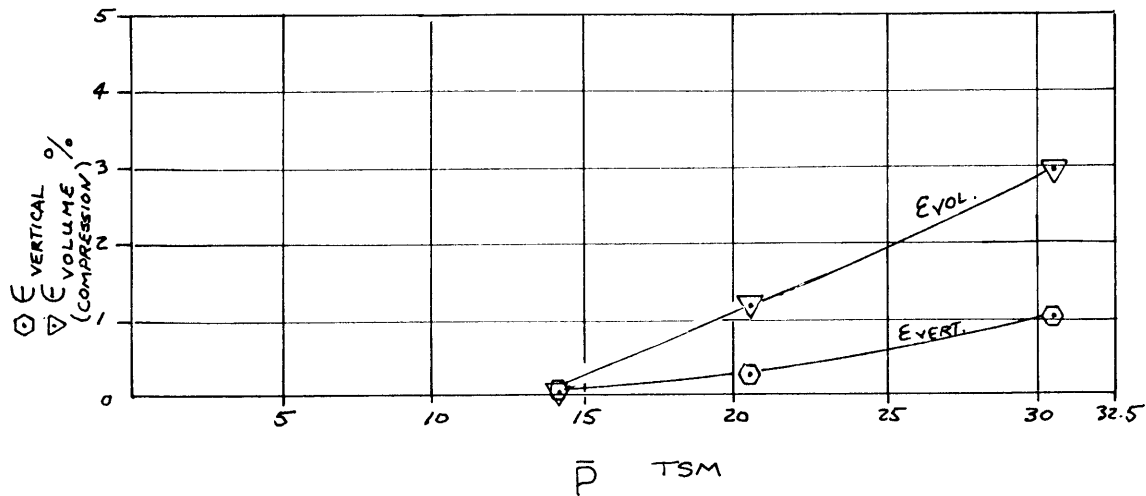
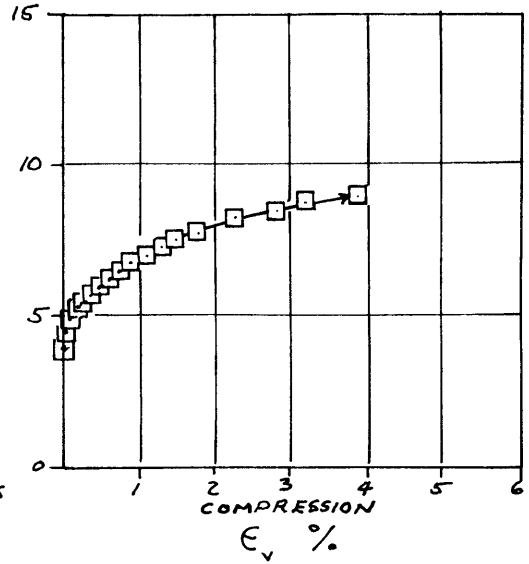
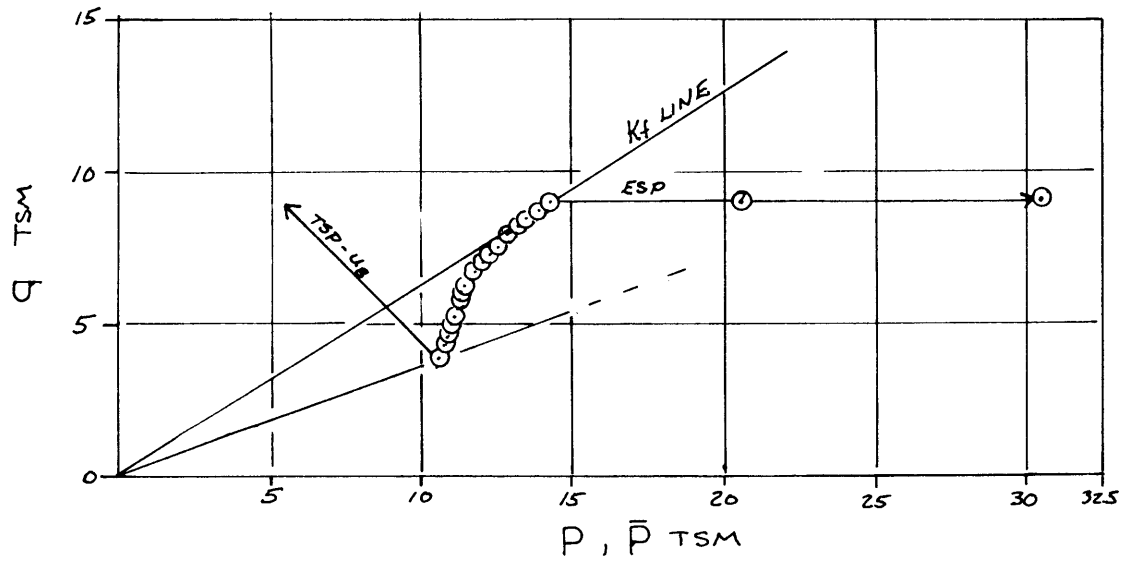


NOTES :

1. STRESS CONTROLLED $CK_0UC(u)$
2. BORING 2-2 DEPTH 10 METERS

STRESS PATH TEST TC-1

FIG.4.4.5_a

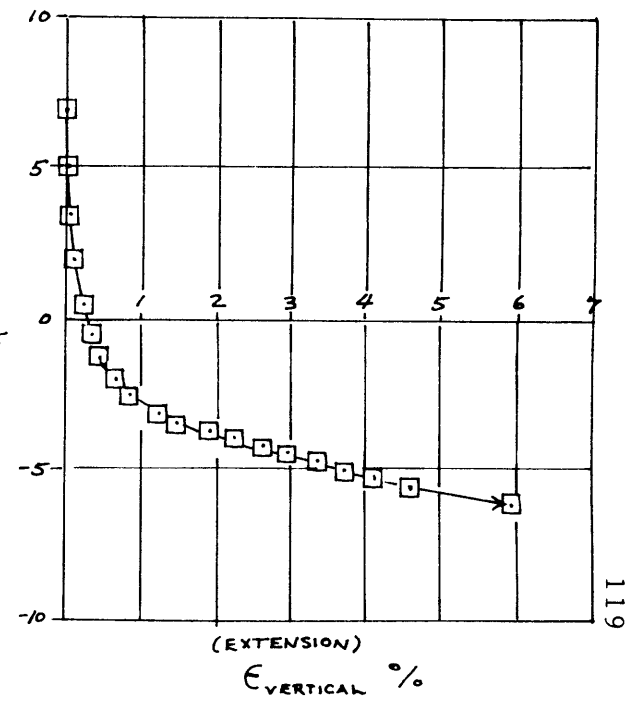
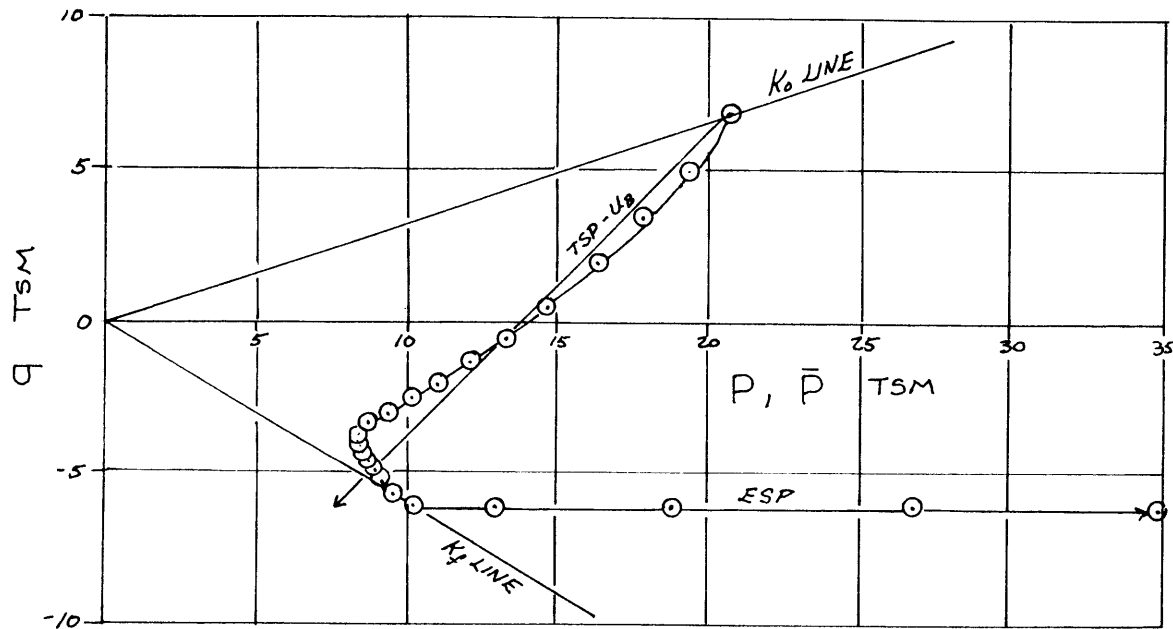


NOTES :

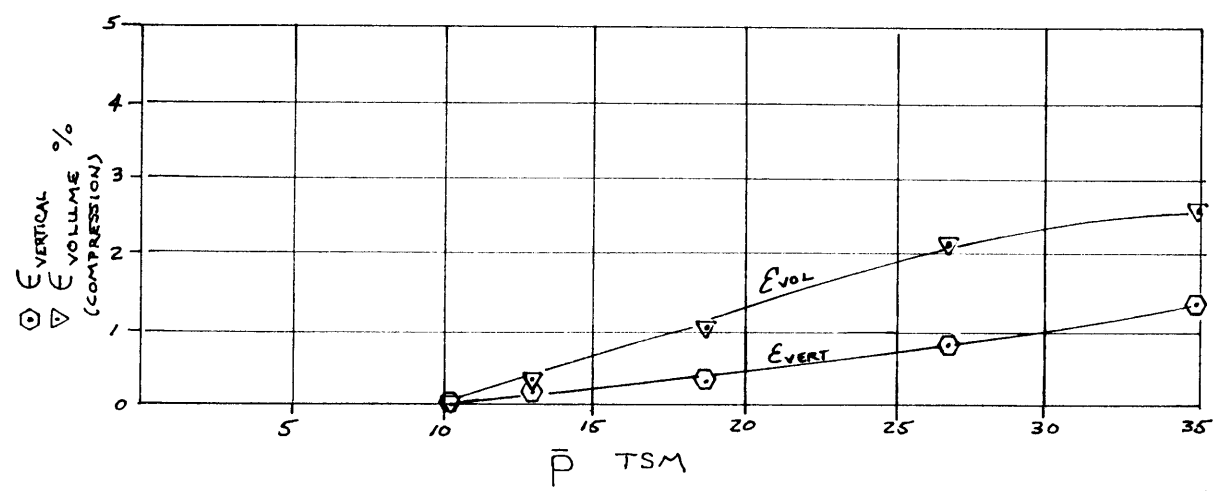
1. STRESS CONTROLLED $\overline{CK}_0 \overline{UC}(U)$
2. BORING 3 DEPTH 19 METERS

STRESS PATH TEST TC-2

FIG.4.4.5b



119

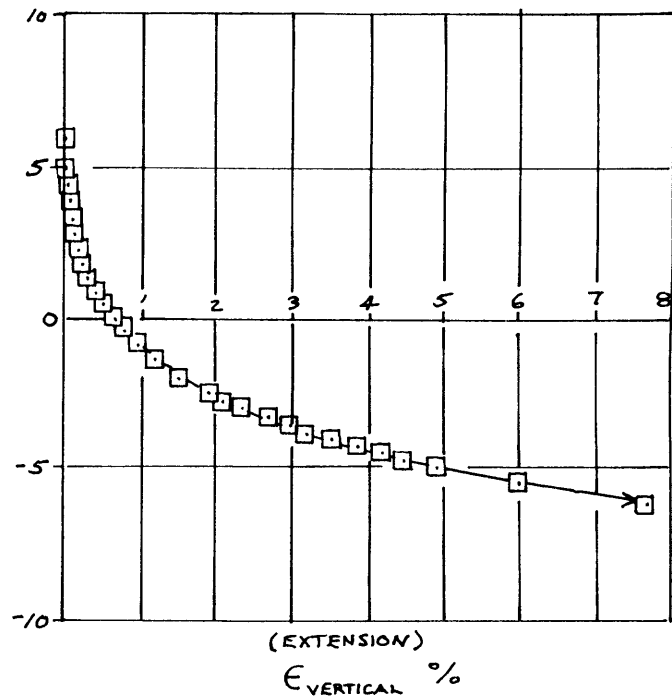
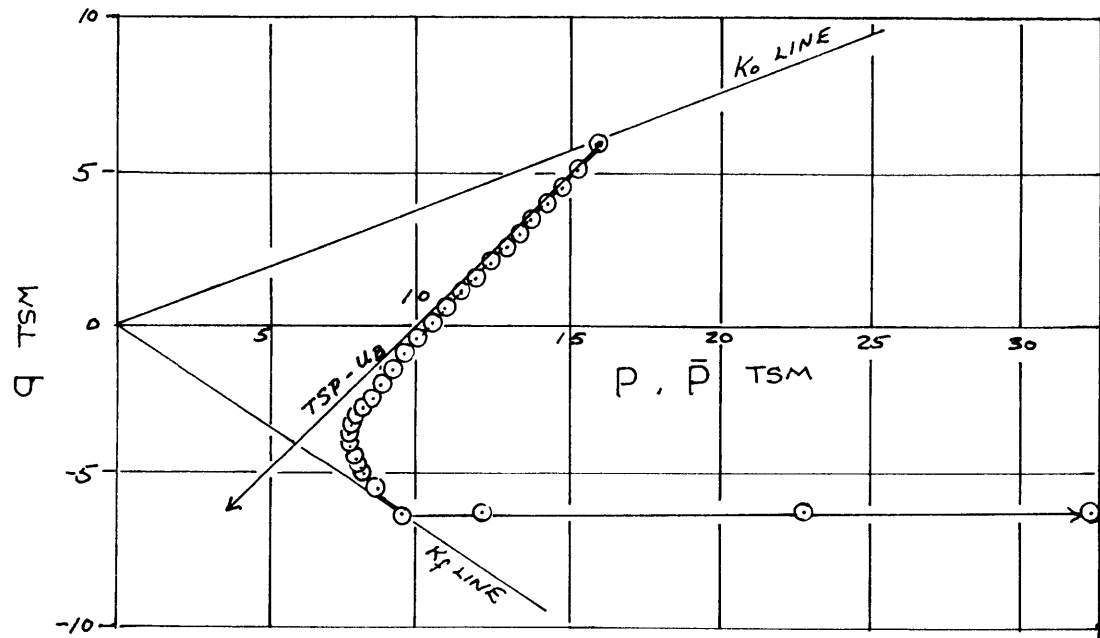


NOTES:

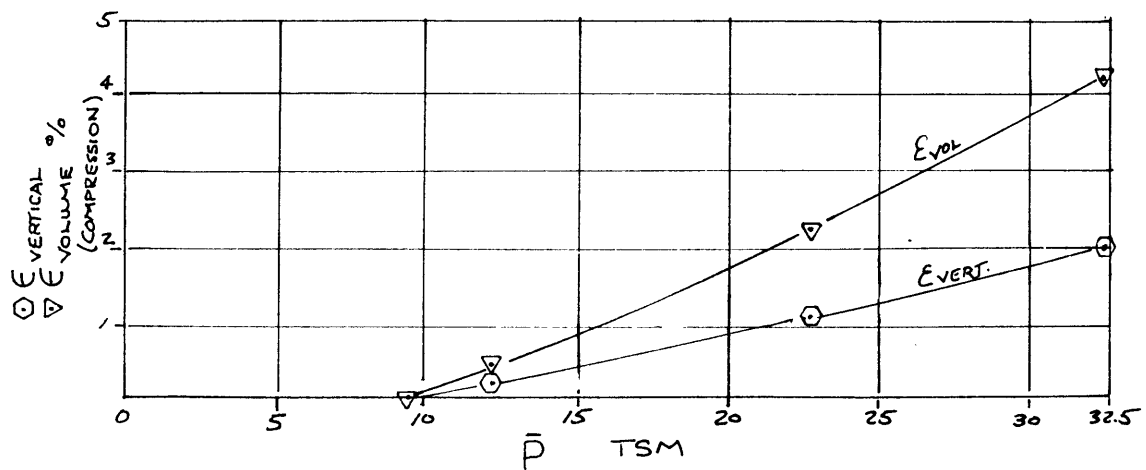
1. STRESS CONTROLLED $C\bar{K}_0\bar{U}\bar{E}(U)$
2. BORING 2-1 DEPTH 34 METERS

STRESS PATH TEST TE-1

FIG. 4.45c



120



NOTES:

1. STRESS CONTROLLED $(\bar{K}_0 \bar{U}E(U))$
2. BORING Z-1 DEPTH 28 METERS

FIG.4.4.5d

STRESS PATH TEST TE-2

Triaxial Test	TC-1		TC-2		TE-1		TE-2	
Depth m	10		19		34		28	
Fitting Method	log t	\sqrt{t}	log t	\sqrt{t}	log t	\sqrt{t}	log t	\sqrt{t}
Pre-Shear	0.27	0.30	7.1	1.1	4.5	0.74	0.26	0.60
	0.03	0.12	3.5	2.0	2.1	0.65	0.22	0.33
			1.4	5.0	0.26	0.85	0.26	0.72
Average	0.15	0.21	3.0	2.7	2.3	1.3	0.25	0.55
Post-Shear		0.08		1.8		1.3		3.1
		0.06		5.0		4.6		0.60
						2.0		0.30
Average		0.07		3.4		2.7		1.3

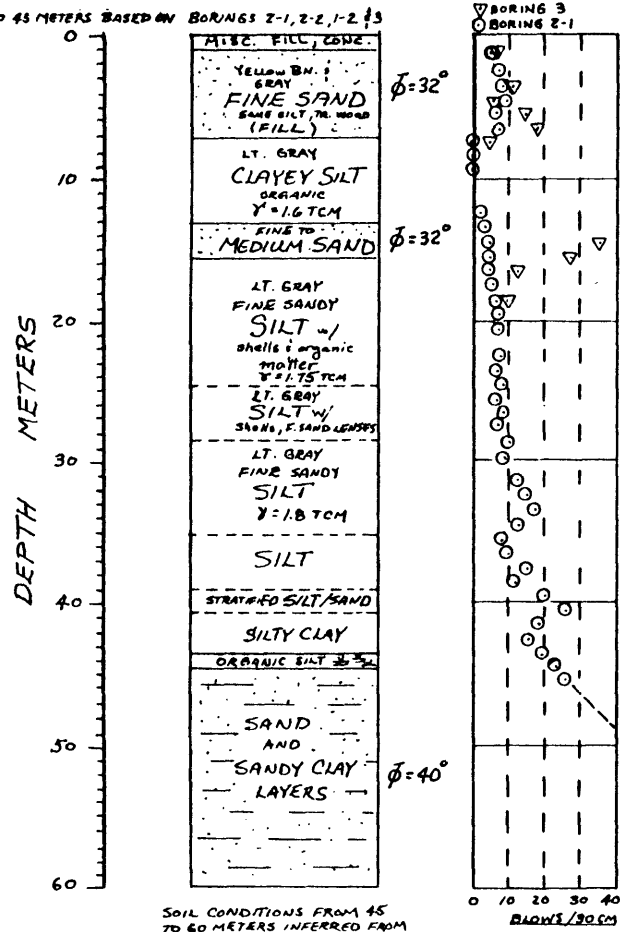
121

COEFFICIENT OF CONSOLIDATION $\text{CM}^2/\text{SEC} \times 10^{-3}$

SUMMARY OF COEFFICIENT OF CONSOLIDATION
DATA FROM STRESS PATH TESTS

TABLE 4.2

0 TO 45 METERS BASED ON BORINGS Z-1, Z-2, 1-2 #3



SOIL CONDITIONS FROM 45 TO 60 METERS INFERRED FROM OLDER BORING DATA FROM SAME GENERAL AREA.

REVISED SOIL PROFILE

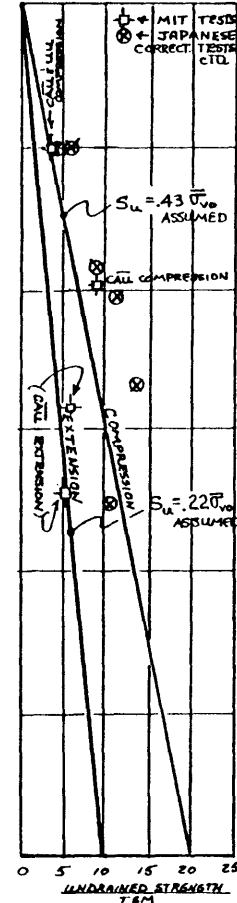
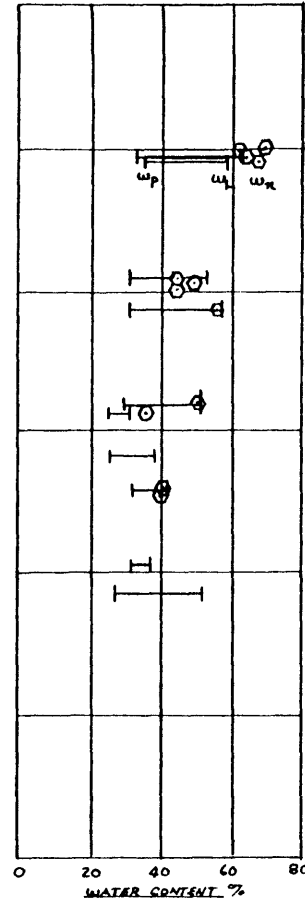
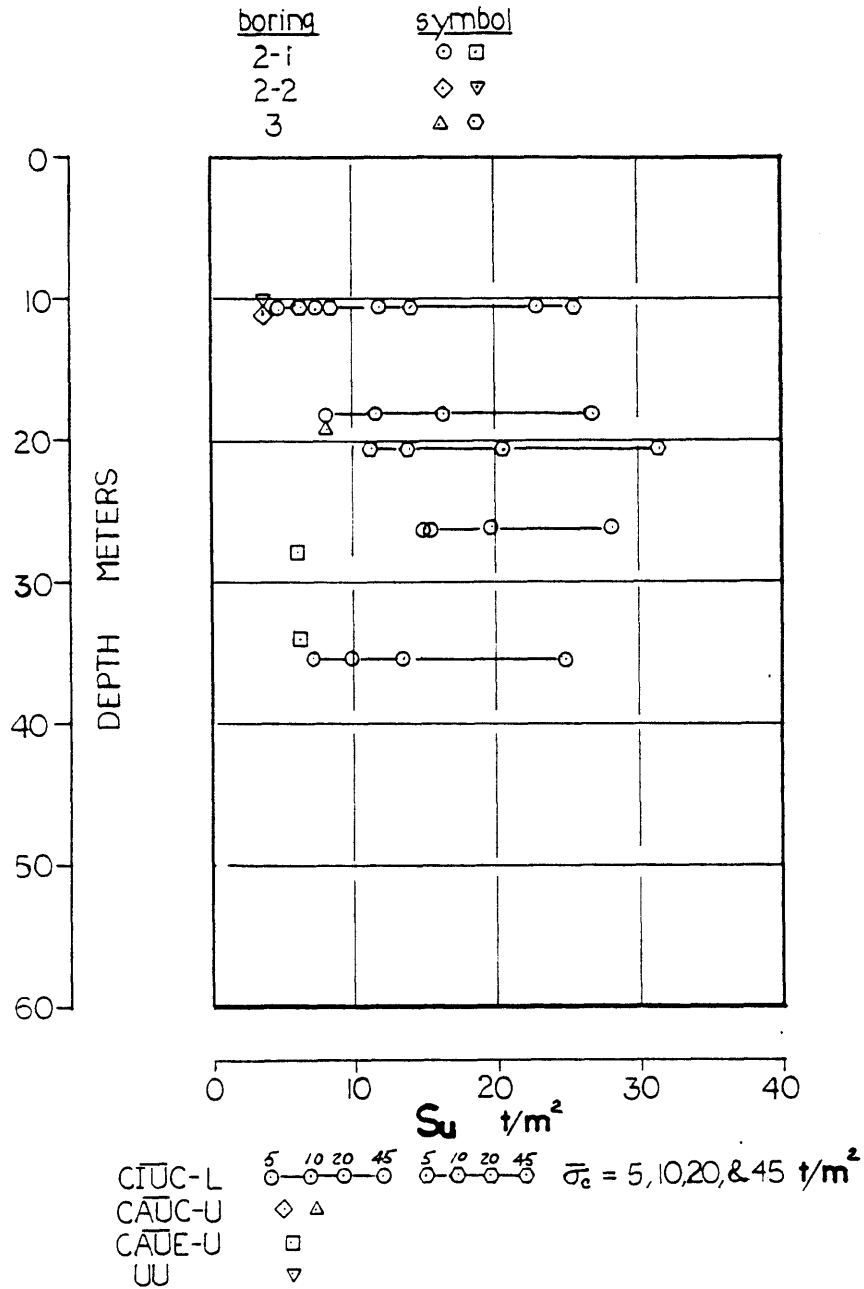


FIG. 44.6



UNDRAINED STRENGTH:
 TRIAXIAL TEST RESULTS VERSUS SAMPLE DEPTH

FIG. 4.4.7

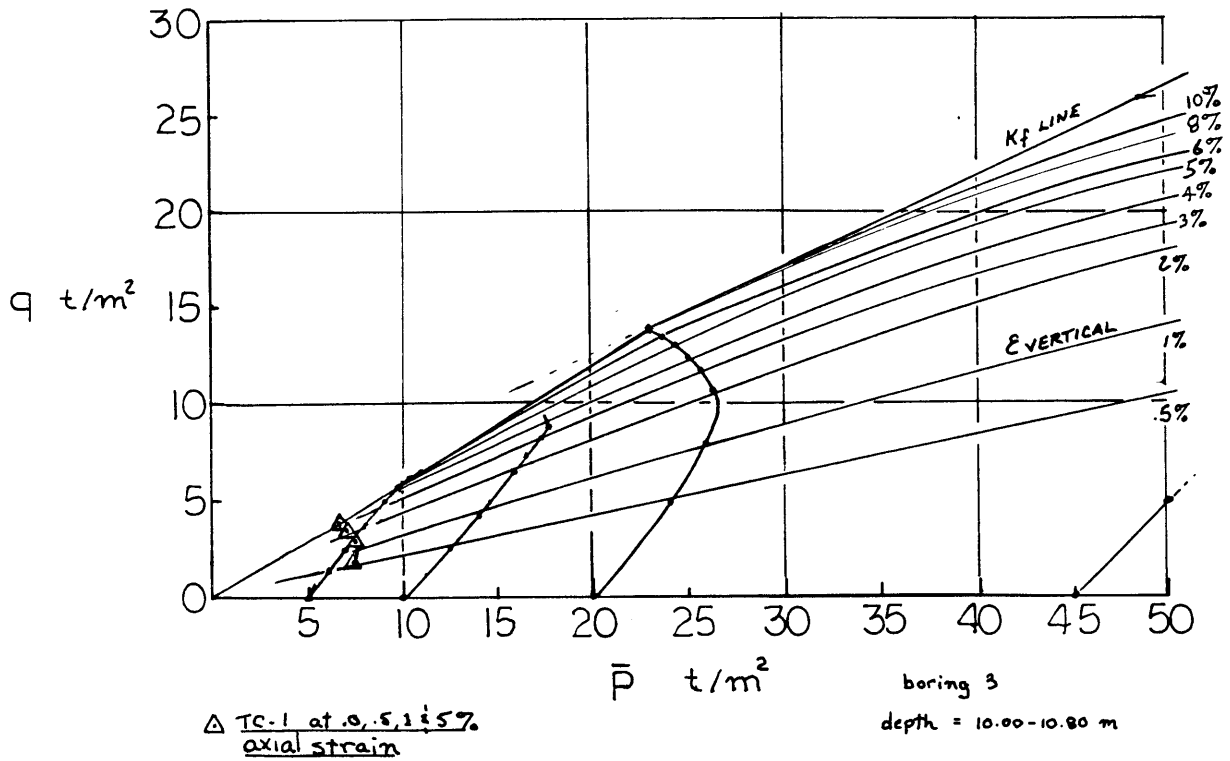
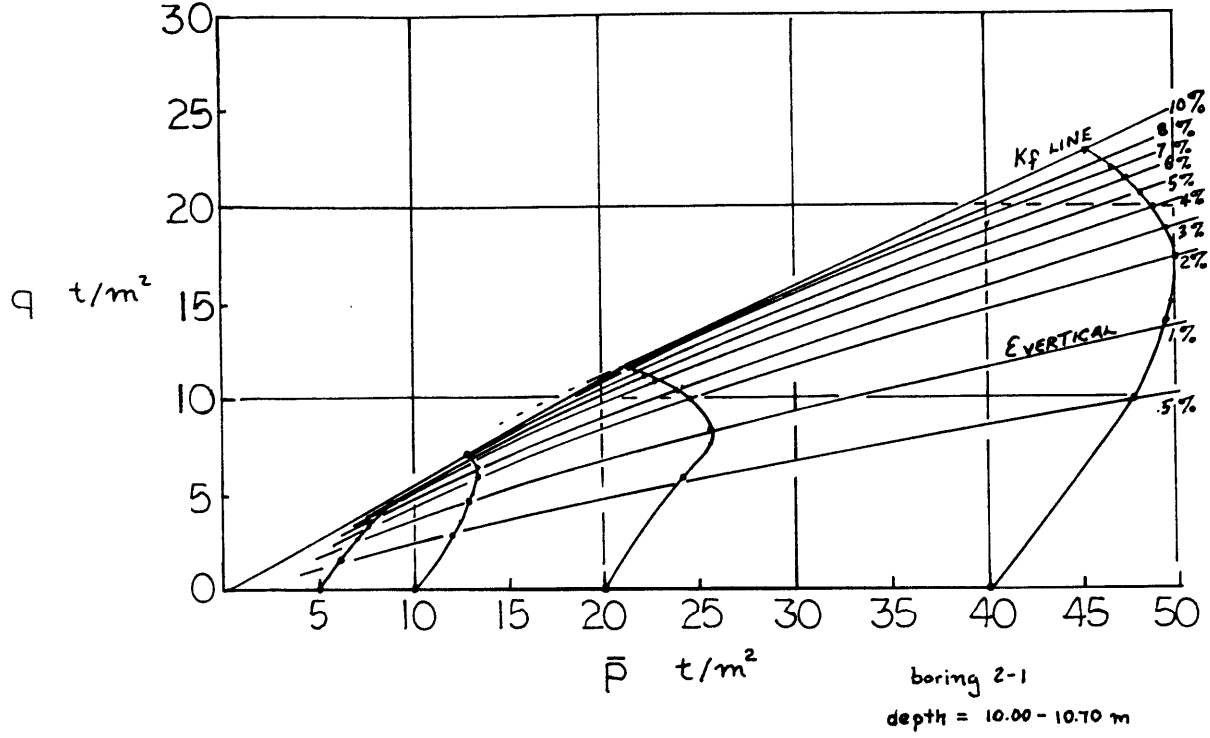
DEPTH	TEST	LAB S_u ①	$\bar{\sigma}_{vo}$ TSM	$\bar{\sigma}_{hd}$ TSM	$\bar{\sigma}_{oct}$ TSM	\bar{C}_{IU} CORRECTED S_u	$S_u / \bar{\sigma}_{vo}$	REMARKS
10.2 ± (METERS)	CIUC(L)	7.1 (TSM)	~9	4.5	6	5.7	.63	②
10.3 ±	CIUC(L)	5.25	~9	4.5	6	4.2	.47	②
10.3 ±	UU(L)	3.9	~9	4.5	6	—	.43	—
10.3 ±	CAUC(U)	3.9	~9	4.5	6	—	.43	TC-1
18.4 ±	CIUC(L)	11.6	~14.5	7.25	9.7	9.3	.64	②
19.3 ±	CAUC(U)	9.0	~15.2	7.6	10.1	—	.59	TC-2
20.4 ±	CIUC(L)	14.4	~16	8	10.7	11.5	.72	②
26.4 ±	CIUC(L)	16.9	~20.5	10.25	13.7	13.5	.66	②
28.3 ±	CAUC(U)	6.0	~22.0	11	14.7	—	.27	TE-2
34.3 ±	CAUC(U)	6.2	~27.5	13.75	18.3	—	.22	TE-1
35.3 ±	CIUC(L)	13.0	~28.3	14.1	18.9	10.4	.37	②

① \bar{C}_{IU} STRENGTHS EXTRAPOLATED FROM A SERIES OF TESTS AT DIFFERENT CONFINING PRESSURES (SEE TEXT)

② TESTS RUN AT A STRAIN RATE OF 0.5% PER MINUTE

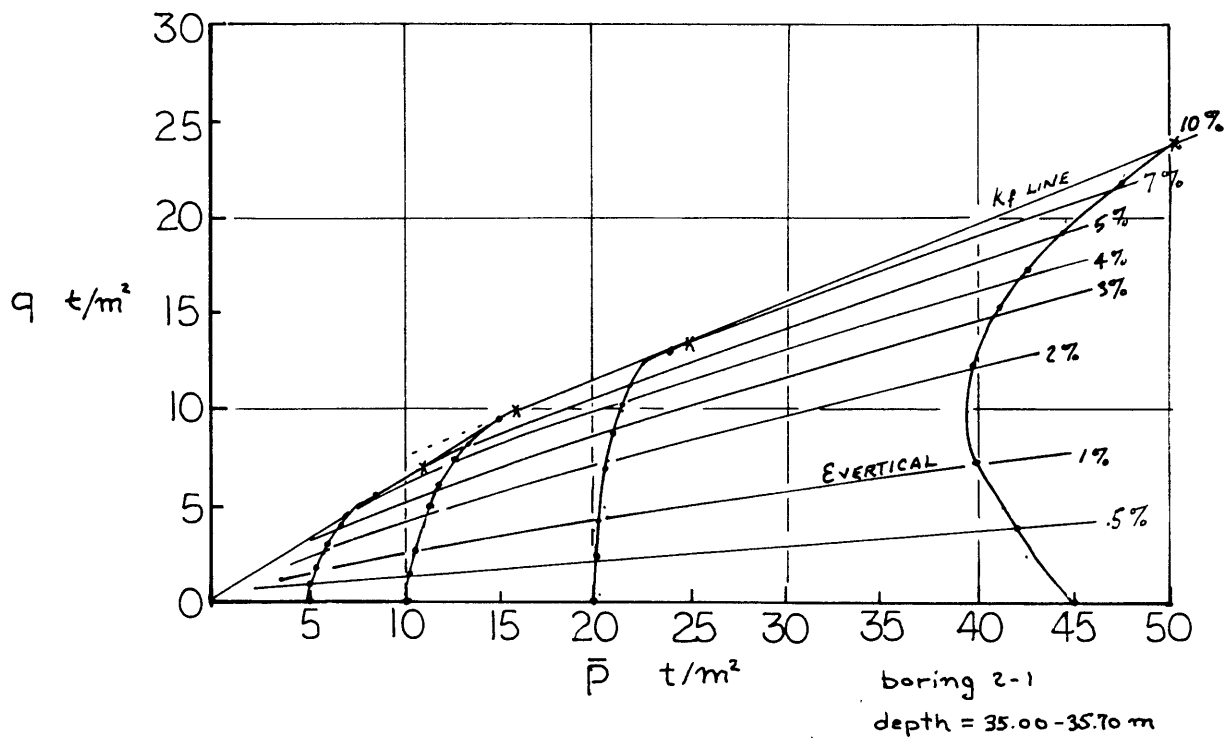
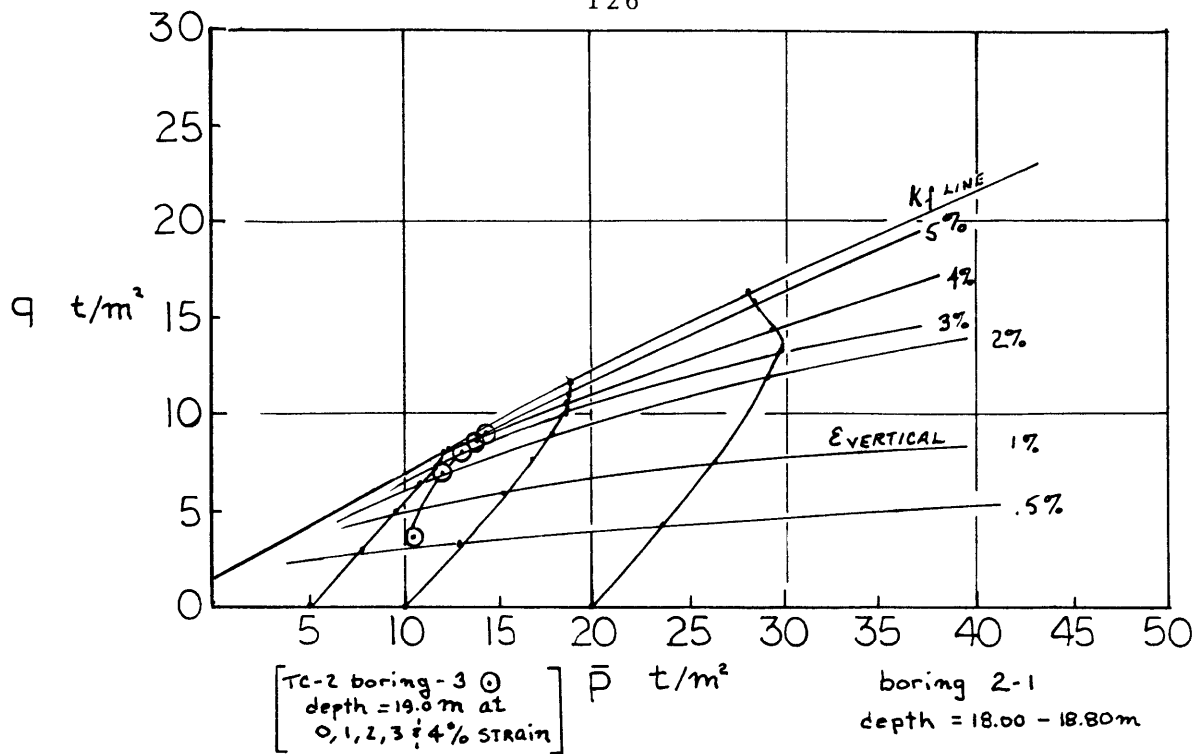
SUMMARY OF SHEAR STRENGTH DATA

TABLE 4.3



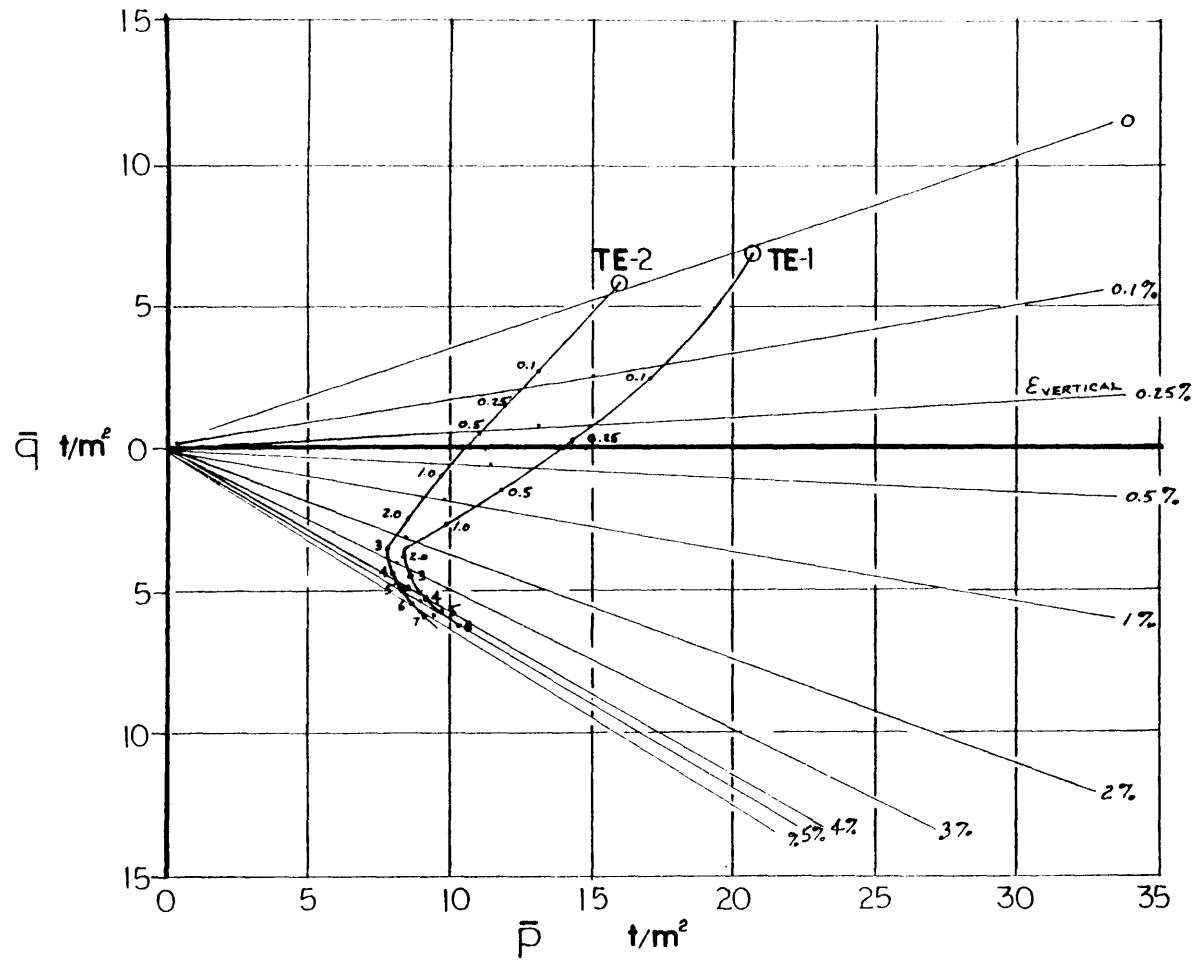
ESTIMATED CONTOURS OF EQUAL STRAIN - COMPRESSION

FIG. 4.4.8a



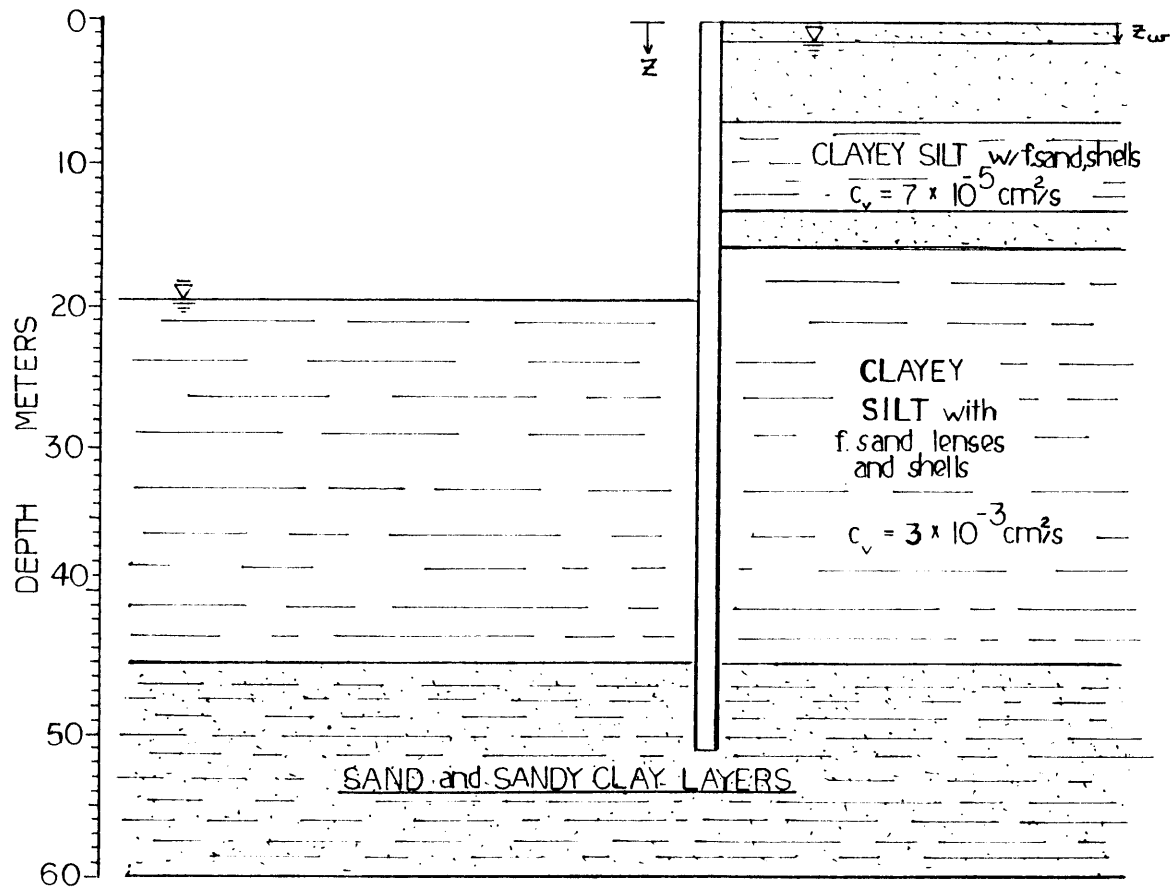
ESTIMATED CONTOURS OF EQUAL STRAIN - COMPRESSION

FIG. 4.4.8b



ESTIMATED CONTOURS OF EQUAL STRAIN - EXTENSION

FIG. 44.8c



SIXTH EXCAVATION STAGE SIMPLIFIED PROFILE

FIG.44.9

INSIDE EXCAVATION

E.L.	DEPTH	P-u _o	q _o	σ ₁	σ ₂	σ ₃	ε _v	EXCESS		EXCESS	DISSIPATED			ε _{vol}	ε _{vc}	ε _{hc}	ε _{vs}	ε _{hs} ^z	ε _{vt}	ε _{nt}	ν	E _v	
								u _p	u _{zd}		u _e	u _{TE}	Δu _D										Δu _E
227	39.3	23.6	7.9	13.5	12.5	10.5	1.55	4.0	—	11.5	0.16	—	1.84	1.84	0.12	0.04	0.04	1.4	0.7	1.36	0.74	.53	382
231	30.8	18.6	6.2	10.6	3.0	9.2	0.89	10.0	—	16.0	0.01	—	0.16	0.15	0.06	0.02	0.02	1.8	0.9	1.78	0.92	.52	333
235	24.8	14.9	5.0	8.6	0.9	8.0	0.42	14.3	.24	17.0	0.17	*3.5	2.9	0.6	0.5	0.17	0.17	1.5	0.75	*1.67	0.58	.35	359
284	43.5	26.1	8.7	15.0	13.1	9.4	1.88	1.1	—	13.0	0.72	—	9.4	9.4	0.27	0.09	0.09	0.4	0.2	*.31	0.29	.93	452
290	29.3	17.6	5.9	10.1	1.2	7.8	0.77	11.1	—	19.0	0.02	—	0.4	0.4	0.18	0.06	0.06	1.1	0.55	*1.04	0.66	.59	365
295	21.8	13.1	4.4	3.9	4.7	5.5	0.18	16.4	63	13.0	0.56	*0.3	7.3	3.0	1.2	0.4	0.4	7.0	3.5	6.6	3.9	.59	300
342	43.5	26.1	8.7	7.7	9.8	8.4	1.88	1.1	—	16.5	0.72	—	11.2	0.3	0.1	0.1	0.1	0.05	0.05	0	0.15	—	∞
344	36.3	21.8	7.3	6.4	3.7	6.3	1.32	6.1	—	17.0	0.64	—	0.7	0.7	0.05	0.017	0.017	0.31	0.155	*.317	0.138	0.43	631
348	29.3	17.6	5.9	5.2	3.9	5.6	0.77	11.1	—	14.0	0.62	—	0.3	0.3	0.1	0.03	0.03	5.0	2.5	5.03	2.47	0.49	457
352	23.3	14.6	4.7	4.1	11.0	4.2	0.30	15.3	.44	18.0	0.33	*6.8	5.9	0.9	0.65	0.22	0.22	4.5	2.25	4.28	2.47	0.58	416
398	43.5	26.1	8.7	7.7	*7.9	6.5	1.88	1.1	—	17.0	0.72	—	12.2	12.2	0.36	0.12	0.12	0.05	*0.25	0.17	0.95	0.56	2588
371	39.3	23.6	7.9	6.9	5.1	6.0	1.55	4.0	—	18.0	0.16	—	2.9	2.9	0.26	0.09	0.09	0.05	*0.25	0.14	0.65	0.46	2714
405	27.8	16.7	5.6	4.9	7.3	3.3	0.65	12.1	.03	15.5	0.045	*0.4	0.7	0.3	0.12	0.04	0.04	2.3	*1.15	2.34	*1.11	.47	760
401	34.6	20.4	6.8	6.0	1.2	4.1	1.14	7.8	—	9.0	0.015	—	0.14	0.14	0.45	0.15	0.15	3.0	*1.5	3.015	1.485	.49	723
427	39.3	23.6	7.9	6.9	3.2	4.0	1.55	4.0	—	6.0	0.16	—	0.96	0.96	0.06	0.02	0.02	2.5	*1.25	2.52	1.23	0.49	952
410	20.3	12.2	4.1	3.6	15.4	2.2	0.06	17.4	.87	22.9	0.86	15.1	19.7	4.6	1.7	0.57	0.57	1.5	*0.75	2.07	*.18	0.09	609
454	43.5	26.1	8.7	7.7	6.0	3.4	1.88	1.1	—	17.0	0.72	—	12.2	12.2	0.36	0.12	0.12	0.15	*0.075	0.27	0.45	0.17	3926
455	39.3	23.6	7.9	6.9	2.4	2.5	1.55	4.0	—	12.0	0.16	—	1.9	1.9	0.15	0.05	0.05	7.0	*0.5	1.05	*.45	.43	1981
457	34.6	20.4	6.8	6.0	3.2	2.1	1.14	7.8	—	13.5	0.015	—	0.2	0.2	0.09	0.03	0.03	1.0	*0.5	1.03	*.47	.46	1728
462	26.8	15.8	5.3	4.6	10.0	2.5	0.57	12.9	.08	17.0	0.08	1.0	1.4	0.4	0.21	0.07	0.07	1.5	*0.75	1.57	*0.68	.43	1032
483	39.3	23.6	7.9	6.9	*1.8	1.1	1.55	4.0	—	13.0	0.16	—	2.1	2.1	0.12	0.04	0.04	0.5	*0.25	0.54	*.21	.40	3333
488	29.3	17.6	5.9	5.2	7.2	*4.3	.77	11.1	—	20.0	0.02	—	0.4	0.4	0.12	0.04	0.04	0.4	*.20	0.44	0.16	.36	2486
494	20.3	12.2	4.1	3.6	15.2	2.2	0.06	17.4	.87	23.0	0.86	*15.1	19.8	4.7	1.7	0.57	0.57	1.5	*0.75	2.07	*.18	.09	609

NOTES
1. COMPRESSIVE STRAINS ASSUMED POSITIVE

SUMMARY OF DETERMINATION OF PARTIALLY
DRAINED STRESS STRAIN MODULI

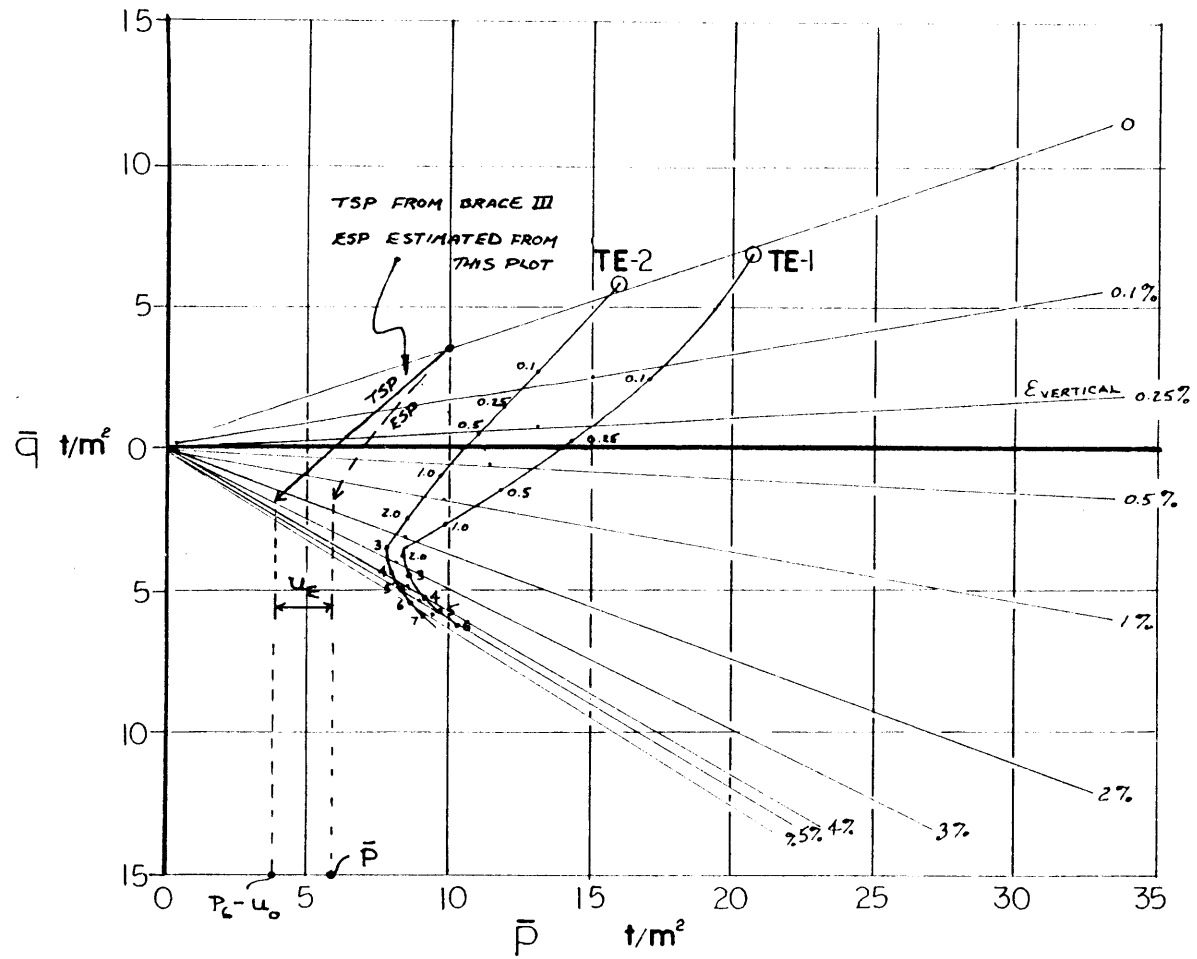
TABLE 4.4

BEHIND EXCAVATION

E.L.	DEPTH	P ₀ -u ₀		z/H _d	EXCESS		EXCESS	EXCESS	DISSIPATED			E _{VOL}	E _{VC}	E _{HC}	E _{VS}	E _{HS}	E _{VT}	E _{HT}	γ	E _V			
		P ₀ -u ₀	q ₀		u ₀	u _{ED}			u _E	u _{ZE}	Δu _D										Δu _E	Δu _T	
13	28.8	17.3	5.8	9.9	16.5	6.7	.88	0	-	-1.3	.01	0	-0.13	-0.13	0	0	0	+0.45	-0.275	+0.45	-0.225	0.50	400
19	34.9	20.9	7.0	12.0	19.3	8.3	1.3	0	-	-2.0	.04	0	-0.8	-0.8	0	0	0	+0.7	-0.35	+0.7	-0.35	0.56	388
21	18.0	10.8	3.6	6.2	9.8	4.8	0.14	0	-	0.0	.64	0	0	0	0	0	0	+0.45	-0.225	+0.45	-0.225	0.50	533
26	38.0	22.8	7.6	13.1	21.8	9.2	1.52	0	-	-2.0	0.13	0	-0.26	-0.26	-0.06	-0.02	-0.02	+0.8	-0.4	+0.78	-0.42	0.54	410
28	25.5	15.3	5.1	8.8	13.9	6.7	0.66	0	-	-2.0	.04	0	-0.8	-0.8	0	0	0	+0.55	-0.225	+0.55	-0.225	0.50	580
30	13.5	8.1	2.7	4.6	7.1	4.0	-	0	-	-	-	0	0	0	0	0	0	+1.25	-0.225	+1.25	-0.225	0.50	208
36	31.8	19.1	6.4	11.0	16.9	8.8	1.09	0	-	-3.9	.01	0	-0.04	-0.04	0	0	0	+1.2	-0.6	+1.2	-0.6	0.5	400
38	19.5	12.7	3.9	7.1	10.1	5.3	0.24	0	-	-3.9	0.42	0	-1.64	-1.64	-1.35	-0.45	-0.45	+1.1	-0.55	+0.65	-1.0	1.54	585
39	13.5	8.1	2.7	4.6	6.7	4.1	-	0	-	-	-	0	0	0	0	0	0	+1.4	-0.70	+1.4	-0.7	0.5	200
44	38.0	22.8	7.6	13.1	19.1	10.7	1.52	0	-	-4.0	0.13	0	-0.52	-0.52	-0.03	-0.01	-0.01	+1.8	-0.9	+1.79	-0.91	0.51	346
46	28.5	17.1	5.7	9.8	13.9	8.45	0.86	0	-	-3.5	0.05	0	-0.05	-0.05	0	0	0	+1.6	-0.8	+1.6	-0.8	0.50	344
48	20.3	12.2	4.0	7.0	9.75	6.3	0.30	0	-	-3.0	0.33	0	-1.0	-1.0	-1.15	-0.38	-0.38	+0.9	-0.45	+0.52	-0.83	1.60	554
56	38.0	27.8	7.6	15.2	16.9	11.3	1.52	0	-	-6.0	0.13	0	-0.78	-0.78	-0.03	-0.01	-0.01	+2.5	-1.25	+2.45	-1.26	0.51	300
59	27.0	16.2	5.4	9.3	11.9	8.1	0.76	0	-	-5.0	0.02	0	-0.10	-0.10	0	0	0	+1.4	-0.7	+1.4	-0.7	0.50	386
65	9.0	6.0	2.0	3.4	5.1	2.75	0.67	0	-	-2.0	0	0	0	0	0	0	0	+0.5	-0.25	+0.5	-0.25	0.50	300
87	41.4	24.8	8.3	14.2	8.5	12.5	1.75	0	-	-17.0	0.42	0	-7.14	-7.14	-0.19	-0.06	-0.06	+2.5	-1.25	+2.44	-1.31	0.52	336
89	33.6	20.2	6.7	11.6	11.6	10.1	1.21	0	-	-9.5	.04	0	-0.38	-0.38	-0.02	-0.00	-0.00	+1.9	-0.95	+1.9	-0.95	0.50	358
92	27.4	16.4	5.5	9.4	5.9	8.0	0.79	0	-	-11.5	.02	0	-0.23	-0.23	-0.10	-0.03	-0.03	+1.25	-0.625	+1.22	-0.625	0.54	490
95	21.4	12.8	4.25	7.3	8.1	6.2	0.37	0	-	-3.0	0.23	0	-0.7	-0.7	-0.6	-0.2	-0.2	+1.0	-0.5	+0.8	-0.70	0.88	489
139	43.5	26.1	8.7	15.0	12.3	13.9	1.90	0	-	-16.0	0.78	0	-12.5	-12.5	-0.36	-0.12	-0.12	+3.5	-1.75	+3.38	-1.87	0.55	308
140	39.3	23.6	7.9	13.5	9.8	12.9	1.61	0	-	-15.0	0.20	0	-3.0	-3.0	-0.15	-0.05	-0.05	+3.2	-1.6	+3.15	-1.65	0.52	317
145	29.3	17.6	5.9	10.1	9.0	8.4	0.92	0	-	-10.0	0.01	0	-1.0	-1.0	0	0	0	+1.5	-0.75	+1.5	-0.75	0.50	333
150	21.8	13.1	4.4	7.5	10.0	3.7	0.40	0	-	-4.0	0.19	0	-0.76	-0.76	-0.75	-0.25	-0.25	+0.4	-0.2	+0.2	-0.05	-	215
158	9.75	6.3	2.1	3.6	5.0	2.05	0.92	0	-	-1.0	-0	0	0	0	0	0	0	+0.33	-0.16	+0.33	-0.16	0.50	~300

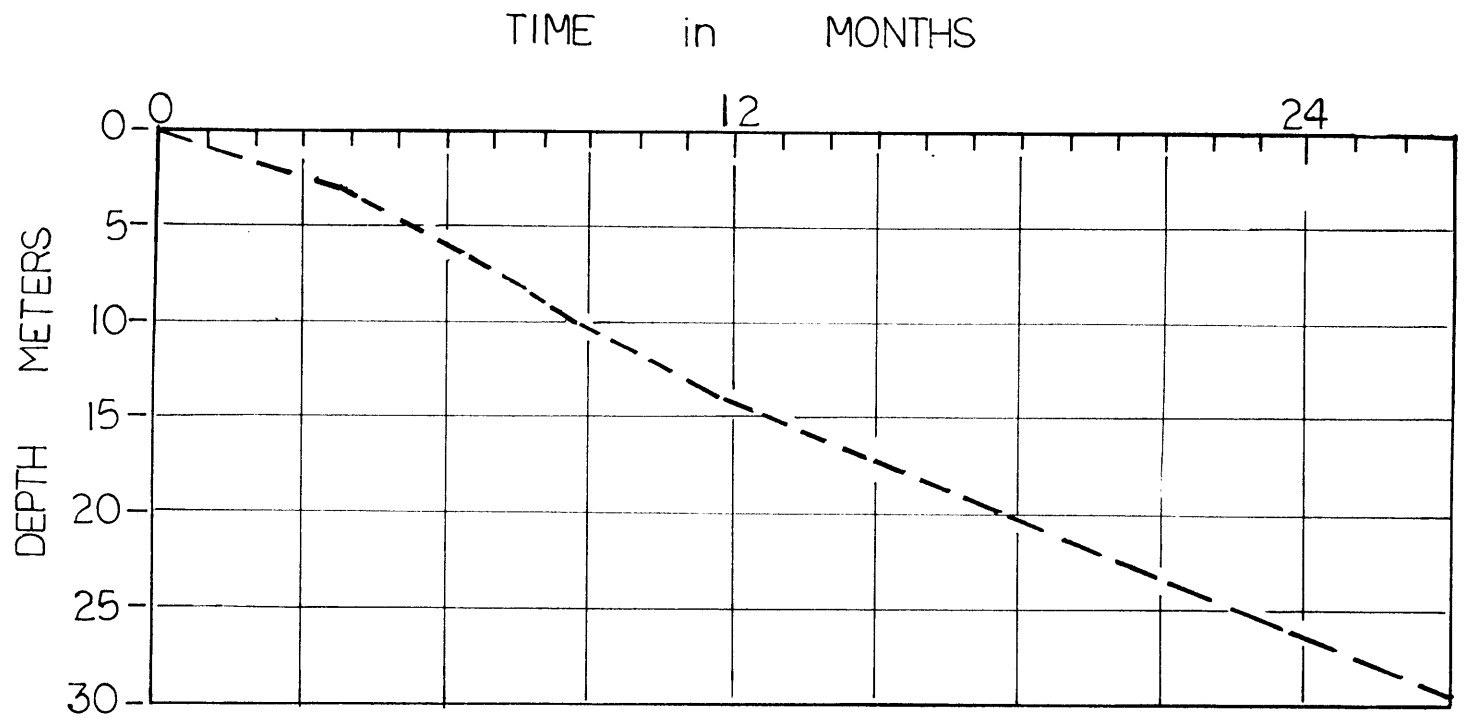
NOTE: MODULUS VALUES 25-10% IN ERROR DUE TO COMPUTING ERRORS

TABLE 4.4
(CONTINUED)



SUPERPOSITION OF TOTAL STRESS PATH
ON CONTOUR PLOT OF EQUAL STRAIN

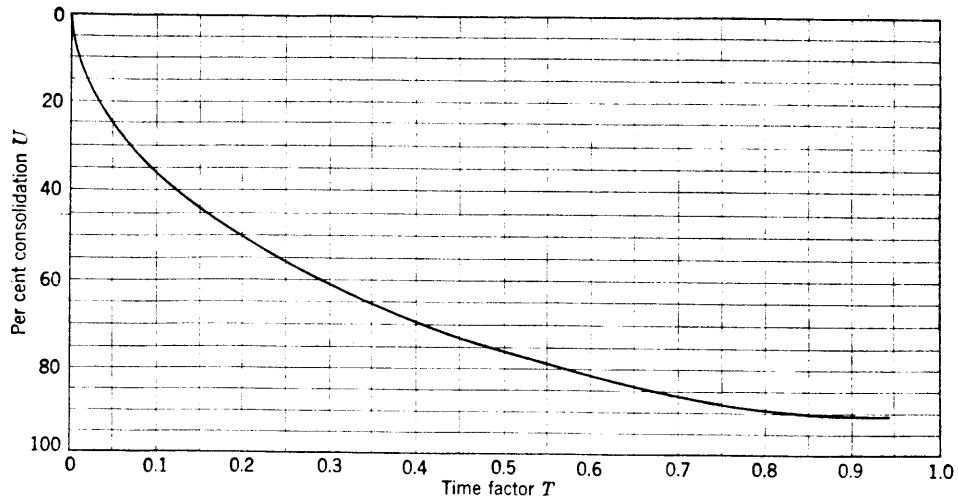
FIG. 44.10



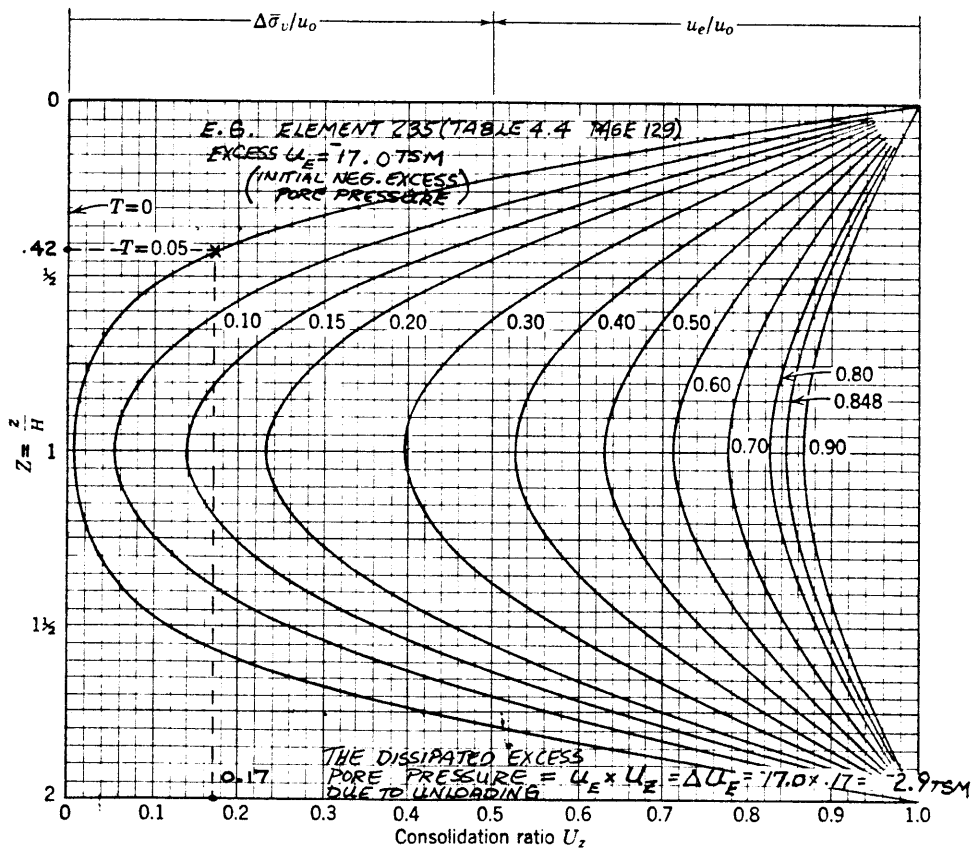
132

DEPTH OF EXCAVATION VS. TIME

FIG.4.4.II



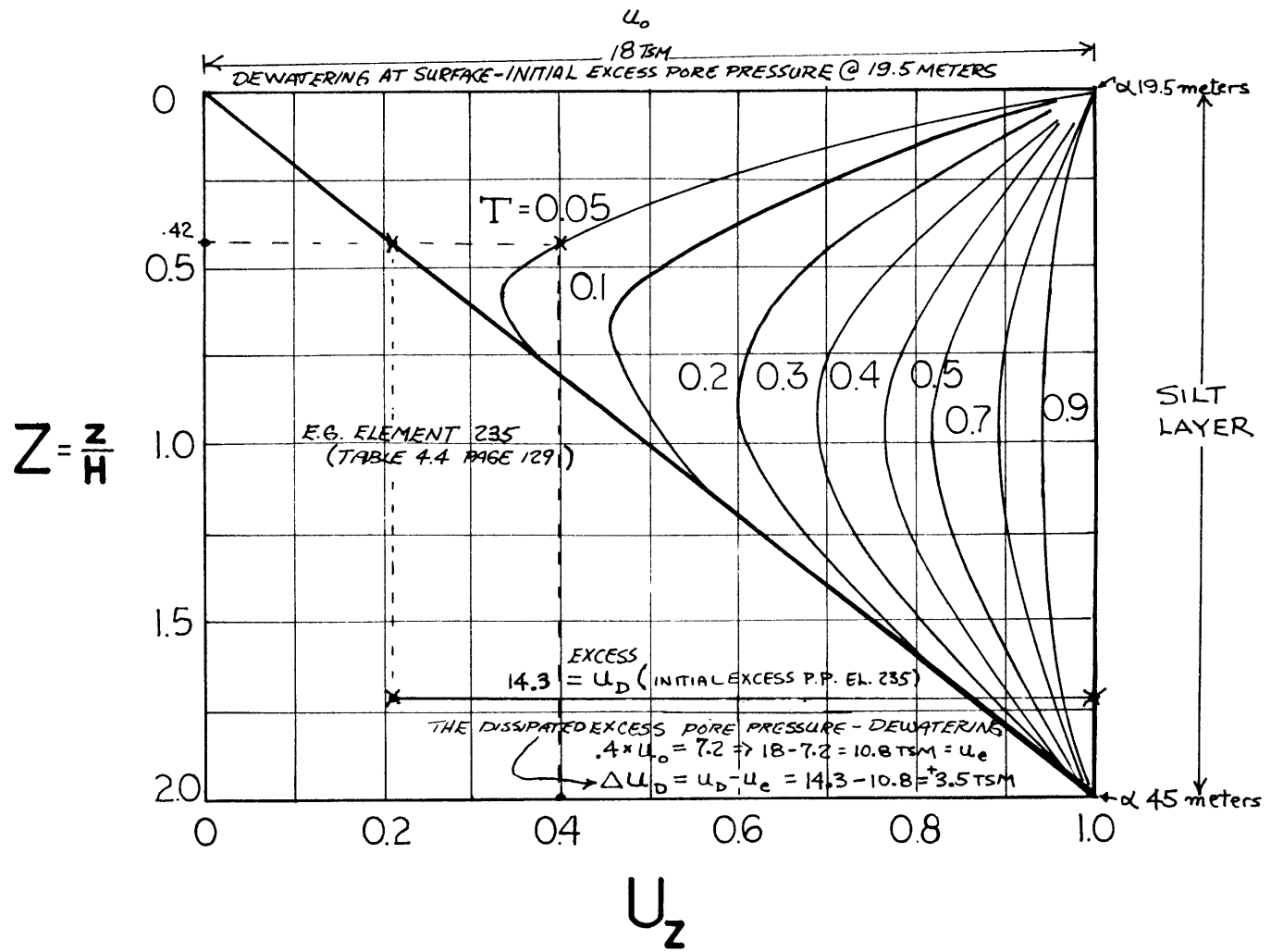
4.4.12a TIME FACTOR VS. AVERAGE DEGREE OF CONSOLIDATION



4.4.12b NORMALIZED DEPTH VS. CONSOLIDATION RATIO

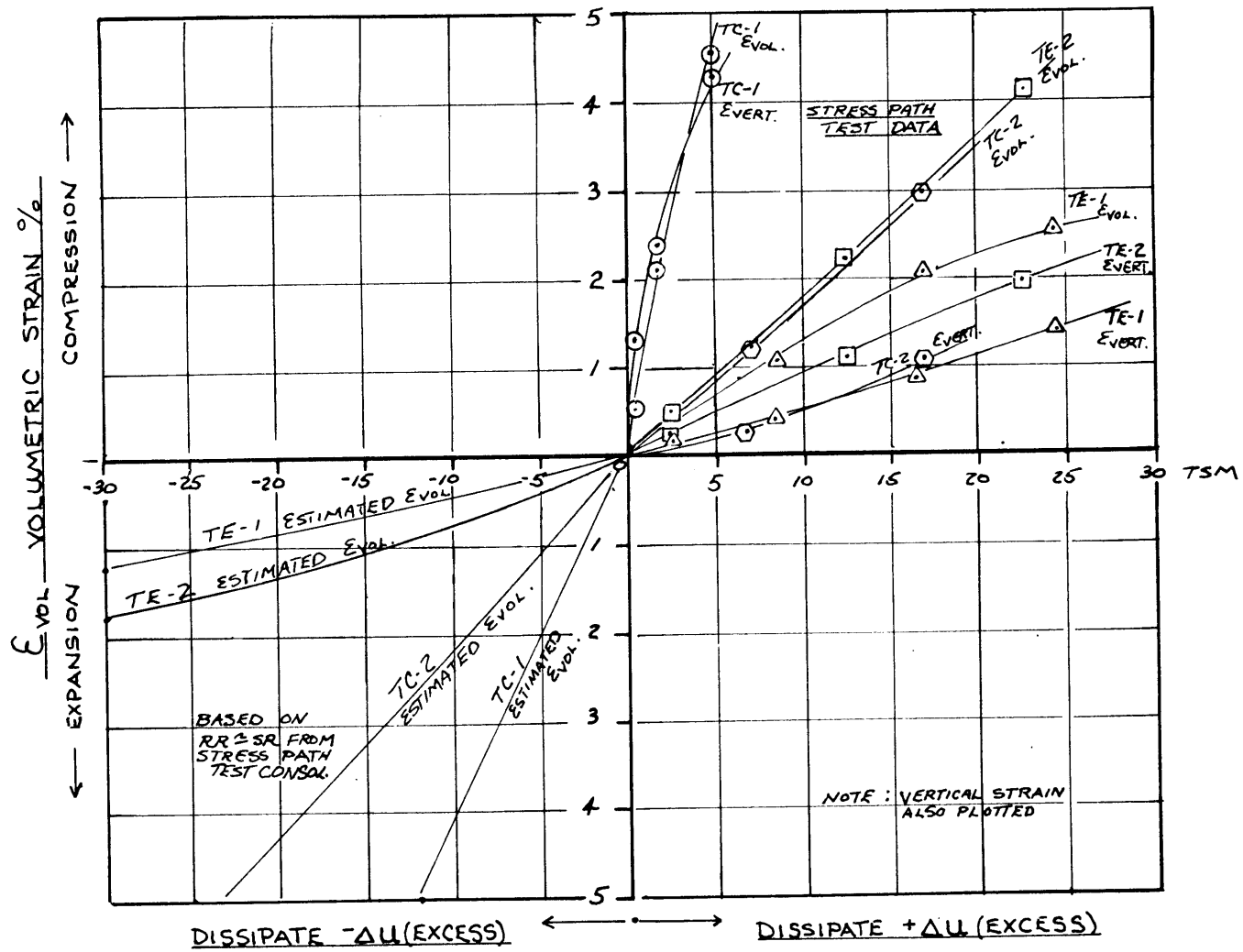
FROM LAMBE & WHITMAN (1969)

FIG. 4.4.12



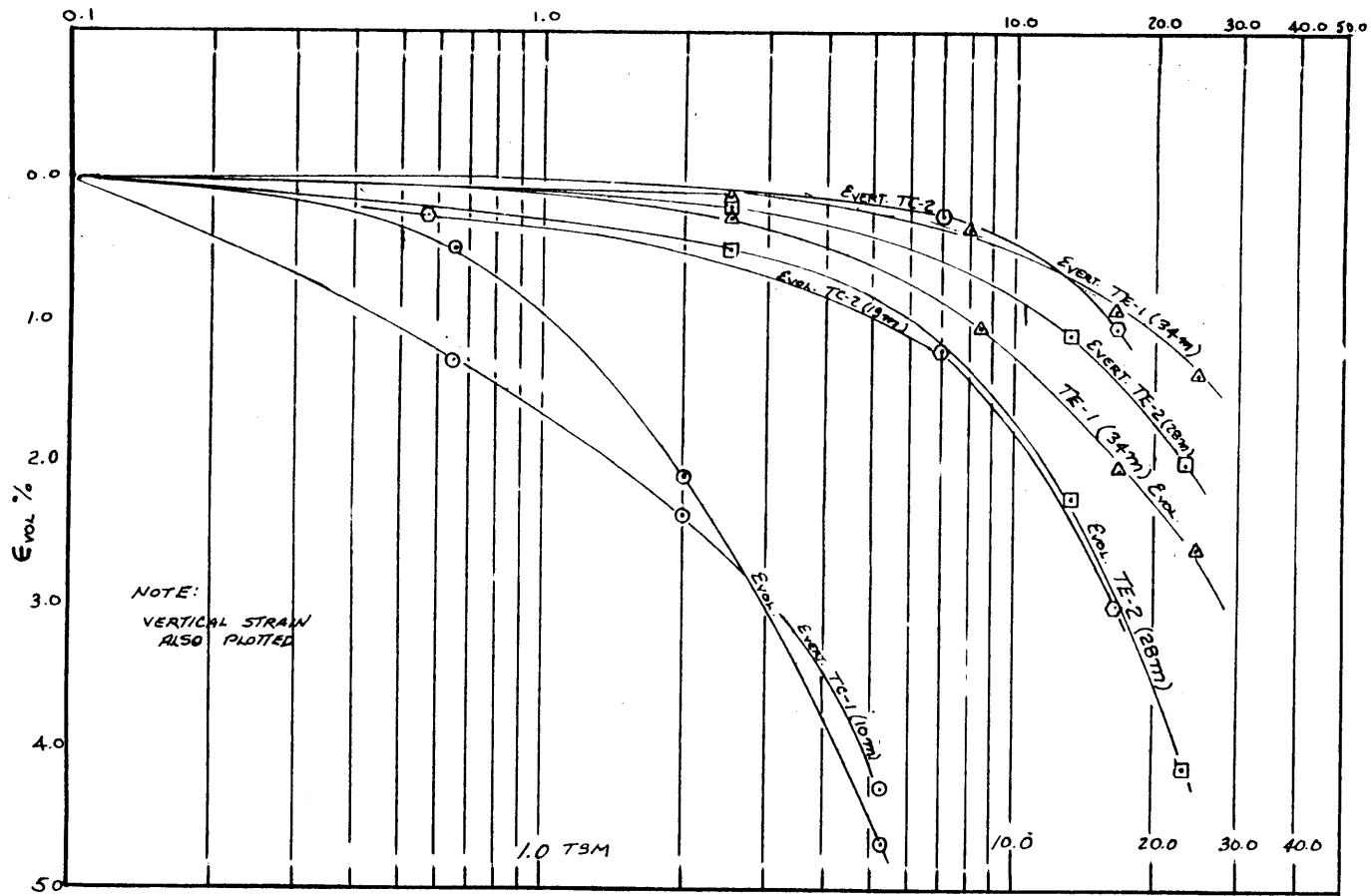
NORMALIZED DEPTH VS. CONSOLIDATION RATIO FOR TRIANGULAR INITIAL EXCESS PORE PRESSURE

FIG. 4.4.13



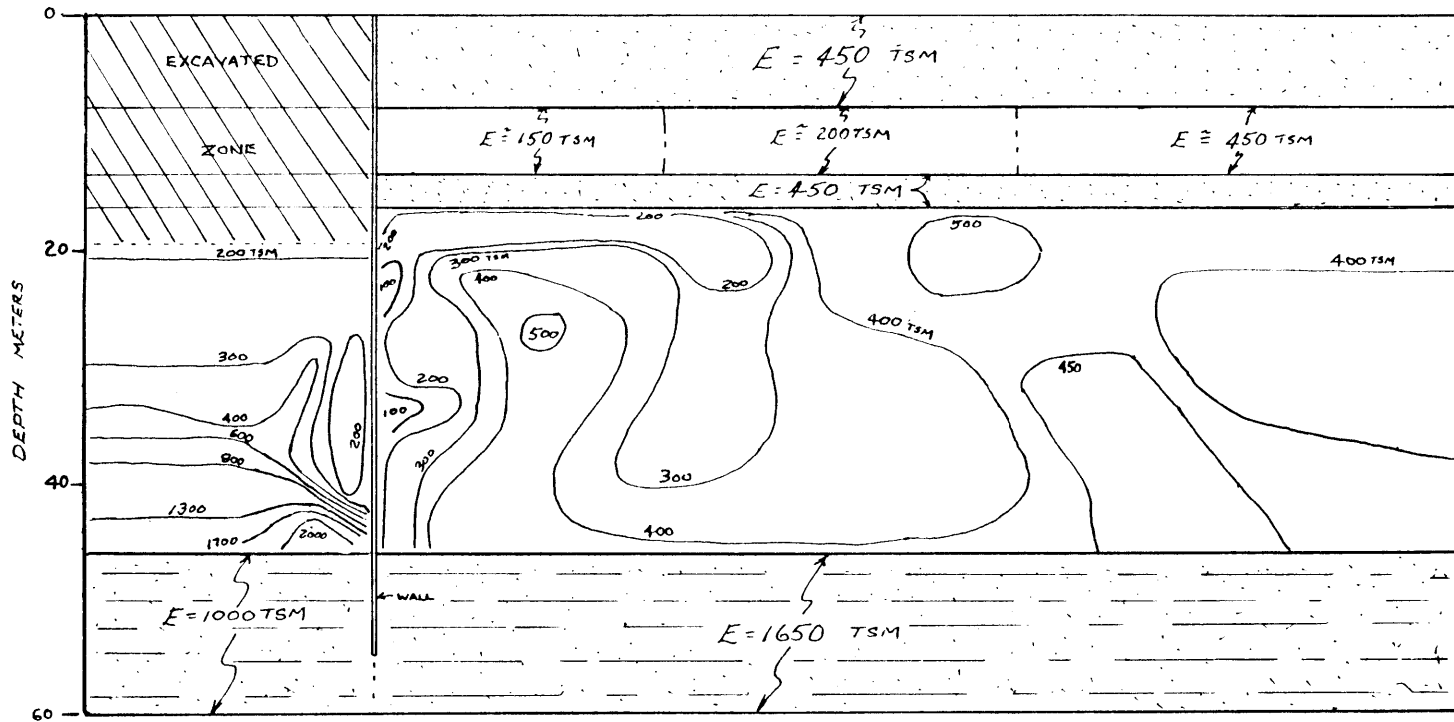
VOLUMETRIC STRAIN VS DISSIPATION OF PORE PRESSURE

FIG.4.4.14a



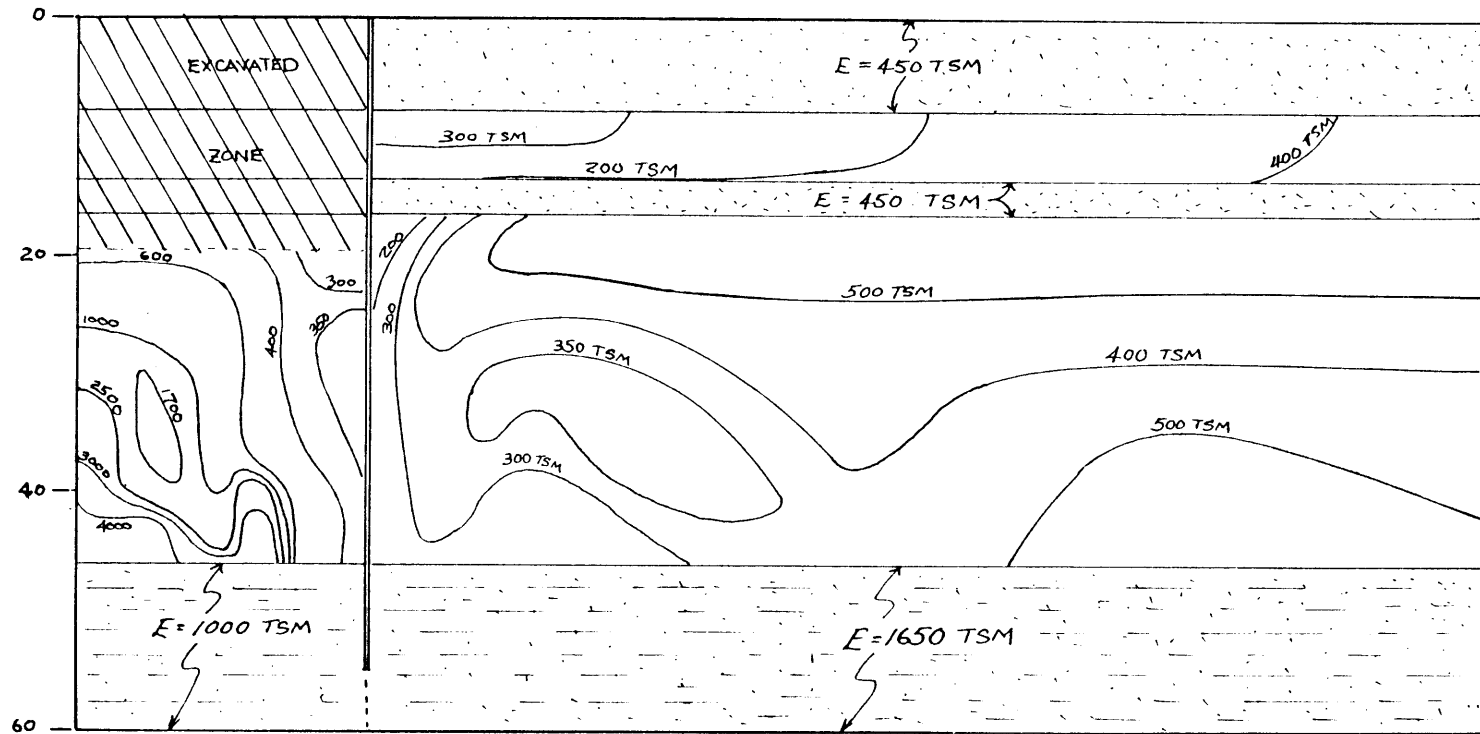
VOLUMETRIC STRAIN VS. LOGARITHMIC DISSIPATION OF PORE PRESSURE

FIG. 44.14b



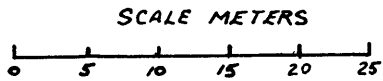
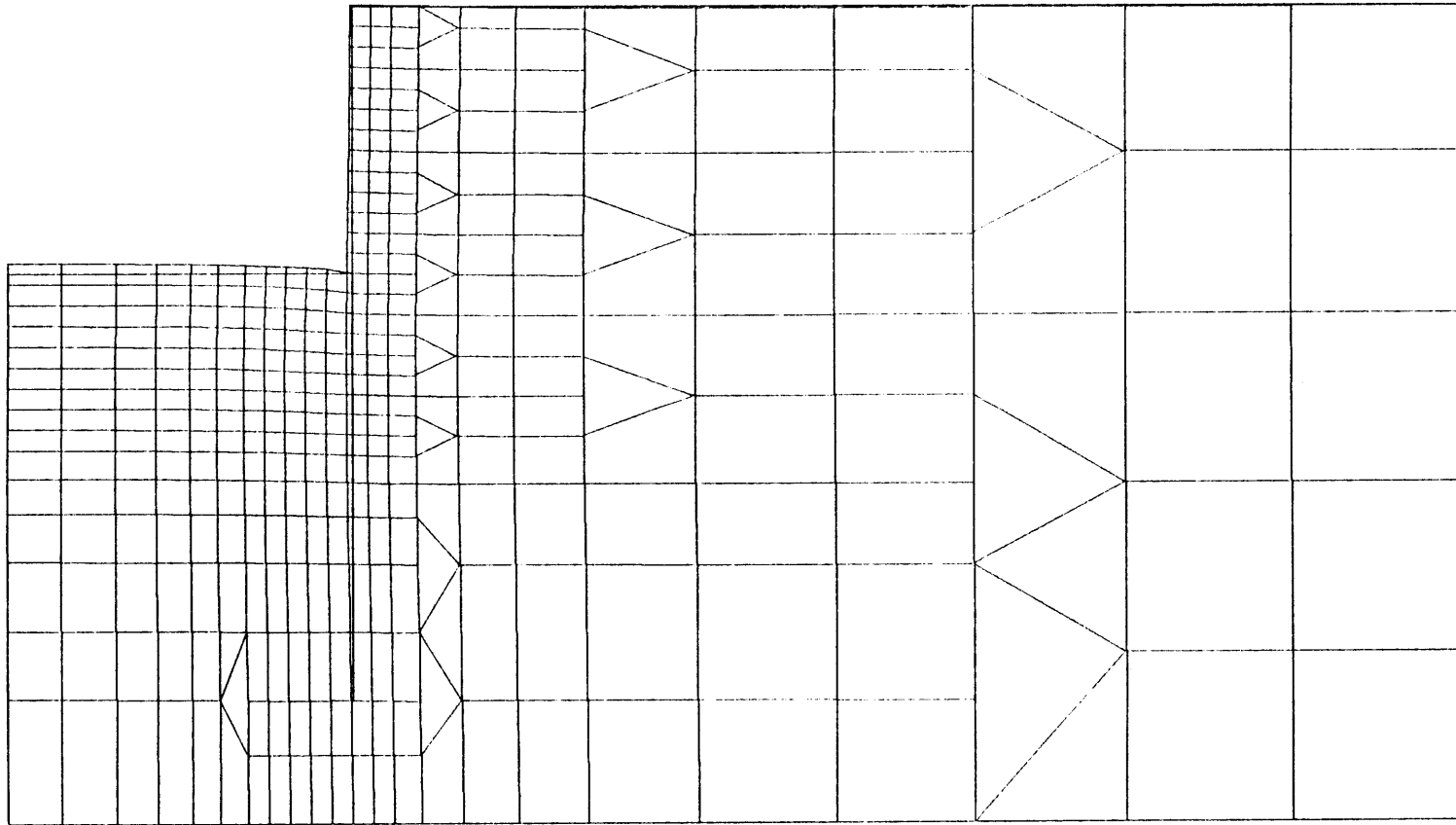
CONTOURS OF MODULI - BRACE III ANALYSIS - REVISED RUN NO. B

FIG. 44.15



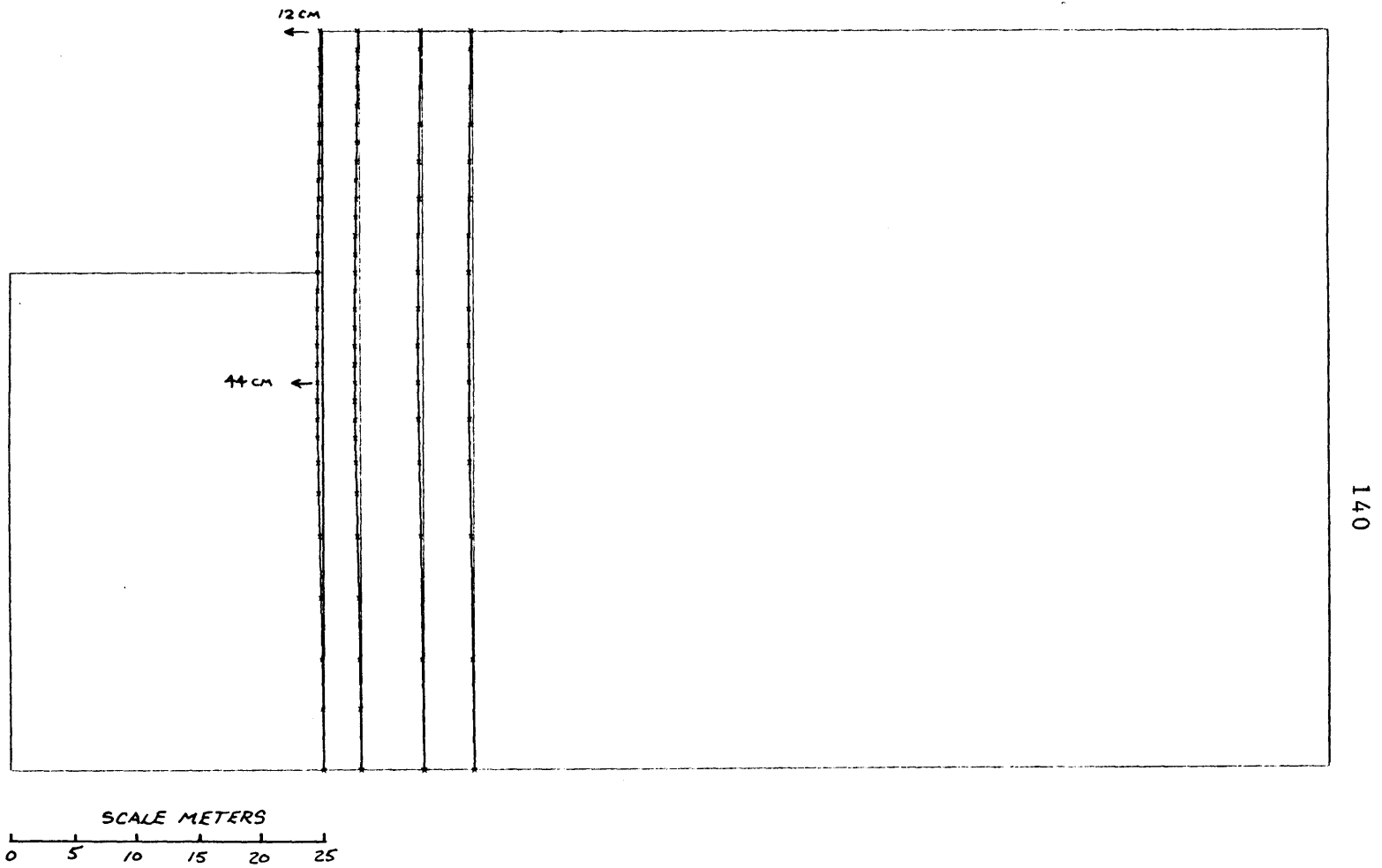
CONTOURS OF MODULI - BRACE III ANALYSIS - FINAL RUN C

FIG.4.4.16



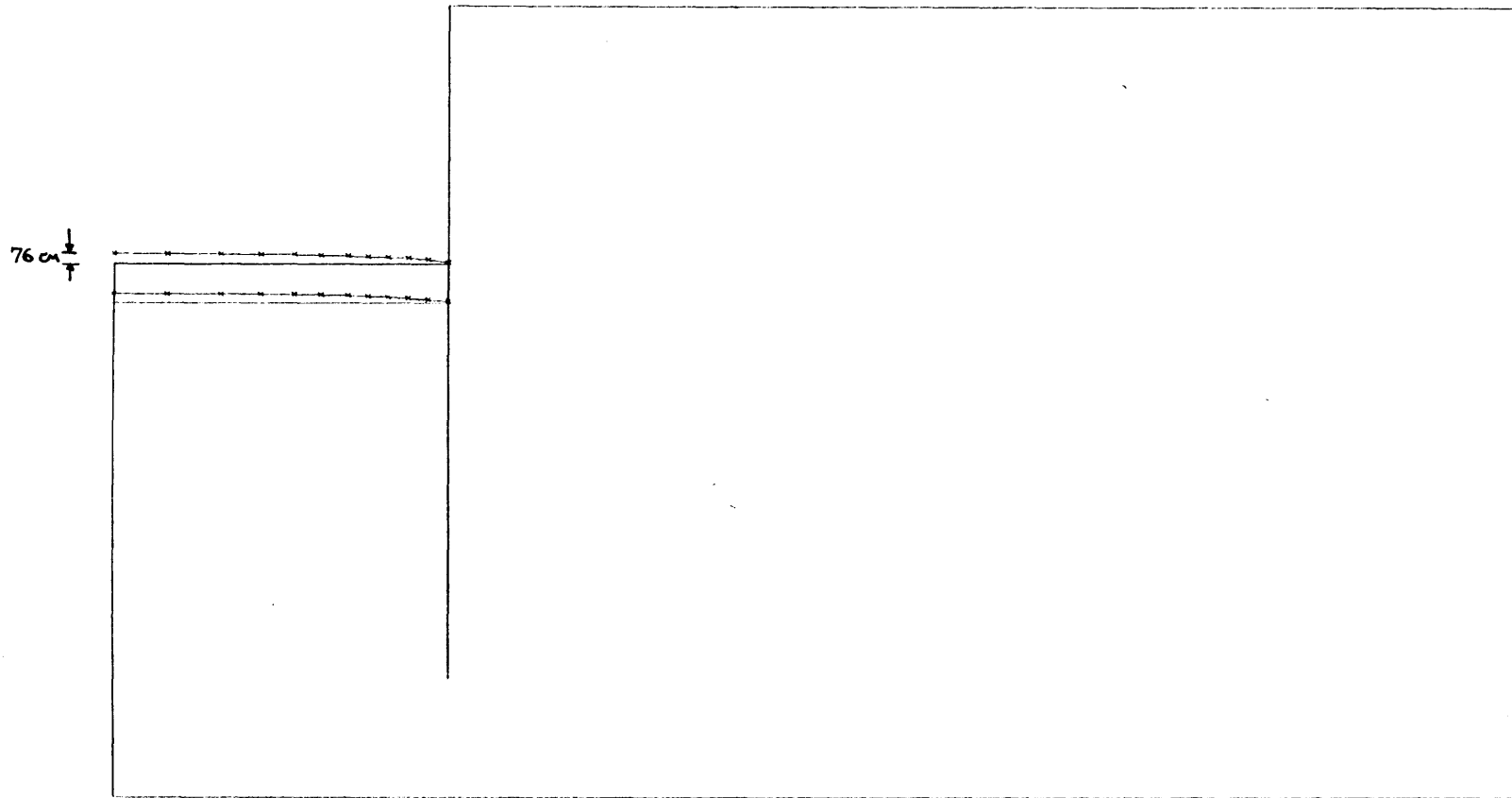
DEFORMED FINITE ELEMENT MESH

FIG.44.17

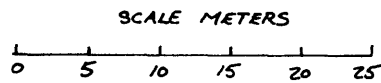


SELECTED LINES OF LATERAL DISPLACEMENT

FIG. 44.18



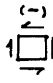
141

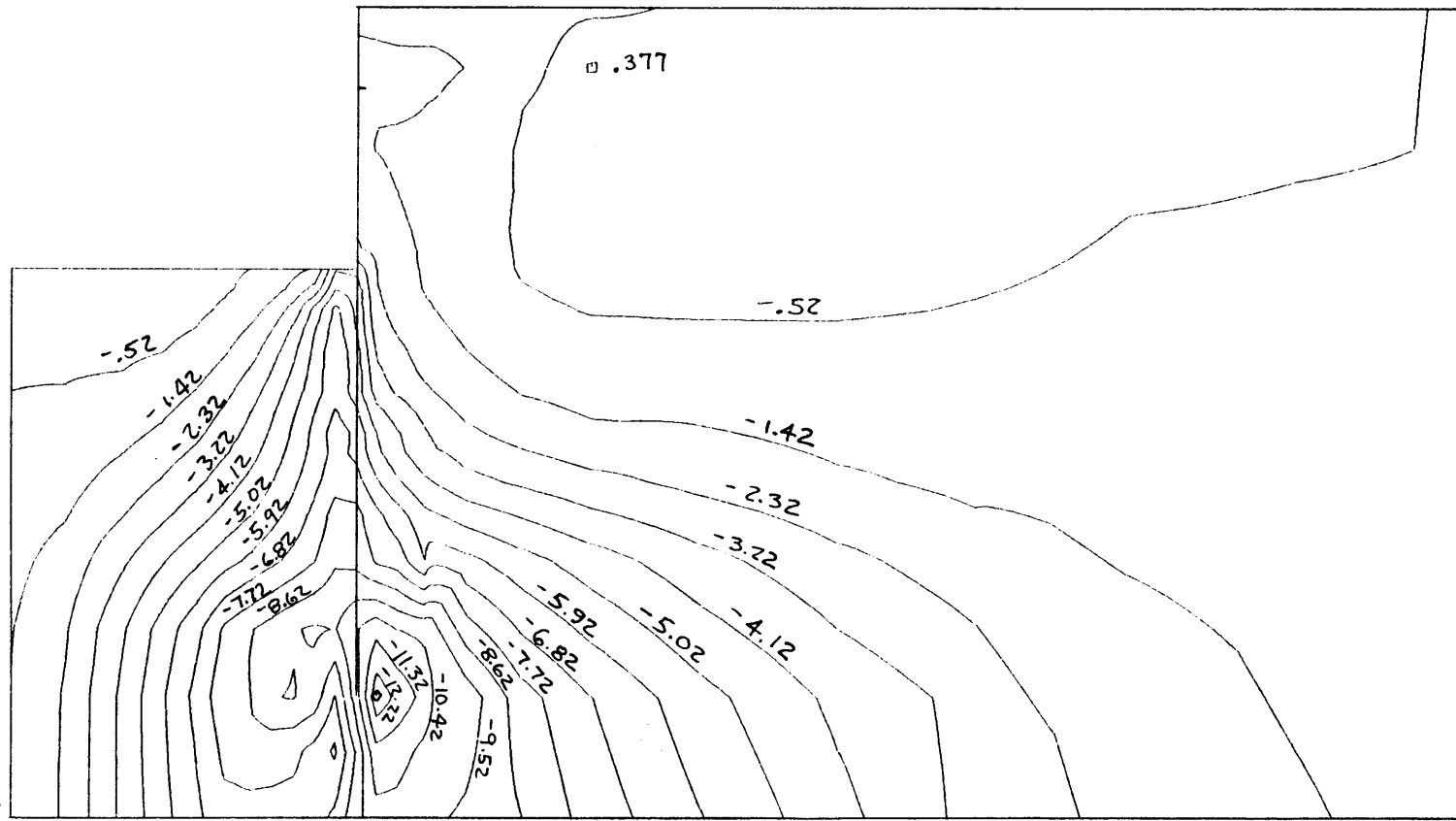


SELECTED LINES OF VERTICAL HEAVE

FIG. 44.19

□ MAXIMUM = 0.377 TSM
◇ MINIMUM = -12.385 TSM
CONTOUR INTERVAL = 0.900

TAU-XZ 

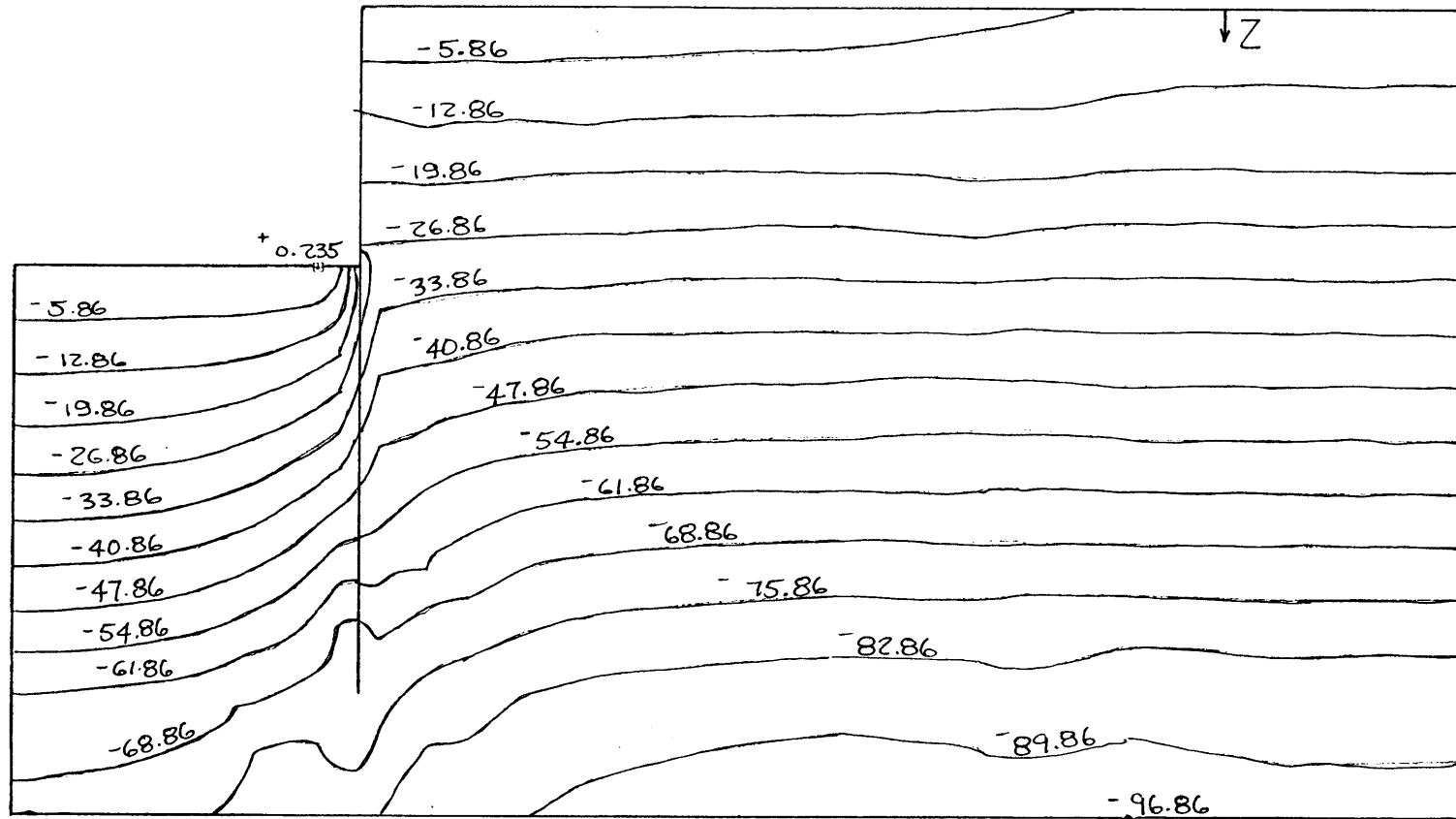


CONTOURS OF SHEAR STRESS

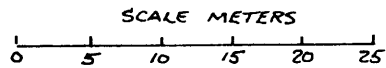
FIG. 44.20

□ MAXIMUM = 0.235 TSM
◇ MINIMUM = -96.860 TSM
CONTOUR INTERVAL = 7.000 TSM

TOTAL SIGMA Z



143

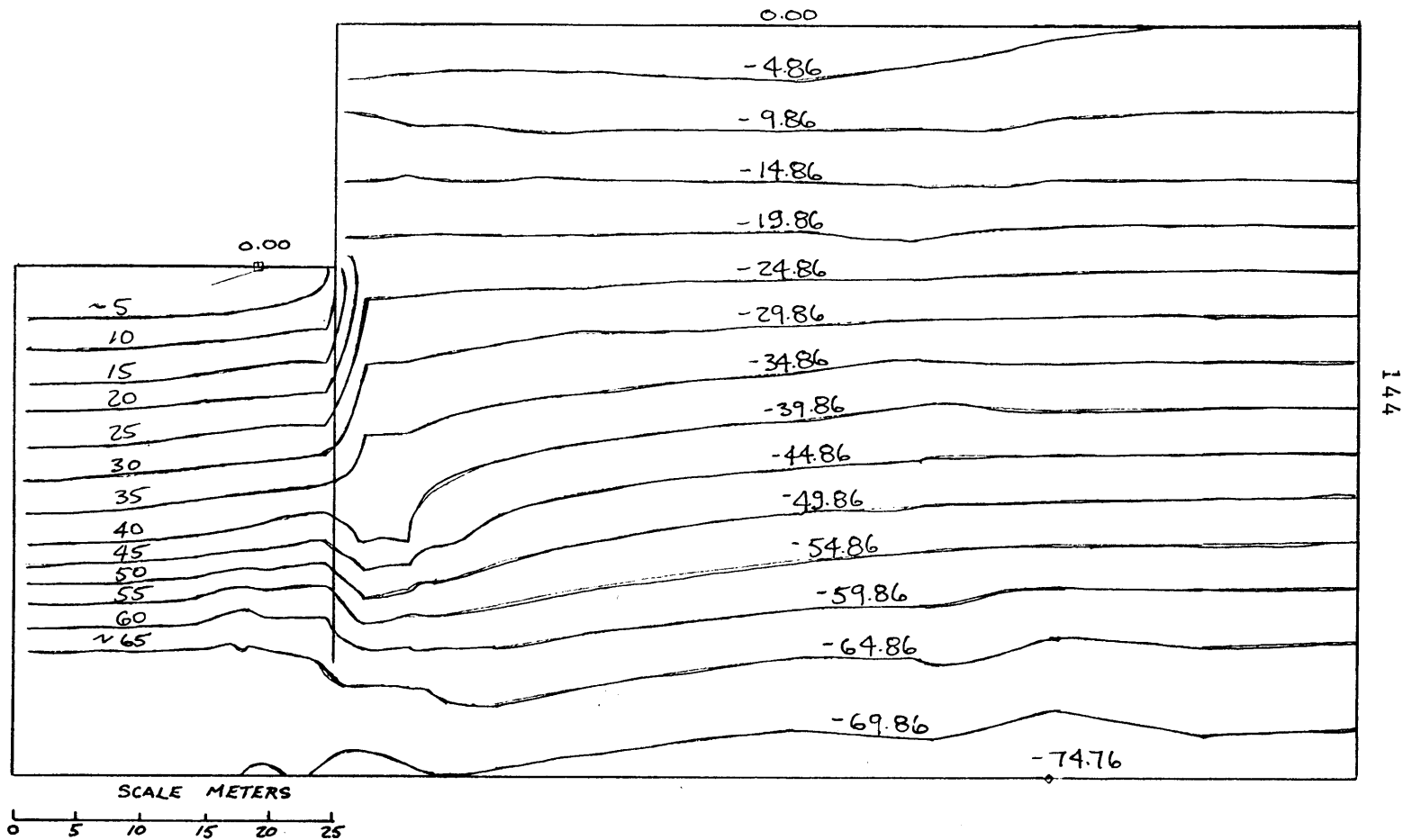


CONTOURS OF TOTAL SIGMA Z

FIG.44.21

□ MAXIMUM = 0.000 TSM
◇ MINIMUM = -74.760 TSM
CONTOUR INTERVAL = 5.000 TSM

TOTAL SIGMA X → □ ←

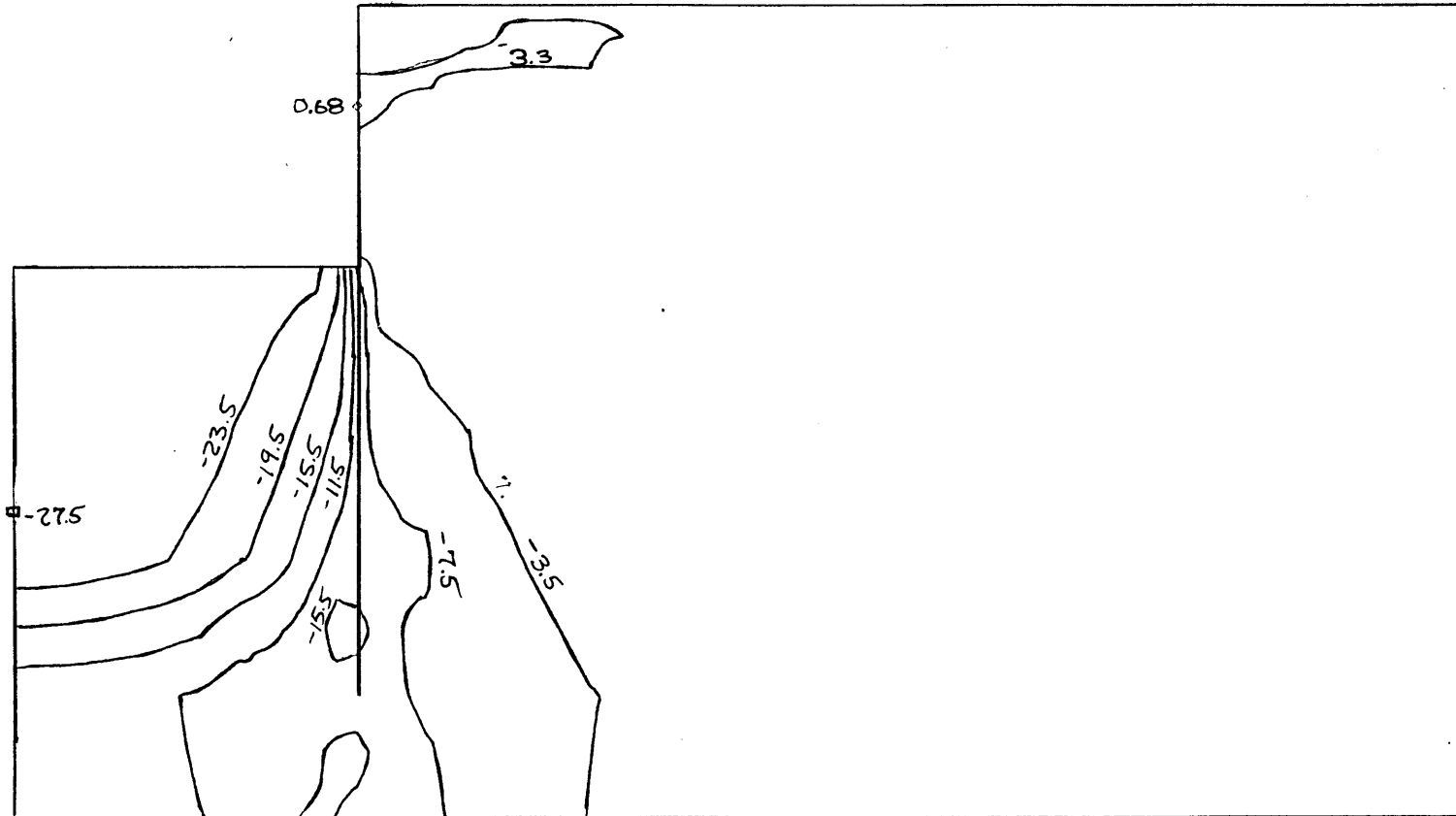
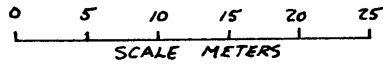


CONTOURS OF TOTAL SIGMA X

FIG.44.22

□ MAXIMUM = -27.500 TSM
◇ MINIMUM = +0.683 TSM
CONTOUR INTERVAL = 4.000 TSM

PORE PRESSURE (UNDISSIPATED)

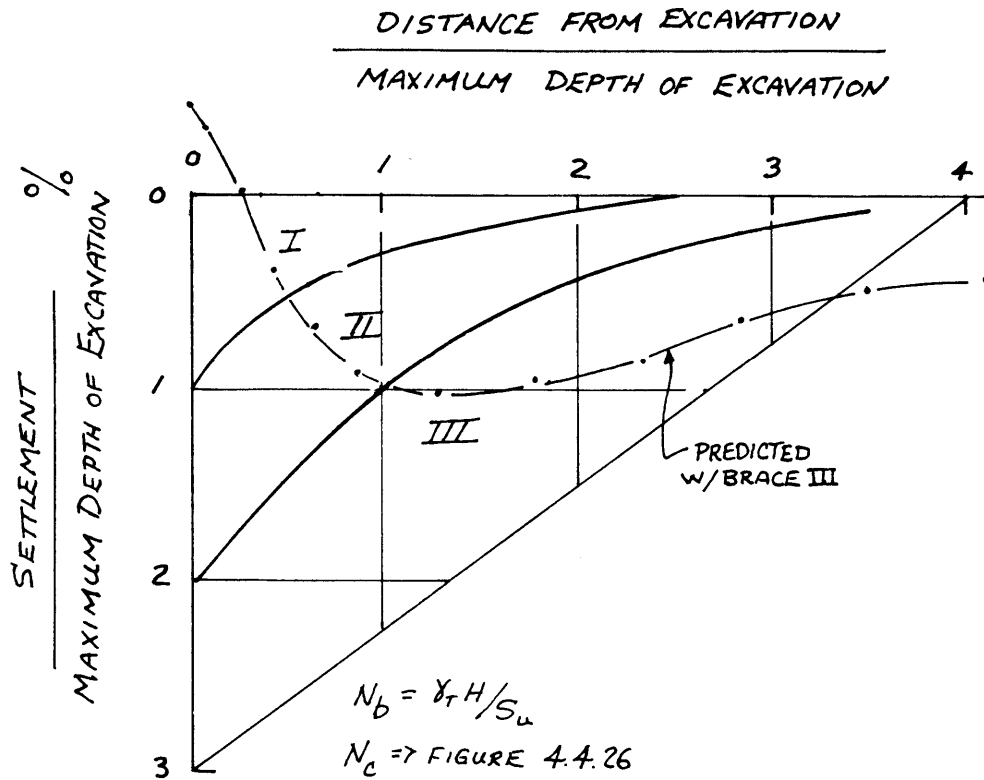


145

CONTOURS SHOWING TRENDS OF NEGATIVE EXCESS PORE PRESSURE

FIG.44.23

SETTLEMENT ADJACENT TO EXCAVATIONS
PECK (1969)



Zone I
Sand and Soft to Hard Clay
Average Workmanship

Zone II
a) Very Soft to Soft Clay
1) Limited depth of clay below bottom of excavation
2) Significant depth of clay below bottom of excavation but $N_b < N_{cb}$

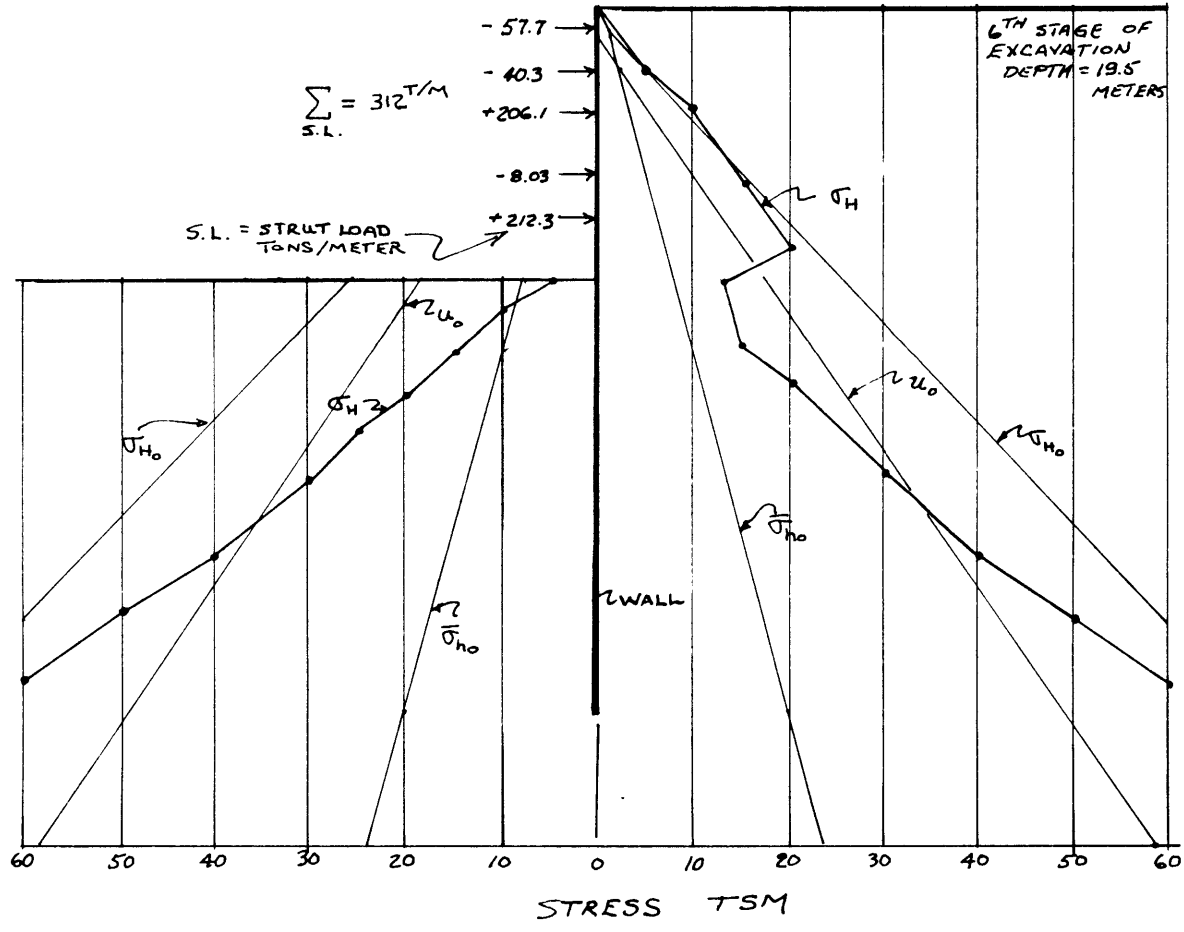
b) Settlements affected by construction difficulties

Zone III
Very Soft to Soft Clay to a significant depth below bottom of excavation and with $N_b \geq N_{cb}$

COMPARISON OF PECK'S CHART WITH SETTLEMENT BEHIND THE NAKAGAWA EXCAVATION

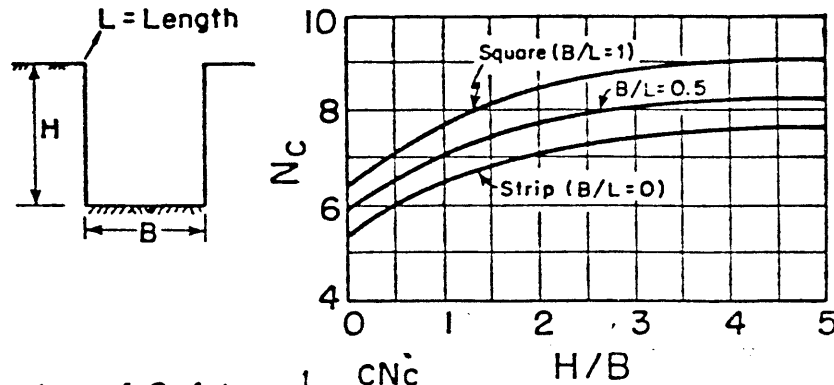
FIG 4.4.24

BRACE III STRUT LOADS AND σ_H DISTRIBUTION



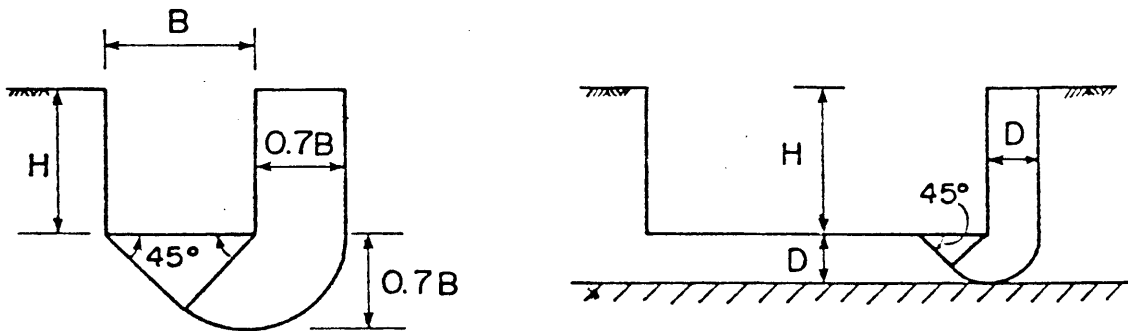
ESTIMATED TOTAL STRESS DISTRIBUTION BEHIND THE STEEL PILE WALL

FIG. 44.25



$$\text{Factor of Safety} = \frac{1}{H} \frac{C N_c}{\gamma}$$

Bottom Heave Analysis for Deep Excavations ($H/B > 1$) - BJERRUM & EIDE (1956)

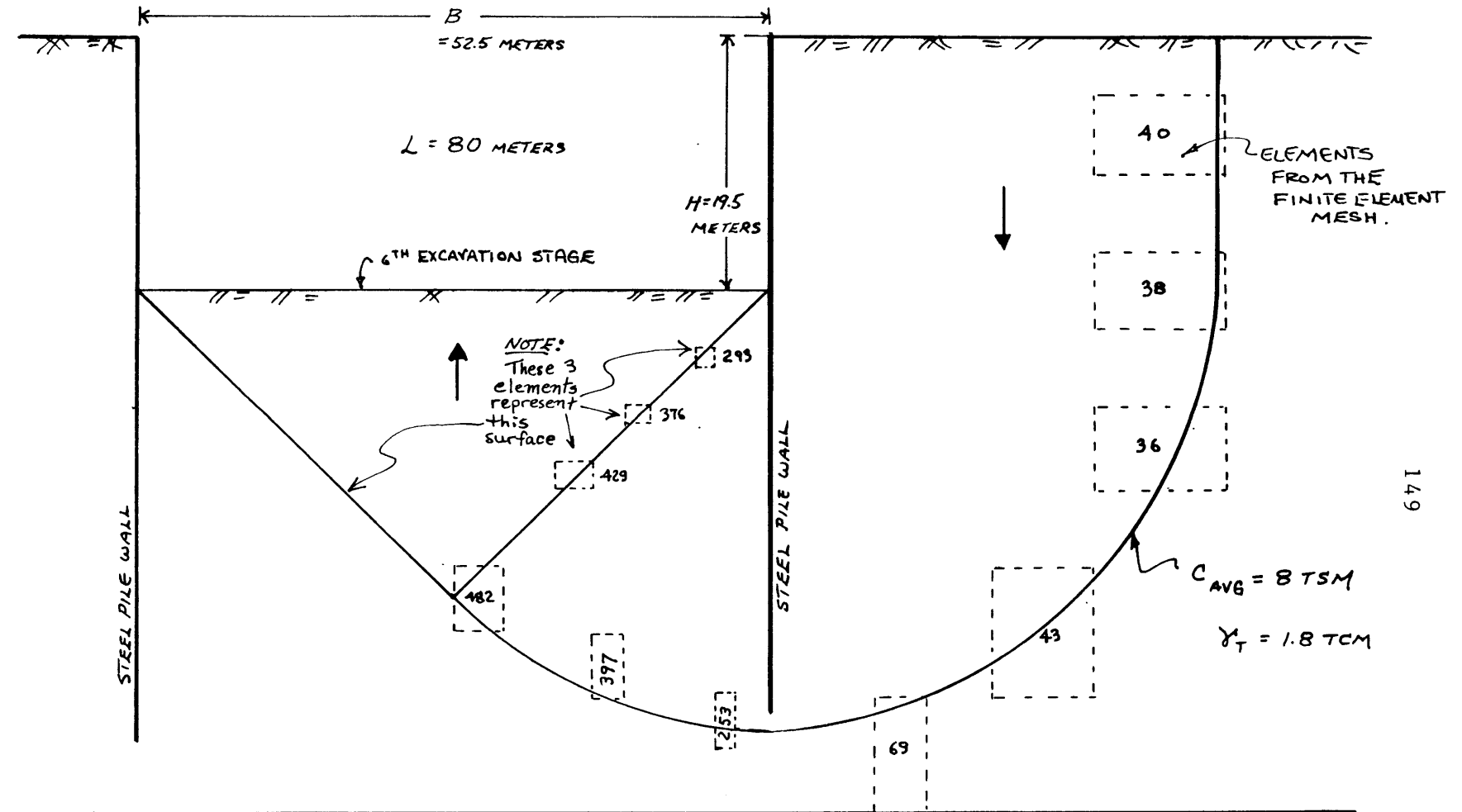


$$\text{Factor of Safety} = \frac{1}{H} \cdot \frac{C N_c}{\gamma - C/0.7B}$$

$$\text{Factor of Safety} = \frac{1}{H} \cdot \frac{C N_c}{\gamma - C/0.7D}$$

Bottom Heave Analysis for Shallow Excavations ($H/B < 1$) - TERZAGHI (1943)

FIGURE FROM CLOUGH & SCHMIDT (1977)

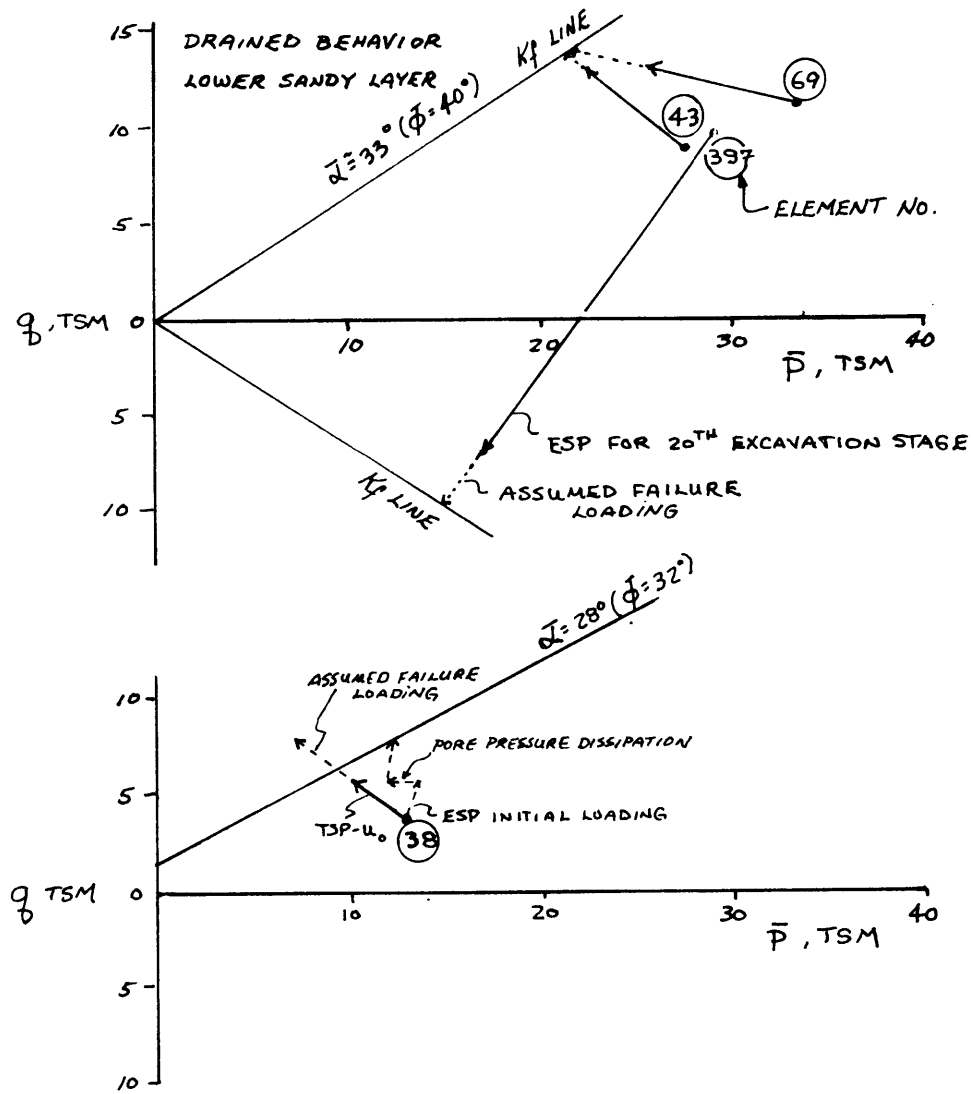


$$H/B = .37 \quad B/L = .66 \quad N_c = 6.3$$

$$F.S. = \frac{1}{H} \cdot \frac{c N_c}{\gamma - c/1B} = \frac{1}{19.5} \cdot \frac{8 \times 6.3}{1.8 - 8/7 \cdot 52.5} = 1.63$$

SIXTH EXCAVATION STAGE - STABILITY ANALYSIS

FIG.4.4.27



STRESS PATHS FOR STABILITY ANALYSIS

FIG.44.28

EL.	DEPTH	$P_c - U_c$	q_c	$P_c - U_c$	q_c	Z/H_d	EXCESS ΔU_b	U_{FD}	EXCESS ΔU_r	U_{ZE}	ΔU_b	ΔU_E	ΔU_T	S
36	31.75	19.1	6.4	16.9	8.8	1.09	0	0	-3.9	.01	0	-0.4	-0.4	11
38	19.5	12.7	3.9	10.1	5.8	0.24	0	0	-3.9	.42	0	-1.64	-1.64	8
40	7.5	5.3	1.76	5.3	3.6	0.17	0	0	-1.0	0.17	0	-0.17	-0.17	3
43	46.0	27.6	9.2	22.4	13.0	—	0	0	0	0	0	0	0	13.5 ^⓪
69	55.5	33.4	11.1	25.8	13.0	—	0	0	0	0	0	0	0	13.5 ^⓪
293	24.8	14.9	5.0	-12.1	3.0	0.57	12.9	.08	-25.0	.08	+1.0	-2.0	-1.0	5
376	27.3	17.6	5.9	-9.6	1.9	0.77	11.1	~0	-23.6	.02	0	-0.47	-0.47	6
397	48.5	29.1	9.7	17.0	-7.0	—	0	0	0	0	0	0	0	10.0 ^⓪
429	34.0	19.4	6.8	-6.3	1.6	1.14	7.8	~0	-20.8	.015	0	-0.31	-0.31	6.2
482	43.5	26.1	8.7	17.6	2.1	1.88	1.1	~0	-22.9	.72	0	-16.5	0	4
253	53.0	30.8	10.6	19.0	8.8	—	0	0	0	0	0	0	0	7.5 ^⓪

ALL TERMS - METER, AND METRIC TONS

S = STRENGTH

AVG. S = 8.0 TSM

⓪ BASED ON FAILURE ENVELOPE WHERE $\phi = 40^\circ$, $\alpha = 33^\circ$

TABLE 45

CHAPTER 5

SUMMARY AND CONCLUSIONS

5.0 GENERAL

Review of case history braced excavations shows that the role of time is important. Dissipation of excess pore pressures, the major time effect influencing the soil response, will often lead to a decrease in factor of safety with time. The writer concludes that an excavation warrants the best technology available because of this time dependent behavior, for the safety of the workers and the surrounding environment (general public, existing structures, etc.). Similarly, deformations are also a function of pore pressure dissipation. The magnitude of movements and deformations which can be tolerated and anticipated are a major concern in braced excavation, particularly in urban areas. This thesis presents the formulation and application of a method intended to better predict such movements by including the effects of pore pressure dissipation. The application of the method shows that one can combine the Stress Path Method with the Finite Element Method to obtain a powerful approach including the effects of non-linear soil behavior and consolidation.

The assumption that undrained conditions prevail in braced excavation in cohesive soil need not be merely

accepted for lack of another method. The proposed method to model partially drained conditions can be applied. Although it is illustrated for a major excavation, the method can also be applied to less complicated problems on a simpler scale to estimate stability and deformation. One does not need a large finite element program to apply The Stress Path Method. However for complex geometries such as the Nakagawa Treatment Plant Excavation, the finite element program BRACE III is a powerful tool, and the use of it is justified.

5.1 LIMITATIONS

One limitation of the proposed method as applied in chapter four is that there is a significant amount of hand work involved. However, compared to the alternative of additional tests and testing time, the amount of handwork is not unreasonable. In this case study only one stage of construction performance was predicted. Figure 5.1 helps to illustrate that for one to predict performance of other excavation stages the entire procedure must be iterated for each stage. A better approach to model all stages would be to execute the hand work for one or two excavation stages and then fit a polynomial curve or hyperbolic equation through the stress strain data. An initial modulus for the earlier stages can be obtained from the undrained stress strain test data. Kondner (1963), and Duncan and Chang (1970) present and discuss utilization of the hyperbolic model (refer to Figure 5.2) where;

$$(\sigma_1 - \sigma_3) = \epsilon / \left[\frac{1}{E'_i} + \frac{\epsilon R_f}{(\sigma_1 - \sigma_3)_f} \right], \quad R_f = (\sigma_1 - \sigma_3)_f / (\sigma_1 - \sigma_3)_{\text{ult}}$$

The current version of BRACE III however, does not have this capability to model such nonlinear stress strain behavior, although the program could easily be modified.

As a practical matter one should be aware of several limitations when using the proposed method.

- (1) Large finite element computer programs such as BRACE III require experience for proper useage and effectiveness. It can also be expensive to run the program and analyze the results.
- (2) Stress path tests are both expensive and difficult to run, although several carefully executed stress path tests may be of significantly more value than a larger number of more common laboratory tests (e.g. UU Tests). Well known factors such as sample disturbance can significantly influence laboratory test results.
- (3) Program modifications to make the proposed method and BRACE III more compatible are needed (i.e., modify and dimension the program to handle input of many varied soil properties)

5.3 SUGGESTIONS FOR FURTHER RESEARCH

Some suggestions by the writer for further research and work in this area of interest include:

- (1) Additional studies of the type made by Clough and Osaimi, applied to actual excavations, i.e., predicted vs. actual performance (e.g., deformations). Such study for a variety of soil

conditions would help evaluate the applicability of the sophisticated numerical technique, and hopefully broaden our understanding of the role of time in braced excavation.

- (2) Evaluation and updating of the prediction in this paper, and other predictions using the proposed method by comparison with actual field results. For the Nakagawa site, additional testing (i.e. oedometer tests) are needed because of the limited test data available to date. From additional test data and field measurements the BRACE III program input can be revised and the prediction updated.
- (3) Improvement of the soil structure interaction modeling in the BRACE III computer program. There is an inherent strain incompatibility between soil and sheeting elements (Jaworski 1973). Displacement compatibility is not maintained along inter-element boundaries between the one dimensional sheeting elements and the two dimensional elements of the soil continuum. The wall elements which have three degrees of freedom per node assume curved deformed positions. Soil elements have only two degrees of freedom and maintain straight boundaries in the deformed position.

- (4) Develop Brace III program capability to model nonlinear stress strain behavior, perhaps by employing a subroutine which uses a hyperbolic relationship as proposed by Kondner (1963).

5.4 CONCLUSIONS

The objective of this thesis was to formulate and apply a method which includes the effects of pore pressure change with time to predict deformation in an excavation. This thesis shows that one can combine the Stress Path Method to obtain soil parameters with the Finite Element Method to perform analysis in a way that includes the effect of time on deformation of a braced excavation. The approach is outlined in Chapter 3 and applied in Chapter 4.

Advantages of the approach outlined in Chapter 3 are:

- (1) Complex nonlinear time analysis is avoided.
- (2) The fundamentals of the field problem are examined by the engineer as he selects his input so that he retains a feel for the problem.
- (3) A few tests can be used and extrapolated to cover an entire geometry.

The proposed approach is an iterative procedure. The application to the example in Chapter 4 suggests that two to three iterations give a reasonable solution, especially for the overall deformations.

For the example case consisting of an excavation in a

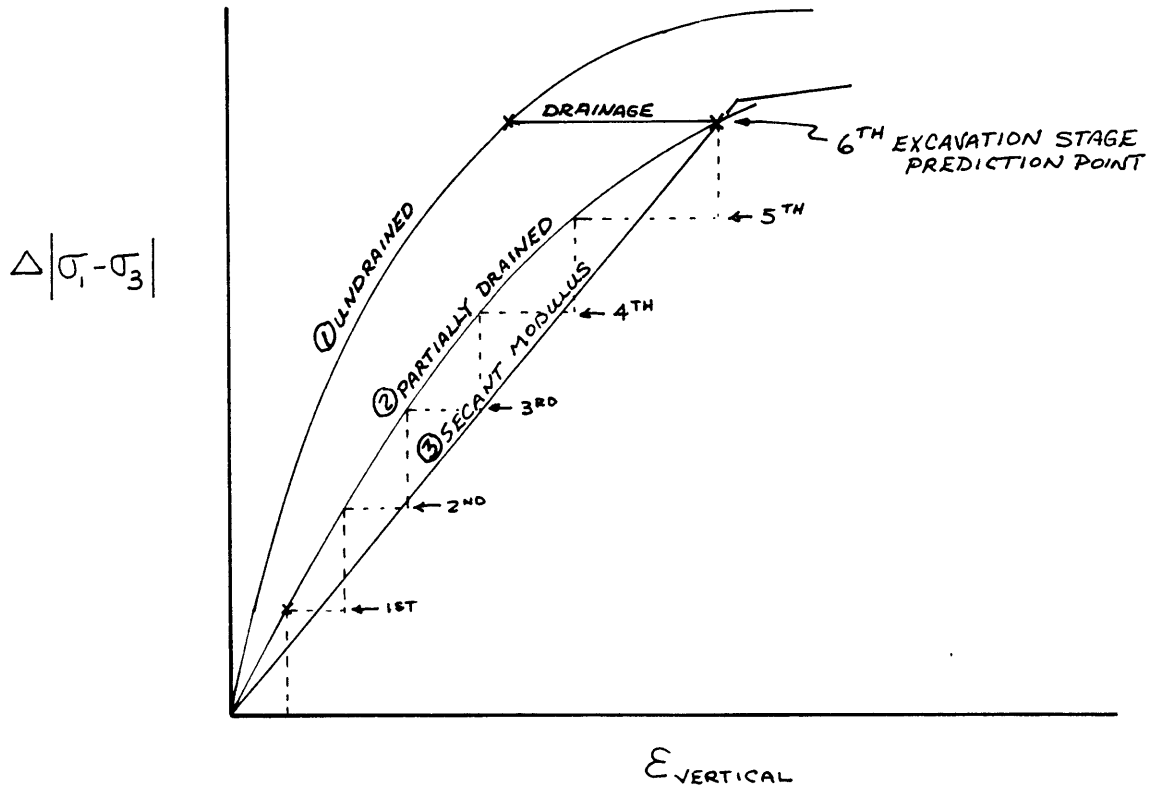
clayey silt, the effect of time on deformations within the excavation is significant although not major. Heave and inward wall movements within the excavation appear to increase by approximately 10 to 20 percent with consolidation.

Within the top 8 meters (depth of 20 to 28 meters) of the bottom of the excavation at the 20 meter excavation depth, the negative excess pore pressures due to unloading and the positive excess pore pressures due to shallow or surficial dewatering, substantially offset each other. This results in a relatively small net excess pore pressure for this case. In other words, because of the dewatering the dissipation of large negative excess pore pressure and resulting heave is minimized.

For this particular soil the negative excess pore pressures due to excavation are offset by the excess pore pressures generated by surficial dewatering. Consequently, the effects of time on predicted movement are relatively small in this case. With other soils and other conditions of flow, the effect of time on deformations could be considerable.

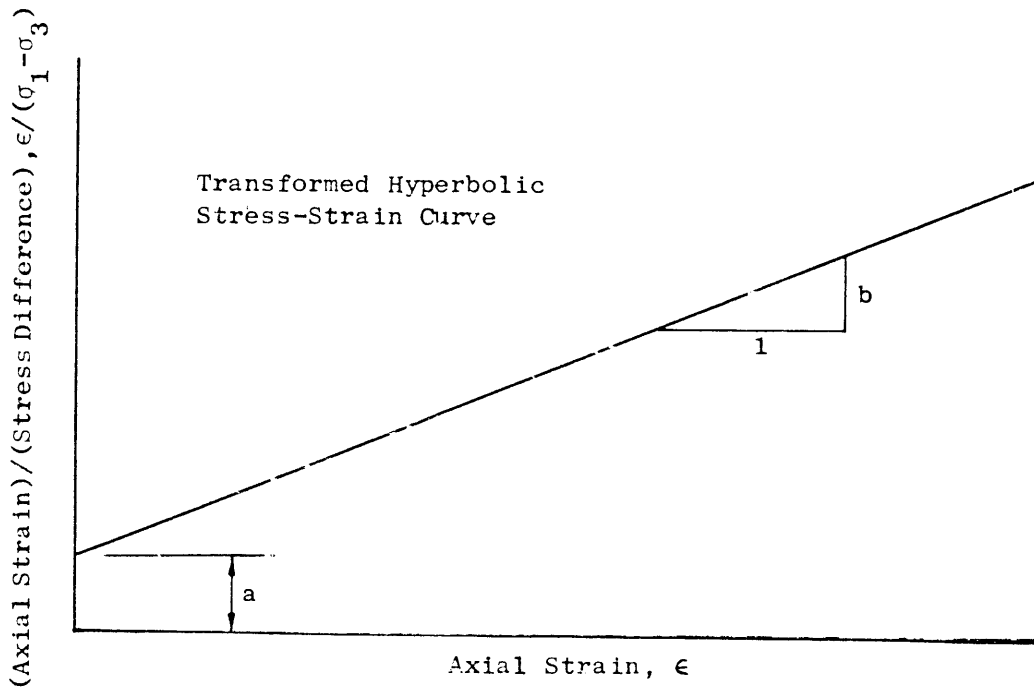
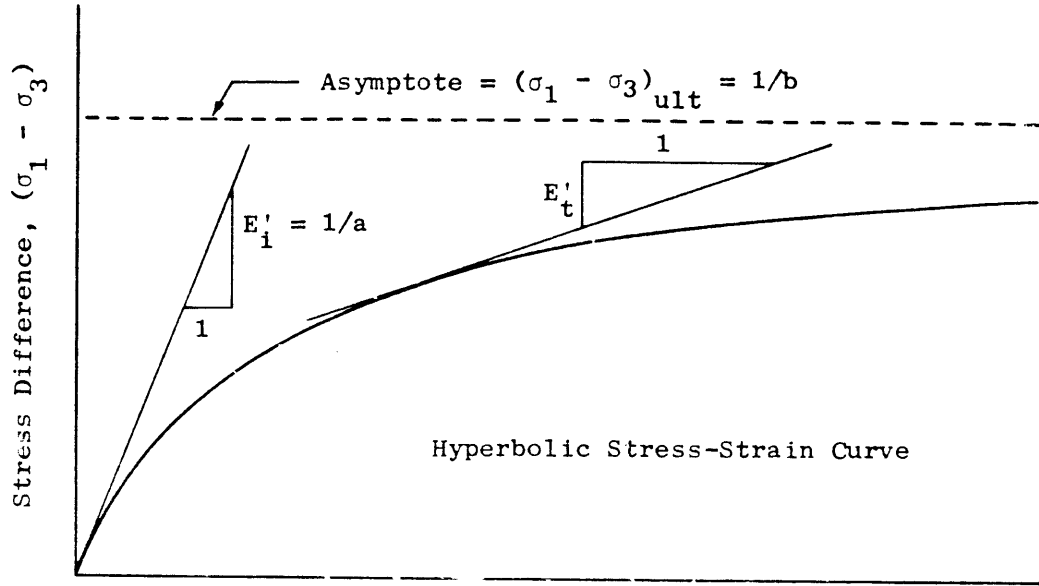
In addition, for this particular case the example shows that the undrained heave is large when compared to the consolidation movements. For other situations involving higher factors of safety against bottom heave the contribution of time to total deformation will be more significant.

Again, a practical advantage of the proposed method is that such fundamental behavior can be observed and quantified by the engineer during his analysis of the field situation.



CURVE ② - ACTUAL BEHAVIOR - FITS ALL STAGES

CURVE ③ - IDEALIZED BEHAVIOR APPLICABLE TO PREDICTION OF 6TH EXCAVATION STAGE - USING THE SAME MODULUS FOR PREVIOUS EXCAVATION STAGES WILL RESULT IN AN OVER-PREDICTION OF STRAIN. USING SAME SECANT MODULUS FOR DEEPER STAGES WILL RESULT IN AN UNDER-PREDICTION OF STRAIN MAGNITUDE.



FROM OSAIMI 1977

HYPERBOLIC STRESS STRAIN CURVES

FIG. 5.2

LIST OF SYMBOLS

\bar{a}	Intercept of K_f line
\bar{c}	Cohesion intercept based on effective stress
CAU	Anisotropically consolidated triaxial test sheared under undrained conditions
CRSC	Constant rate of strain consolidation test
CAES	Center for Advanced Engineering Study
CIU	Isotropically consolidated triaxial test sheared under conditions of no drainage
c_v	Coefficient of consolidation
E_i	Initial tangent modulus
ESP	Effective stress path
H	Height of cut
h_e	Elevation head
h_p	Pressure head
h_t	Total head
H_d	Length of drainage path
K_a	Active earth pressure coefficient
K_o	At rest earth pressure coefficient, horizontal ground surface
OCR	Overconsolidation ratio
P.I.	Plasticity index
p, \bar{p}	$\frac{\sigma_v + \sigma_h}{2}, \frac{\bar{\sigma}_v + \bar{\sigma}_h}{2}$
q	$\left[\left(\frac{\sigma_v - \sigma_h}{2} \right)^2 + \tau_{vh}^2 \right]^{1/2}$
S_u	Undrained shear strength of soil
TSP	Total stress path
$TSP - u_o$	Total stress path minus initial pore pressure

u	Pore pressure
u_{ss}	Steady state pore pressure
u_e	Excess pore pressure
u_D	Excess pore pressure due to excavation unloading
u_E	Excess pore pressure due to dewatering
UU	Unconsolidated undrained triaxial test
w_n	Water content, natural
w_l	Liquid limit
w_p	Plastic limit
z	Depth
z_w	Depth to water table
U_z	Consolidation ratio
\bar{U}	Average degree of consolidation
α	Slope of the K_f line
γ	Unit weight
γ_T	Total unit weight of soil
γ_w	Unit weight of water
ϵ	Strain
E	Young's modulus
σ_v	Total vertical stress
σ_H	Total horizontal stress
σ_{oct}	Octahedral stress
$\bar{\sigma}_v$	Vertical effective stress
$\bar{\sigma}_H$	Horizontal effective stress
$\sigma_{vo}, \bar{\sigma}_{vo}$	Initial total and effective stresses, vertical
$\sigma_{Ho}, \bar{\sigma}_{Ho}$	Initial total and effective horizontal stresses
$\phi, \bar{\phi}$	Friction angle, friction angle based on effective stress

REFERENCES

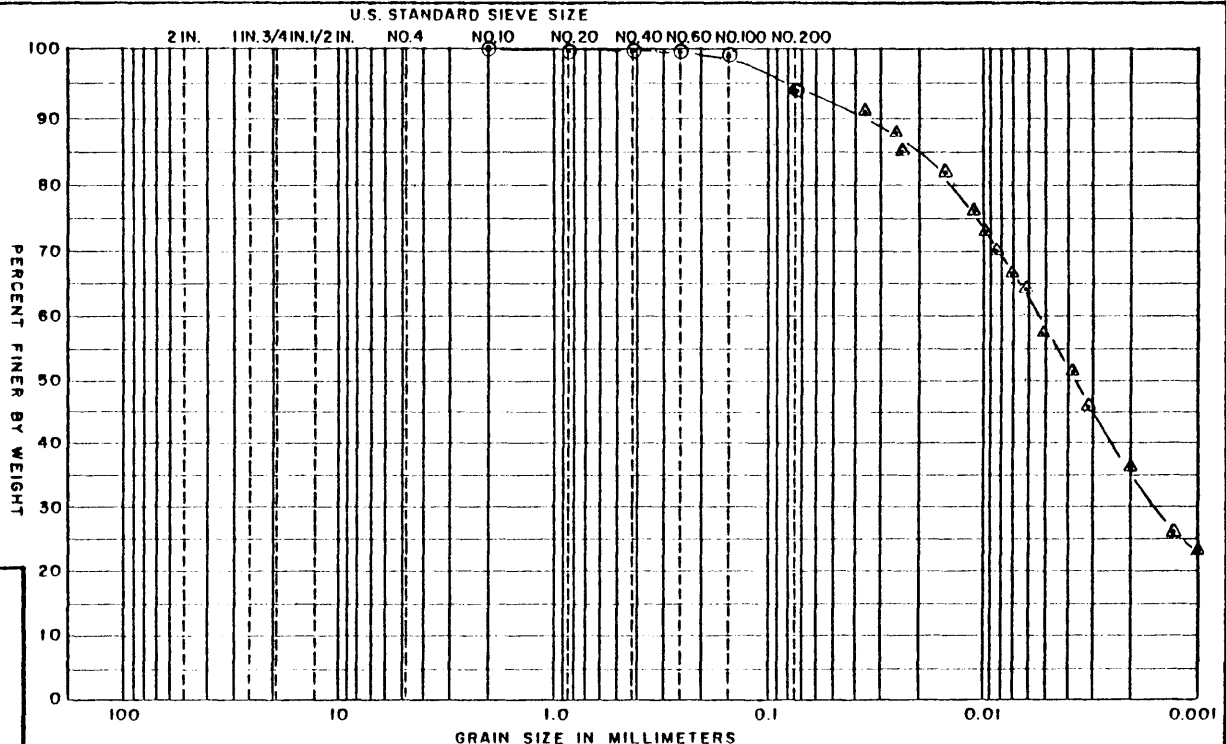
- Bathe, K.J., Wilson, E.L., Numerical Methods in Finite Element Analysis, Prentice-Hall 1976
- Bjerrum, L, and O, Eide (1956). "Stability of Struttred Excavations in Clay," Geotechnique 6, No. 1.
- Bjerrum, L., C.J. Clausen, and J.M. Duncan, (1972). "Earth Pressures on Flexible Structures - A State-of-the-Art Report," Proc. of the Fifth European Conference on Soil Mechanics, Madrid, Vol 2, pp 169-196.
- Clough, G.W., and Davidson, R.R., "Effects of Construction on Geotechnical Performance", Dept. of Civil Engineering, Technical Report No. CE-214, January 1977.
- Clough, G.W., Duncan, J.M., "Finite Element Analysis of Retaining Wall Behavior", JSMFD, ASCE, Vo. 97, December 1971.
- Clough, G.W., Personal Communication 1980
- Clough, G.W., and Schmidt, B, "Design and Performance of Excavations and Tunnels in Soft Clay", Dept. of Civil Engineering, Technical Report No. CE-235, 1977
- Clough, G.W., Tsui, Y., "Performance of Tied Back Walls in Clay", Paper presented at the National ASCE Meeting, Cincinnati, Ohio, April, 1974.
- Cole, K.W., Burland, J.B., "Observations of Retaining Wall Movements Associated With a Large Excavation", Proc. 5th European Conf. on Soil Mech. and Foundation Engineering, Madrid 1972
- Corbet, B.O., Davies, R.V., Langford, A.D., "A Load Bearing Diaphragm Wall at Kensington and Chelsea Town Hall at London", Proc. Diaphragm Walls and Anchorages, Inst. of Civil Eng., London, 1975.
- D'Appolonia, David J., (1971). "Effects of Foundation Construction on Nearby Structures," Pan American Conference on Soil Mechanics and Foundations, Puerto Rico, pp. 189-236.
- Desai, C.S., Abel, J.F., Introduction to the Finite Element Method, Van-Nostrand-Reinhold,
- Department of the Navy (1971). " Design Manual DM-7" Navfac Naval Facilities Engineering Command, Washington, D.C.

- Davis, E.H., and Christian, J.T. (1971), "Bearing Capacity of Anisotropic Cohesive Soil", ASCE, JSMFD, Vol. 97, Sm5, pp. 753-769.
- Duncan, J.M. and Chang, C-Y., "Nonlinear Analysis of Stress and Strain in Soils", JSMFD, ASCE, No.- SM5, Vol. 96, 1970.
- Duncan, J.M., and Chang, C-y., "Analysis of Soil Movement Around a Deep Excavation", JSMFD, ASCE, No. SM5, Sept. 1970.
- DiBiagio, E., and L. Bjerrum (1957). "Earth Pressure Measurements in a Trench Excavated in Stiff Marine Clay," Proc. 4th Int. Conf. on Soil Mech. and Found. Eng., London, 2, pp. 196-202.
- DiBiagio, E., Roti, J.A. "Earth Pressure Measurements on a Braced Sherry Wall in Soft Clay, Proc. 5th European Conf. Soil Mech. Found. Eng., Madrid 1972
- Henkel, D.J., "Geotechnical Considerations of Lateral Stresses", State-of-the-Art Paper, presented at the Specialty Conference on Lateral Stresses in the Ground and Design of Earth Retaining Structures, ASCE, Cornell Univ. N.Y., June 22-24, 1970
- Jaworski, Walter E., An Evaluation of the Performance of a Braced Excavation, Phd Thesis, M.I.T., June 1973
- Kondner, R.L., (1963), "Hyperbolic Stress Strain Response : Cohesive Soils," JSMFD, ASCE, VOL.89, No. SM1.
- Ladd, C.C., (1973), "Estimating Settlements of Structures Supported on Cohesive Soils", MIT Class Handout.
- Ladd, C.C.. (1971), "Strength Parameters and Stress Strain Parameters of Saturated Clays", MIT Class Handout.
- Ladd, C.C. Wissa, A.E.Z. "Geology and Eng. Properties of Conn. Valley varved Clays with Special Reference to Embankment Construction", Dept. Civil Eng. Report R-70-56
- Lambe, T.W., Wolfskill, L.A., and Wong, I.H., "Measured Performance of Braced Excavation," Journal of Soil Mechanics and Foundations Division, ASCE, Vol. 96, May 1970, pp. 817-836.
- Lambe, T.W., and Whitman, Soil Mechanics, Wiley & Sons, New York, 1969.

- Lambe, T.W., "Interpretation of Field Data", paper from Proc. of Lecture Series in Observational Methods in Soil and Rock Engineering, University of Illinois, pp. 116-148, Dec. 1970.
- Lambe, T.W., "Predictions in Soil Engineering", 13th Rawkin Lecture, Geotechnique 23, No. 2, 149-202. 1973.
- Lambe, T.W., (1970). "Braced Excavations," ASCE Conference on Lateral Stresses in the Ground and Design of Earth-Retaining Structures, pp. 149-218.
- Lambe, T.W. (1968). "The Behavior of Foundations During Construction", JSMFD, ASCE Vol. 94, No. SM1, pp 93.
- Lambe, T.W., "The Stress Path Method", JSMFD, ASCE, Vol. 93, No. SM6, Proc. Paper 5613, Nov. 1967.
- Lambe, T.W., Marr, W.A. "The Stress Path Method, Second Edition" JGED, ASCE, Vol. 105, No. GT6 pp. 727, June 1979
- M.I.T., Dept of Civil Engineering, "M.I.T. Test Section Instrumentation MBTA Haymarket - North Extension Project" Mass -MTD-2, March 1972.
- Mitchell, J.K., and W.S. Gardner(1975), "In-Situ Measurement of Volume Change Characteristics, 6th PSC, ASCE, pp. 379-391.
- Peck, Hansen, and Thornburn, Foundation Engineering, Wiley, 1974.
- Osaimi, A.E. and G.W. Clough (1979) "Pore-Pressure Dissipation During Excavation, Proc. of ASCE, JGED Vol. 105, No. GT4, pp. 481-499.
- Osaimi, A.E., "Finite Element Analysis of Time Dependent Deformations and Pore Pressures in Excavations and Embankments" Phd Thesis, Stanford University Dept. of Civil Engineering 1977.
- Palmer, J.H. Laverne, and Kenney, T.C. "Analytical Study of a Braced Excavation in Weak Clay" Can. Geotechnical Journal Vol. 9, No. 2 pp. 145-164 May 1972.
- Peck, Ralph B., (1969). "Deep Excavations and Tunnelling in Soft Ground," State-of-the-Art Volume, Seventh International Conference on Soil Mechanics and Foundation Engineering, Mexico City, pp. 259-281.

- Ries, Carol, "Predicting Lateral Earth Pressures for the Design of Tie-Back Retaining Walls", Master of Science Thesis, M.T.T. 1974.
- Skempton, A.W. and P. LaRochelle, (1965). "The Bradwell Slip: A Short Term Failure in London Clay" Geotechnique, No. 15 pp. 222-242.
- Taylor, R.L. and Brown, C.B., "Darcy Flow Solutions With Free Surface, "Journal of the Hydraulics Division, ASCE, Vol. 93, No. HYZ, pp. 25-33, 1967.
- Terzaghi, K., Theoretical Soil Mechanics, John Wiley and Sons, New York 1942.
- Terzaghi, K. and R.B. Peck (1967). Soil Mechanics in Engineering Practice, Wiley and Sons, New York.
- Tschebotarioff, Gregory P., (1973). Foundations, Retaining Walls and Earth Structures, McGraw Hill, New York.
- Wong, I.H., Analysis of Braced Excavations, Phd. Thesis, M.I.T. 1971
- Zienkiewicz, O.C., Cheung, Y.K., The Finite Element Method in Structural and Continuum Mechanics, London, McGraw-Hill Publishing Co., Ltd 1967.

APPENDIX A
GRAINSIZE PLOTS AND SQUARE ROOT OF TIME
CONSOLIDATION PLOTS - NAKAGAWA SOIL SPECIMENS



COBBLES	GRAVEL		SAND			SILT OR CLAY
	COARSE	FINE	COARSE	MEDIUM	FINE	

UNIFIED SOIL CLASSIFICATION SYSTEM

TEST NO.	SYM.	MATERIAL SOURCE	REMARKS
S-1	⊙	Tokyo, Japan	Hakagawa Treatment Plant
H-1	△		Site B

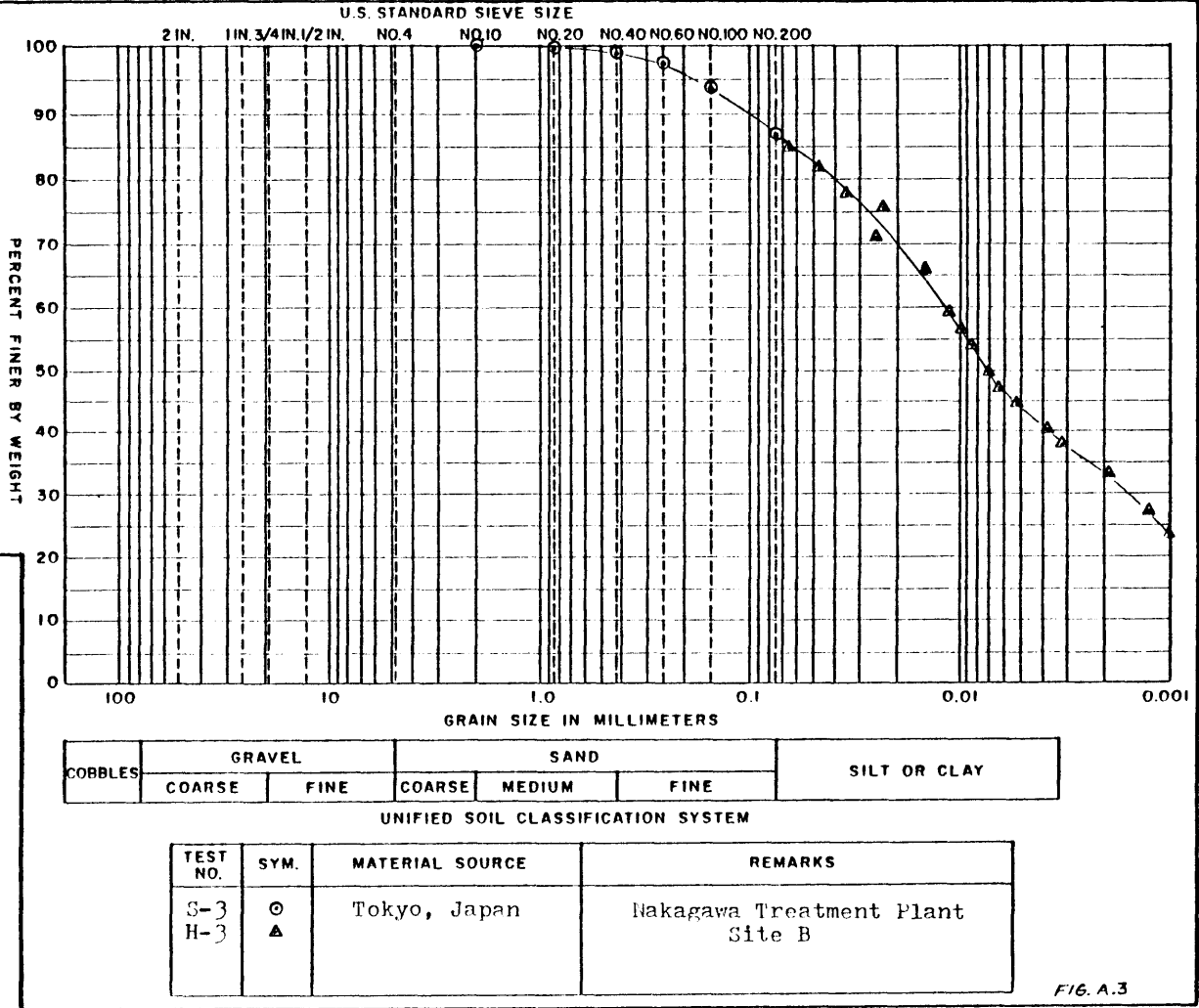
FIG. A.1

GRADATION TESTS

BORING NO. 2-2
 SAMPLE NO. 42.15 m
 DEPTH 42.15 m
 TECH. MY
 REVIEWER _____
 TEST SERIES NO. _____
 DATE 5-5-80
 FILE _____

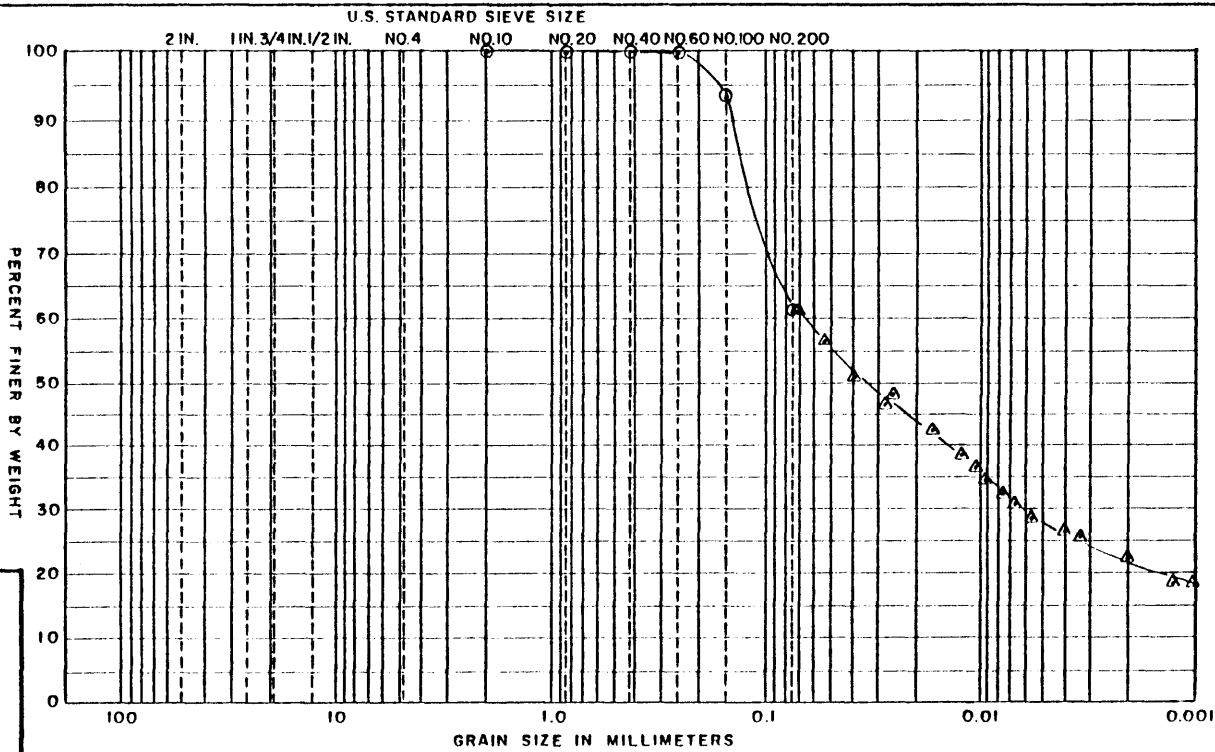
BORING NO. 2-1
 SAMPLE NO. 3
 DEPTH 28.0 m
 TECH. TYR
 REVIEWER _____
 TEST SERIES
 NO. 3
 DATE 5-5-80
 FILE

GRADATION TESTS



BORING NO. 3
 SAMPLE DEPTH 19.0 m
 TECH. MVP
 REVIEWER _____
 TEST SERIES NO. 5
 DATE 5-5-80
 FILE _____

GRADATION TESTS



COBBLES	GRAVEL		SAND			SILT OR CLAY
	COARSE	FINE	COARSE	MEDIUM	FINE	

UNIFIED SOIL CLASSIFICATION SYSTEM

TEST NO.	SYM.	MATERIAL SOURCE	REMARKS
S-5	○	Tokyo, Japan	Nakagawa Treatment Plant Site B
H-5	△		

FIG. A.5

GRADATION TESTS

BORING NO. 2-1
 SAMPLE DEPTH 34.0 m
 TECH. MVP
 REVIEWER _____

TEST SERIES NO. _____
 DATE 5-5-80
 FILE _____

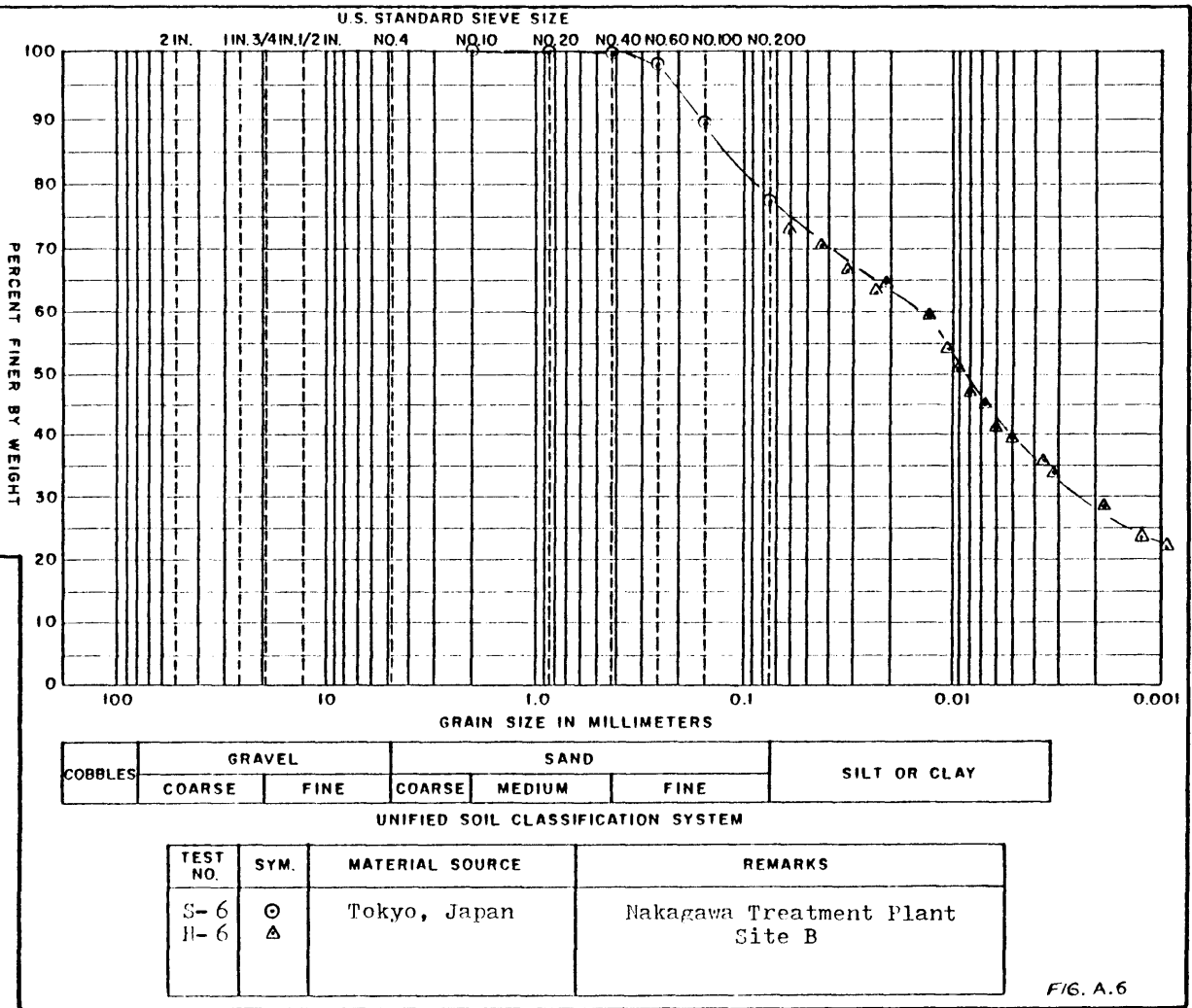


FIG. A.6

TE-1 PRE-SHEAR

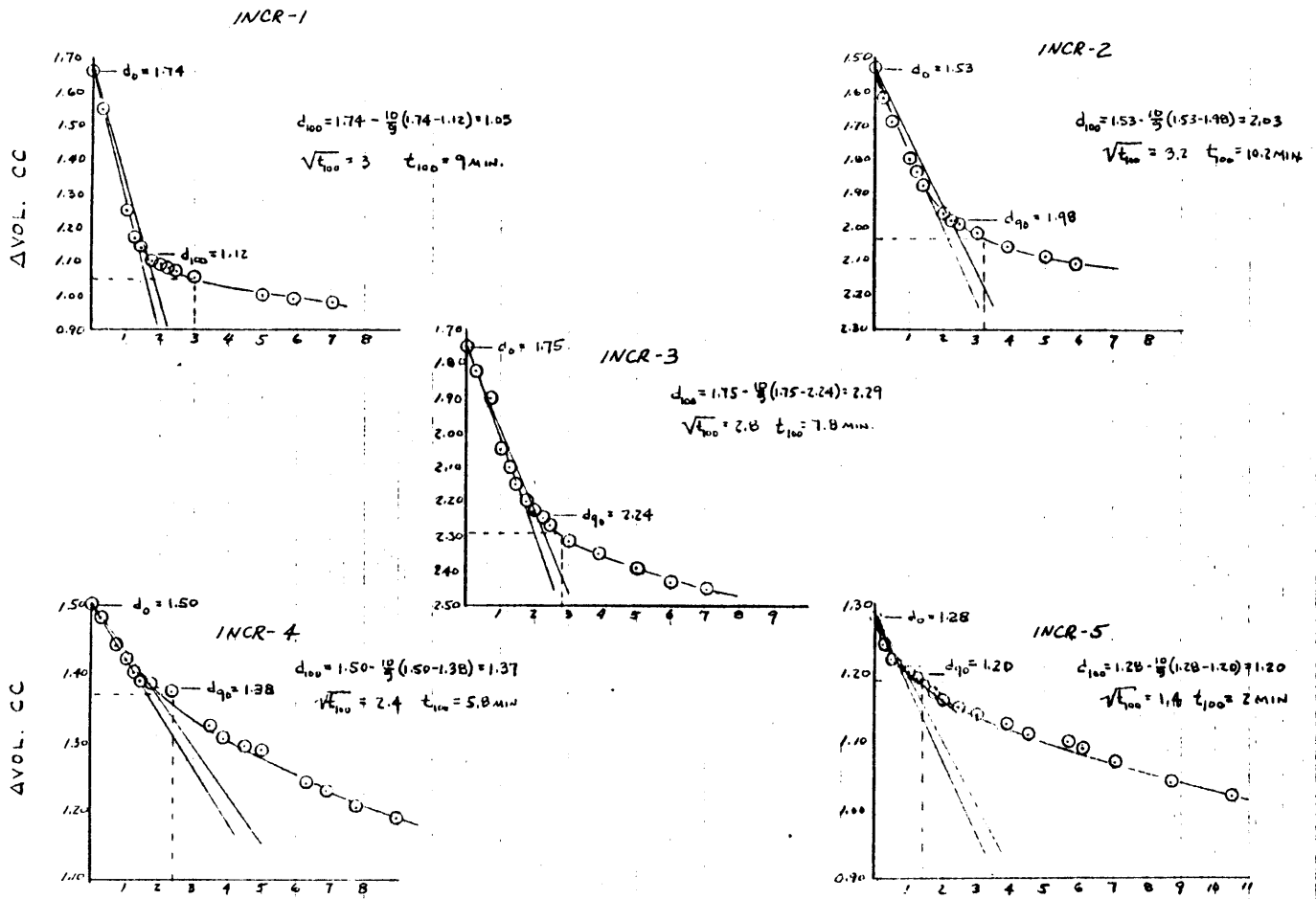


FIG. A.7

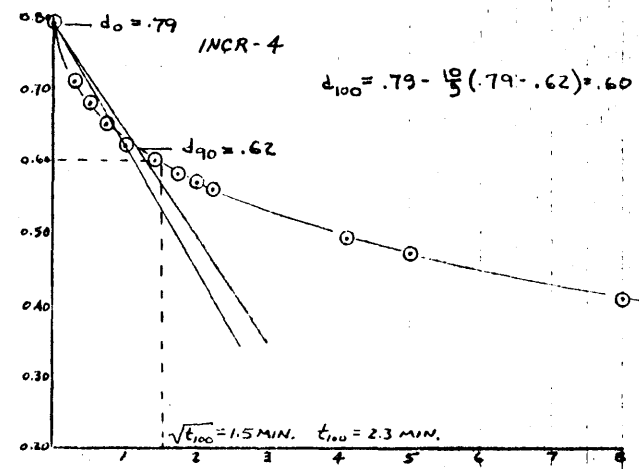
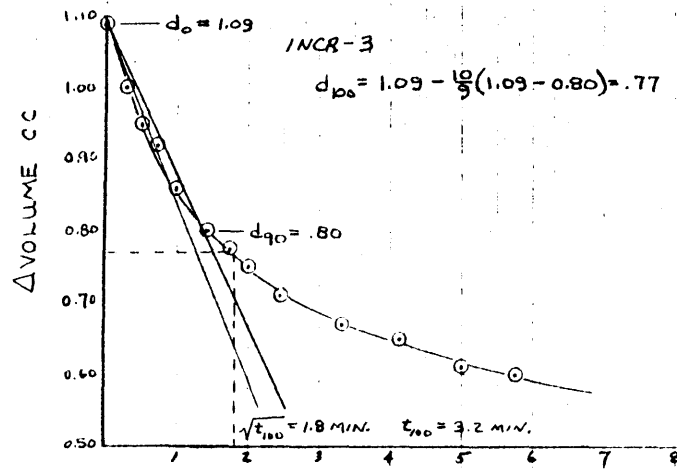
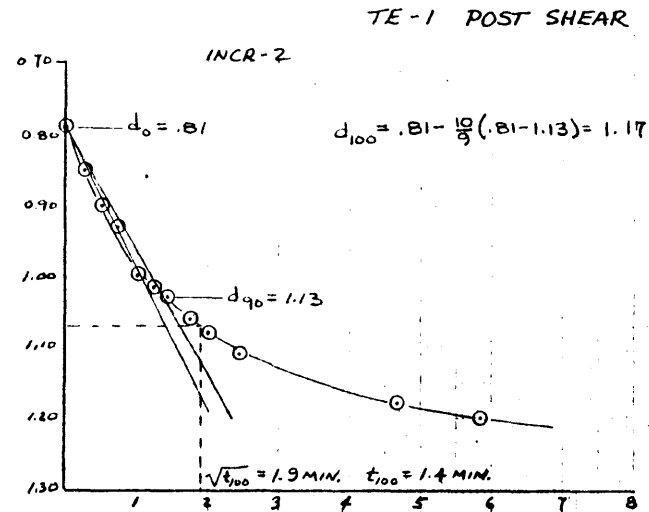
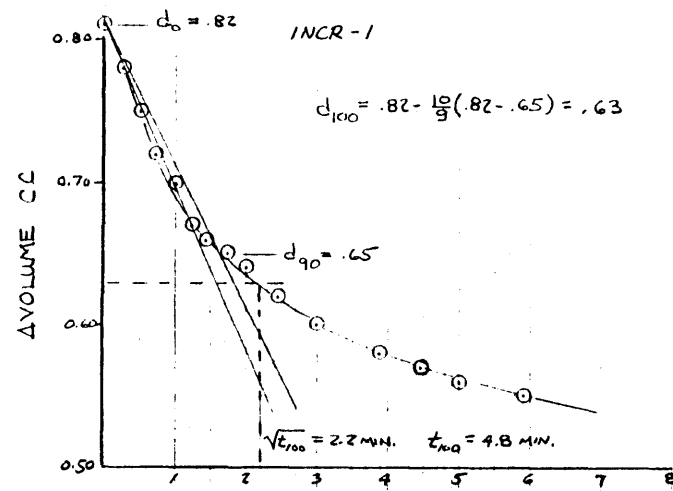


FIG. A. 8

TE-2 PRE-SHEAR

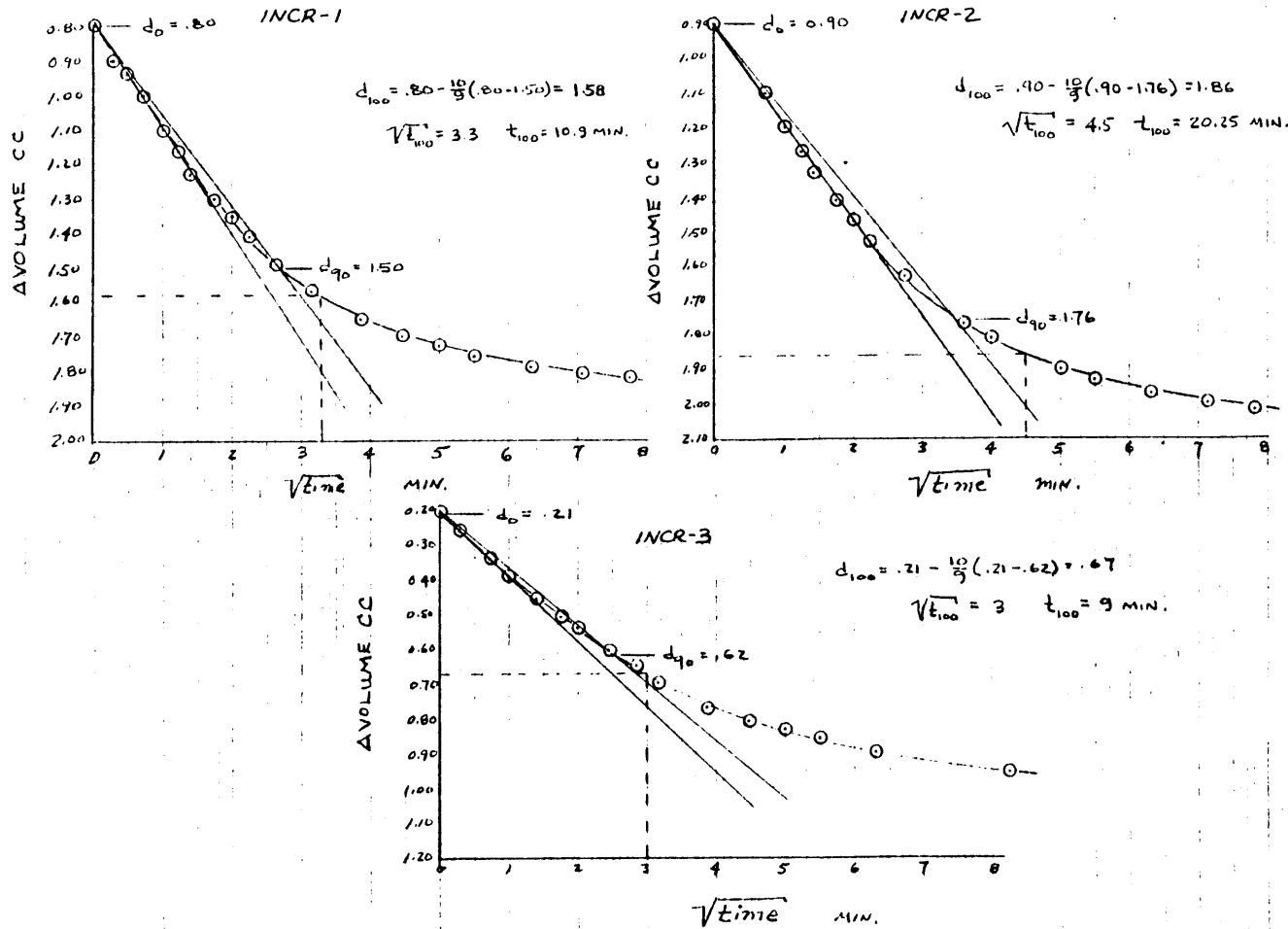


FIG. A.9

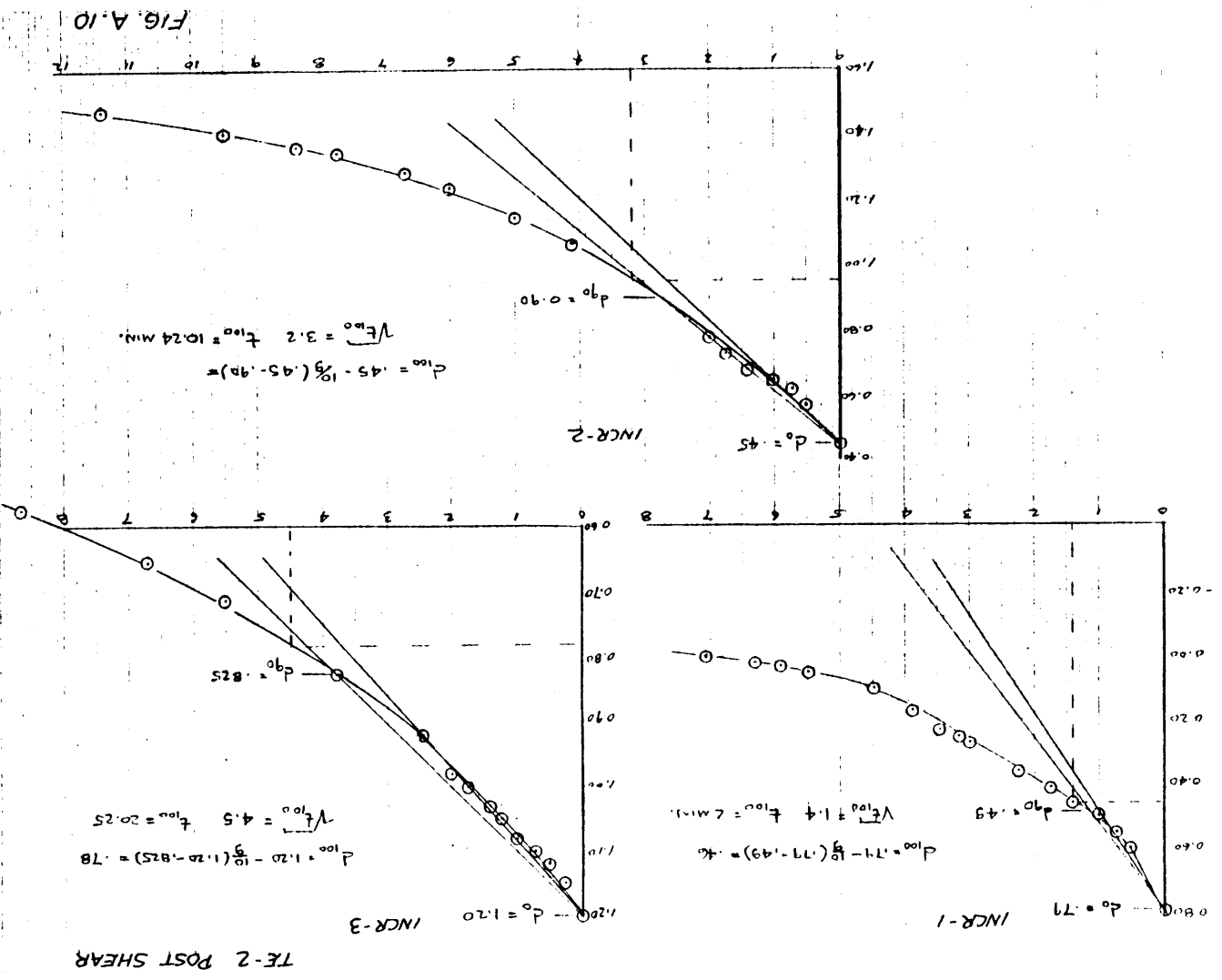
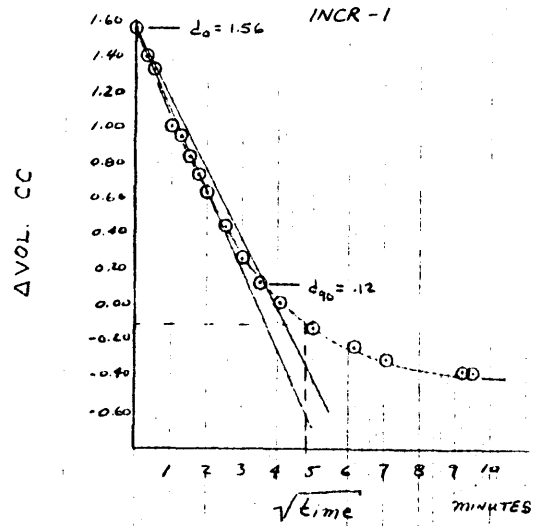


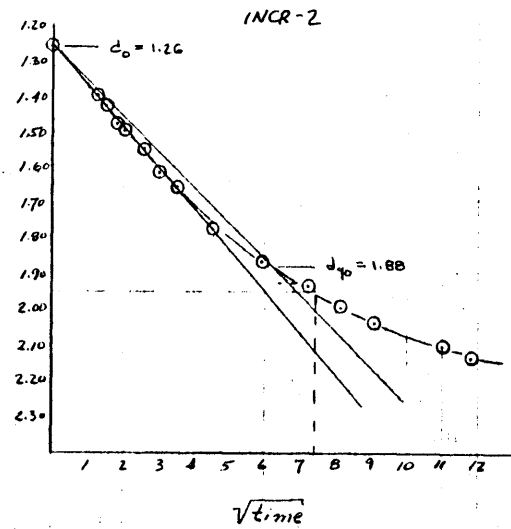
FIG. A.10

TC-1 PRE-SHEAR



$$d_{100} = 1.56 - \frac{10}{9}(1.56 - 0.12) = 0.10$$

$$\sqrt{t_{100}} = 4.8 \quad t_{100} = 23 \text{ MINUTES}$$

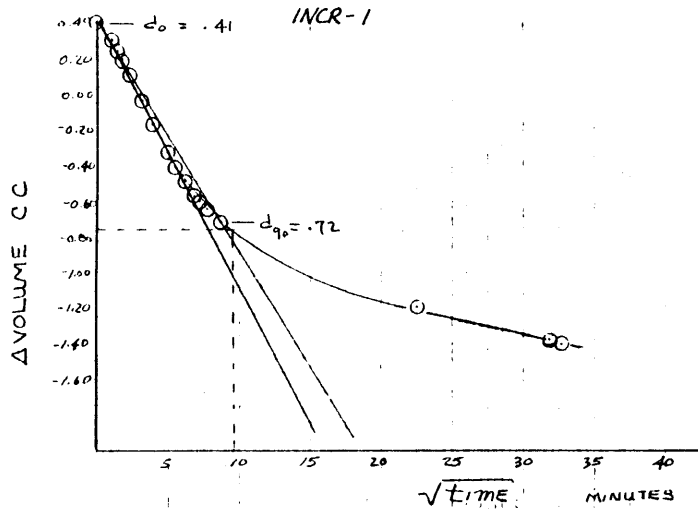


$$d_{100} = 1.26 - \frac{10}{9}(1.26 - 1.88) = 1.95$$

$$\sqrt{t_{100}} = 7.4 \quad t_{100} = 55 \text{ MINUTES}$$

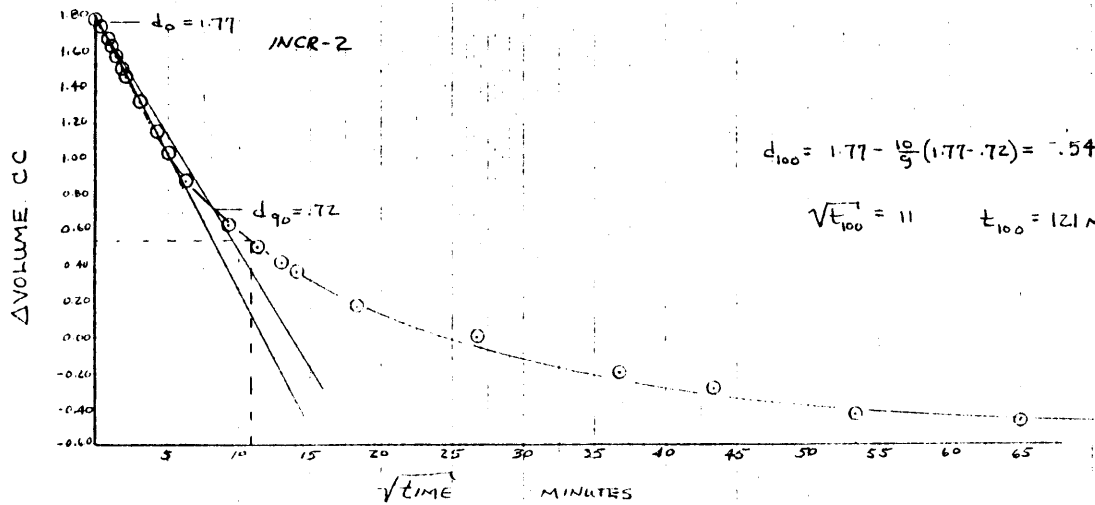
FIG. A-11

TC-1 POST SHEAR



$$d_{100} = .41 - \frac{10}{9}(.41 - .72) = .754$$

$$\sqrt{t_{100}} = 9.5 \quad t_{100} = 90 \text{ MIN.}$$



$$d_{100} = 1.77 - \frac{10}{9}(1.77 - .72) = .54$$

$$\sqrt{t_{100}} = 11 \quad t_{100} = 121 \text{ MIN.}$$

FIG.A.12

TC-2 PRE-SHEAR

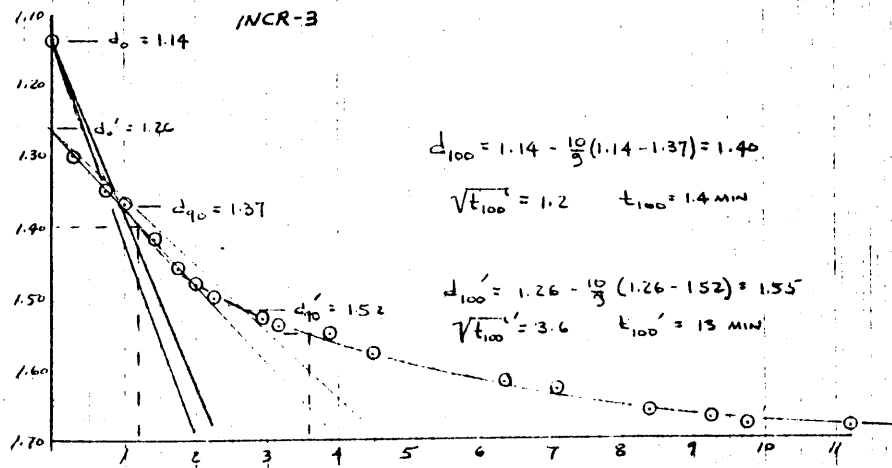
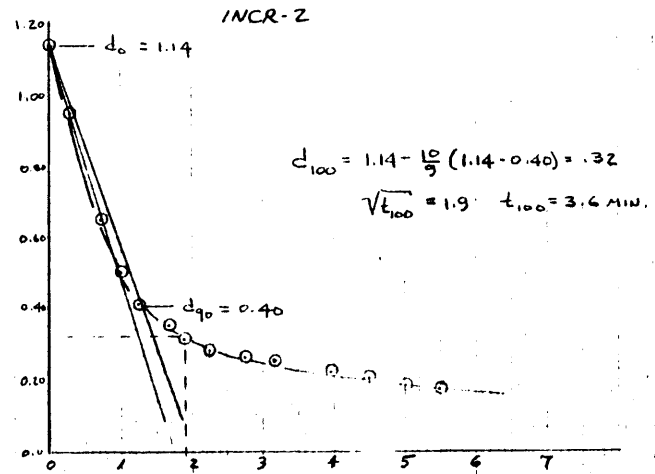
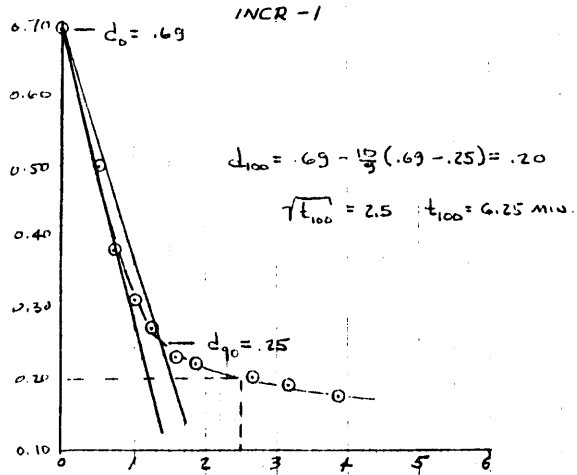


FIG. A.13

TC-2 POST SHEAR

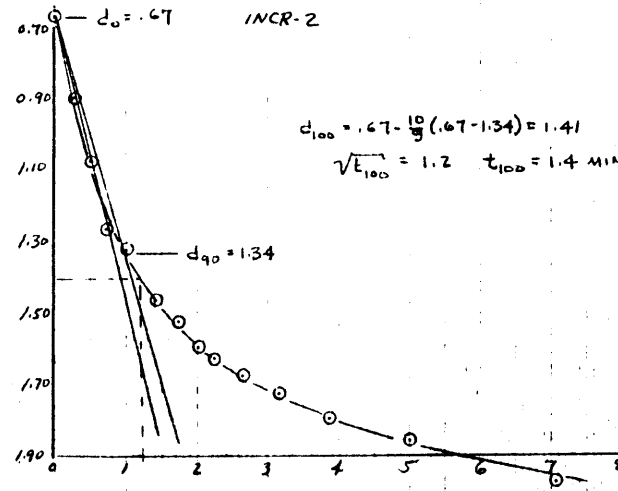
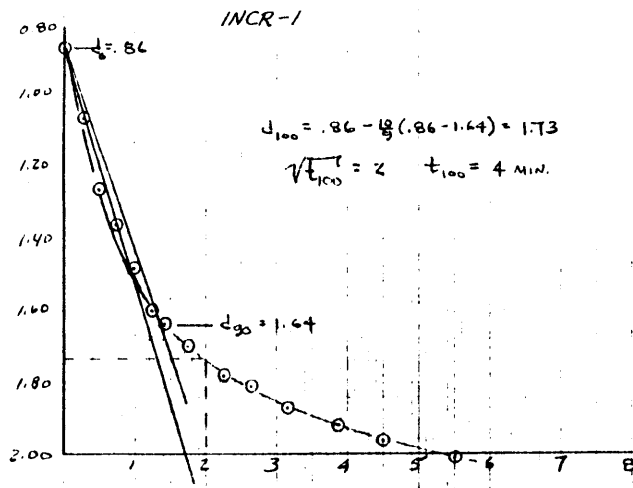
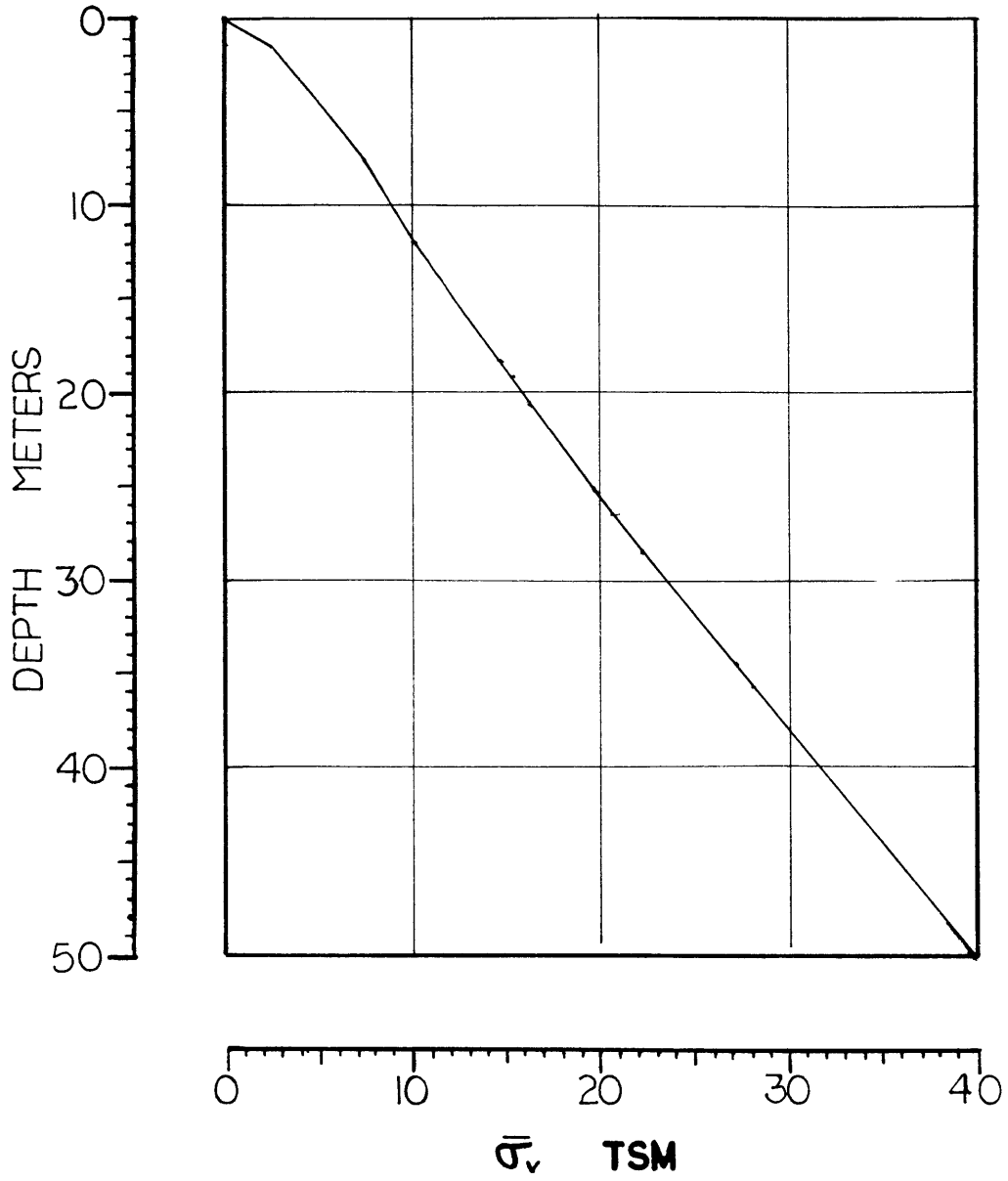


FIG. A.14

APPENDIX B

VERTICAL EFFECTIVE STRESS VERSUS DEPTH - NAKAGAWA



NAKAGAWA

VERTICAL EFFECTIVE STRESS VS. DEPTH

FIG.B.1